

Study of the High Rate Chemical Mechanical Polishing of Heavily Boron-doped
Polysilicon for 3D Applications

by

Hamidreza Pirayesh

A thesis submitted in partial fulfillment of the requirements for the degree of

Doctor of Philosophy

in

Materials Engineering

Department of Chemical and Materials Engineering
University of Alberta

© Hamidreza Pirayesh, 2014

Abstract

The chemical mechanical polishing of polysilicon is a complex process and is not well understood. Despite this, it is used in the semiconductor industry for applications such as via filling and 3D packaging. Although the doping of polysilicon enables applying a wide range of conductivities, boron-doped polysilicon has shown a poor polish removal rates. This is mainly due to role of boron ions in limiting the chemical agent transportation to the surface. Some applications require the removal of more than 10 μm of B-doped polysilicon and improvement in the polish rate would reduce the fabrication costs and significantly improve throughput. In this study, it is shown that the adverse effects of boron on polysilicon polishing rate can be minimized by increasing the mechanical interactions during CMP. This was achieved by control of the lubrication behavior during polishing. In addition, enhancement of the process methodology and slurry properties led to an increase of up to 100% in polish rate compared to standard boron-doped polysilicon polish methods. The increase in polish rate was not accompanied by any polish induced damage to the wafer surface.

Acknowledgements

Foremost, I would like to express my sincere gratitude to my supervisor, Professor Ken Cadien, for the continuous support of my study and research, and for the patience and encouragement. His guidance helped me in all the time of the research and writing this thesis.

I would also like to thank my supervisory committee members, Dr. Thomas Thundat and Dr. Hongbo Zheng for their encouragement and insightful comments.

Many others have contributed to the accomplishment of this work. I am very grateful to the staff of NanoFab and Micralyne, particularly Alexander Janzen, Joshua Krabbe, Les Schowalter, Shiraz Merali and Shiau-Yin Wu. I would like to acknowledge the faculty and staff of the Department of Chemical and Materials Engineering. I am also grateful to my colleagues, particularly Lucy Nolan for her helpful advices and guidance during my program. I would additionally like to acknowledge the Alberta Innovates Technology Futures Nanoworks for the financial support of this research.

Contents

Chapter 1. Literature review	1
1.0 Introduction.....	1
1.1 General background.....	3
1.2 Literature review- CMP mechanisms for metals, silicon dioxide, and polysilicon	8
1.2.1 Metals.....	8
1.2.2 Silicon dioxide	9
1.2.3 Polysilicon.....	10
1.3 Literature review- CMP process	17
1.3.1 Chemical aspects of polysilicon CMP	18
1.3.2 Mechanical aspects of polysilicon CMP- Tribology	20
1.3.3 Effect of temperature on CMP	24
1.3.4 CMP models.....	25
1.3.5 CMP processing parts	27
Chapter 2. Experimental procedure	32
2.1 Wafer fabrication	32
2.2 Wafer polishing.....	32
2.3 Polish measurements.....	36
2.3.1 Pad and wafer rotational velocity	36
2.3.2 Friction force.....	38
2.3.3 Polish temperature	41
2.4 Wafer characterization.....	42
2.4.1 Film conductivity	42
2.4.2 Film thickness	44
2.4.3 Surface characterization.....	45
2.4.4 Dopant concentration.....	45

2.4.4.1 Hole carrier concentration.....	46
2.5 Slurry characterization.....	46
Chapter 3. Lubrication behavior of boron doped polysilicon.....	48
3.1 Polish rate study.....	48
Case 1: Hydrodynamic to partial lubrication (3psi pressure).....	54
Case 2: Partial to boundary lubrication (4.5, 6 psi) at low and moderate velocities.....	55
Case 3: Hydrodynamic lubrication at high flow rates and dry lubrication at low flow rates for the high velocity (110 rpm).....	57
3.2 The influence of polish temperature.....	59
3.3 Surface quality (AFM).....	61
3.4 Conclusions.....	61
Chapter 4. Effect of chemical and mechanical components on high rate CMP of boron-doped polysilicon.....	63
4.1 The effect of slurry flow rate and velocity on polish rate and temperature.....	63
4.2 The effect of slurry temperature of polish rate behavior.....	70
4.3 The effect of chemical and mechanical forces on the polish rate model.....	74
4.4 Effect of optimized high rate polish on surface quality.....	76
Conclusions.....	77
Chapter 5. Effect of slurry and abrasive properties on boron-doped poly CMP.....	80
5.1 Colloidal silica abrasive.....	81
5.2 Zeta potential.....	82
5.3 Silica abrasive dissolution.....	82
5.4 Polish rate as function of pH and silica abrasives.....	86
5.5 Conclusion.....	92
Chapter 6. Boron doping effects on polysilicon CMP.....	93
6.1 Conclusion.....	102
Chapter 7. Summary.....	103
Future work.....	106
Bibliography.....	108

List of Tables

Table 2-1. Summary of process conditions.....	35
Table 3-1. Preston's coefficient for various polish conditions.	52
Table 4-1. Surface roughness measurement of a few polish conditions. The results are the average of six measurements, including the standard deviation (SD).	77
Table 5-1. Zeta potential of colloidal silica at different pH values.	82
Table 5-2. Atomic absorption results (in ppm) for colloidal silica with different particle size and 6wt% concentration, remaining in pH 12 and 13 solutions for 24 hrs.....	83
Table 5-3. Particle size measurement of solutions before and after remained in the high pH solution for 24 hrs (in nm).	84

List of Figures

Figure 1-1. Prediction of semiconductor industry evolution by Moore’s law [1].	4
Figure 1-2. Schematic illustration of CMP process. The inset represents the interaction between pad asperities and slurry abrasives.	6
Figure 1-3. The role of CMP in chip fabrication process.	7
Figure 1-4. CMP mechanism of metals. The abrasives easily remove the softened oxide of metal. New oxide forms after it faces the slurry and the process continues.	9
Figure 1-5. Atomic configuration of n-type (phosphorous) and p-type (boron) silicon based semiconductor.	11
Figure 1-6. Relation between the carrier concentration and resistivity for phosphorous and boron doped polysilicon.	12
Figure 1-7. Effect of slurry pH on polish rate of polysilicon[19].	13
Figure 1-8. Polishing mechanism of polysilicon proposed by Pietsch <i>et al</i> [19].	14
Figure 1-9. Deposition rate of arsenic, boron and phosphorous doped polysilicon in the CVD process [24]. Adding boron shows a significant increase of the deposition rate [24].	15
Figure 1-10. Electrical effects of dopants on CMP of doped polysilicon [29].	17
Figure 1-11. Stribeck curve and the relation between polish parameters and the COF.	23
Figure 1-12. Role of conditioner in preventing the pad glazing effect during polishing.	29
Figure 1-13. SEM micrograph of polymeric pads [70].	30
Figure 2-1. Axis 372M polisher.	34
Figure 2-2. Relative velocity of point A on the rotating wafer with respect to the rotating pad.	37
Figure 2-3. Direction of lateral force, linear velocity and friction force of the wafer when pad and carrier have the same speed.	39
Figure 2-4. Schematic of the 13 points measurement with 4-point probe.	43
Figure 2-5. Cross-sectional SEM micrograph of wafers. The top layer is boron-doped polysilicon, second one is thermal oxide film and the bottom layer is single crystal silicon.	44
Figure 3-1. Polish rate as a function of PV and flow rate. The negative slope of the graph is due to hydroplaning at high polish velocities. The 4.5 psi polish data is not shown for clarity.	50
Figure 3-2. Relationship of removal rate to the pressure velocity product at different flow rates for highly boron doped wafers. The dashed lines represent the hydrodynamic lubrication with reducing the polish rate.	51
Figure 3-3. COF as function of velocity for low polish pressure (3psi), hydrodynamic lubrication regime.	53

Figure 3-4. COF as function of velocity for high polish pressure (6psi), boundary lubrication regime.	56
Figure 3-5. Phase diagram representing the lubrication behavior as function of PV and flow rate.....	58
Figure 3-6. Effect of PV on the maximum polish temperature, after 1 minute of polishing.	60
Figure 3-7. AFM images of wafers before and after polishing.....	62
Figure 4-1. Effect of flow rate and polish velocity on polish rate at 6psi pressure for 2.2 $m\Omega.cm$ resistivity films.	64
Figure 4-2. The pad temperature during polishing of boron doped polysilicon at 6psi pressure and various flow rates and velocities.....	66
Figure 4-3. Coefficient of friction versus a) pad/wafer velocity at low slurry flow rates (50ml/min), b) flow rate for high pad/wafer velocity (110rpm). All experiments at 6psi pressure and for 2.2 $m\Omega.cm$ resistivity films.....	69
Figure 4-4. Pad hardness as a function of temperature (Courtesy of NexPlanar Inc.)	70
Figure 4-5. The effect of flow rate and polish velocity on the removal rate of polishing with HT slurry (70°C) and high pressure (6psi) for 2.2 $m\Omega.cm$ resistivity films.....	73
Figure 4-6. The pad temperature during the polishing of boron doped polysilicon (2.2 $m\Omega.cm$ resistivity films) at 6psi pressure with HT (70°C) and various flow rates and velocities.	73
Figure 4-7. Schematic illustration of the effect of mechanical and chemical factors on removal rate for low, moderate and high pad/wafer velocities.....	76
Figure 4-8. AFM images of sample, a) before polishing; b) after polishing at 6psi and 90rpm and 200ml/min.	79
Figure 5-1. TEM micrograph of silica abrasives used in our experiment. 5-1a and 5-1b are 30/50 and c is 300/30 slurry.....	81
Figure 5-2. pH change of colloidal silica as function of time.....	85
Figure 5-3. The colloidal silica pH change after 24 hours as function of initial pH.	86
Figure 5-4. Polish rate as function of pH for different polish conditions and slurries.	87
Figure 5-5. Effect of polish condition and particle size on the polish rate at 6psi pressure and with 6 and 12wt.% of silica abrasive. Case 1 is 90rpm and 200ml/min, Case 2 is 110rpm and 50ml/min.....	90
Figure 5-6. Effect of slurry chemistry, silica abrasive properties and polish condition on polish temperature.	91
Figure 6-1. Effect of dopants on the polysilicon CMP rate [28].	94
Figure 6-2. SRP and SIMS results for the 2.2 $m\Omega.cm$ sample.	95
Figure 6-3. Polish rate at different flow rates and velocity with 6psi pressure.	97
Figure 6-4. Comparison of polish rate as function of doping level for 200ml/min flow rate and 6psi pressure.....	98
Figure 6-5. The effect of boron-doped polysilicon conductivity on the CMP rate, for the condition of 6pi pressure, 90rpm speed and 200ml/min flow rate. Other conditions follow the same trend as well.	99

Figure 6-6. Removal rate ratio at highly mechanical condition of 50ml/min (RR50) and optimum flow rate of 200ml/min (RR200) vs. the polish velocity..... 101

Figure 7-1. Polish rate comparison for different conditions: A. Undoped poly, commercial polish slurry (Fujimi) and moderate polish condition (6psi pressure, 80rpm speed, 200ml/min flow rate) B. Heavily boron-doped poly, commercial polish slurry and moderate polish condition C. Heavily boron-doped poly, commercial polish slurry and mechanically enhanced condition D. Heavily boron-doped poly, moderate polish condition and developed silica slurry E. Heavily boron-doped poly, mechanically enhance polish condition and developed silica slurry. 105

Chapter 1. Literature review

1.0 Introduction

This thesis explores high rate chemical mechanical polishing of heavily boron-doped polycrystalline silicon based on a fundamental comprehension of the chemical and mechanical components of the polish using a commercial slurry. In order to completely explore the research space and basically investigate the chemical components, a research grade slurry was developed for the final part of the thesis. By understanding the mechanism of polishing and enhancing the mechanical and chemical forces, the polish rate is expected to be improved. The research was funded by an Alberta Innovates Technology Futures Nanoworks grant for a Micralyne Inc. project that involved development of through silicon via technology.

The role of mechanical components was studied by improving the mechanical interactions during the process. By maximizing the friction force through controlling the pressure, temperature, velocity and slurry flow rate the mechanical abrasion of the surface and consequently the surface removal is expected to increase. The research grade slurry with various abrasive sizes was also assisting the improvement of the polish process.

Investigation on the role of chemical etching was carried out by studying the effect of slurry chemistry on the polish rate. Besides, preheating the commercial slurry showed an improvement in the chemical etching and minimizing the mechanical buffing.

Therefore, it could be used as a suitable method to explore the role of chemical components of polishing apart from mechanical forces.

Lastly, the effect of activated boron concentration (doping level) on the polysilicon polishing is studied. It has been shown in earlier works in industry that doping polysilicon with boron can significantly suppresses the polish rate. By understanding the role of boron on the chemical and mechanical components of polysilicon polish rate, it is expected to minimize this retardation effect and achieve higher polish rates. An outline of the thesis is given below.

In this work CMP of heavily boron-doped polysilicon has been investigated by developing a fundamental understanding of the chemical and mechanical aspects of the polish with the ultimate goal of increasing the polish rate.

In chapter (Chapter 1) a brief introduction of the CMP of different materials and doped polysilicon particularly is outlined.

Chapter 2 presents the experimental techniques used to explore this problem.

Chapter 3 discusses the lubrication behavior of polishing. It is shown that lubrication behavior plays the key role in CMP and increasing the slurry flow rate and polish speed do not necessarily improve the polish rate.

Chapter 4 demonstrates the role of chemical and mechanical components of polishing. The mechanical interactions are shown to have a significant effect on polishing and by improving the mechanical and friction forces the polish rate improves considerably.

Chapter 5 examines the slurry chemistry and abrasive properties on polishing. The optimum polish behavior is achieved by high pH, small abrasives, relatively low abrasive concentration and high mechanical interactions in polishing.

Chapter 6 discusses the boron doping level effect on polishing. Increasing the doping level and consequently the conductivity led to a significant polish rate reduction. This effect is investigated and hindrance of the chemical agent transportation is shown to play a critical role in this phenomenon.

1.1 General background

The invention of the transistor in 1947 and the modern integrated circuit (IC) in 1959 led to the rapid growth of the microelectronic industry and the increase in the number of chip devices led to the development of ultra large scale integration (ULSI). Higher performance and lower IC production costs were achieved by increasing the number of transistors and other devices on each integrated circuit (density of parts). Moreover, shrinking the IC size, increasing the density and reducing the interconnect length improves the device speed and reduces the power consumption. Gordon Moore predicted that the density of transistors on each chip doubles approximately every two years and this is now called Moore's Law [1], [2]. Figure 1-1 shows the accuracy of Moore's law for the last four decades. By increasing the number of transistors and other critical parts such as resistors and capacitors on ICs, the parts were required to shrink in size [2], [3].

fabrication technology. Furthermore, CMP has enabled several fabrications advanced such as copper polish and gate last high k metal transistor technology, and is currently enabling 3D interconnecting technology.

In CMP, the rotating wafer is pushed into a pad that is attached to a rotating platen (pad). Meanwhile a polish slurry is flowed onto the platen surface and reacts chemically and interacts mechanically with both the wafer and the pad surface. This process is illustrated schematically in Figure 1-2. The pad usually has a polymeric fibrous or cellular structure and has a surface roughness in the micron range. As shown in Figure 1-2 CMP tools come equipped with a pad conditioner that is used to prevent the pad glazing and maintain a constant polish rate during polishing [3], [6]. The wafer is typically supported by a wafer carrier while a back pressure is applied on the back of the wafer. There are many parameters affecting the final polished surface and the polish rate which make CMP a complicated process. The chemistry of the abrasives and slurry, the pad and wafer carrier rotation speed, the polish force, the hardness and the structure of the pad and the flow rate of the slurry are some of these critical factors.

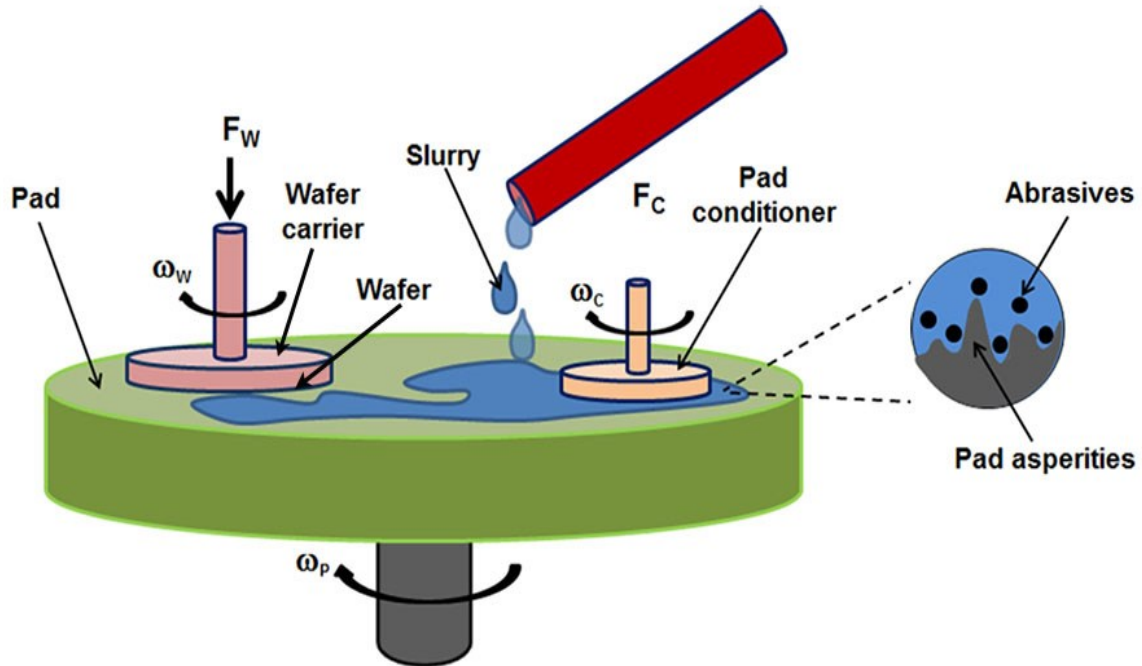
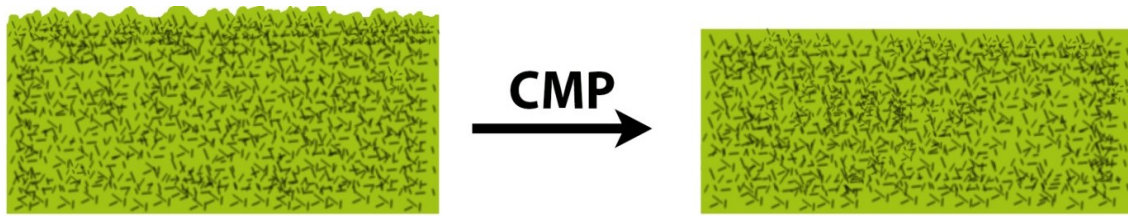
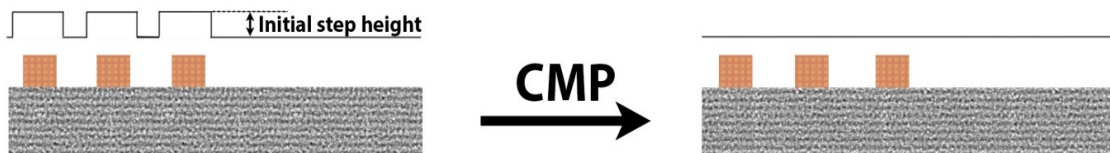


Figure 1-2. Schematic illustration of CMP process. The inset represents the interaction between pad asperities and slurry abrasives.

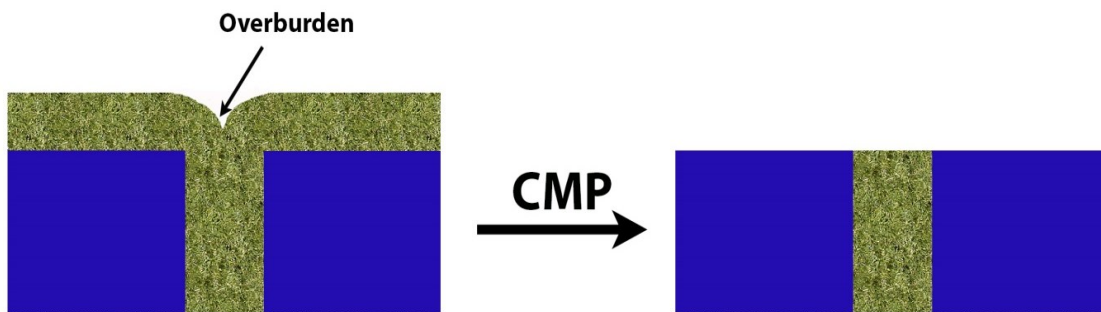
In general, CMP has three major fabrication attributes: 1. Improving the surface quality by smoothing the surface and removing defects, 2. Planarization and maximum surface uniformity 3. Removal of excess materials and overburdens to enhance the packaging process. Overburden is formed during the deposition of fill materials for silicon via (TSV) and shallow trench isolation (STI) processes. Figure 1-3 schematically shows the role of CMP in ULSI fabrication process.



Roughness reduction



Planarization



Removing overburden

Figure 1-3. The role of CMP in chip fabrication process.

CMP process mainly depends on the properties of the material that is being polished. The slurry chemistry, the abrasive properties and the polish process are functions of the polished material properties. For instance oxidizers such as hydrogen peroxide play a key role in metal polishing while in semiconductors and ceramics the pH of the solution is the critical parameter. In addition, the abrasive properties should be tailored for the material to be polished. Harder materials require harder abrasives.

1.2 Literature review- CMP mechanisms for metals, silicon dioxide, and polysilicon

As discussed earlier, the CMP process depends on the material to be polished. For different materials different slurry, polish condition and pad properties is needed. This is due to different mechanisms for the removal of materials. In this section the mechanisms for the CMP of metals, silicon dioxide and polysilicon will be reviewed.

1.2.1 Metals

CMP of metals such as copper and tungsten usually occurs first by oxidizing their surface via strong oxidizers such as hydrogen peroxide (H_2O_2). The oxidized surface will then be abraded by abrasives in the slurry. The process of oxidation and abrasion is shown in Figure 1-4 where the oxidized surface is polished mechanically and the fresh metal surface (after removal of the oxide) will be oxidized by reacting with the slurry oxidizer. This process goes on repetitively until the desired surface removal is achieved. Surface oxidation has important effects on CMP. Mainly, the oxide layer becomes hydrated in the slurry solution. In most cases this hydrated surface is much softer than the underlying metal and it is easier for abrasives to remove it. The role of the oxide is different for different metals. For metals that are capable of forming a passive layer such as tungsten and aluminum, the passive layer will protect the metal surface from further oxide or damage such as pitting while they are not in solid contact with the pad[3], [8]. For metals with no natural passive layer, such as copper, corrosion inhibitors are added to the slurry.

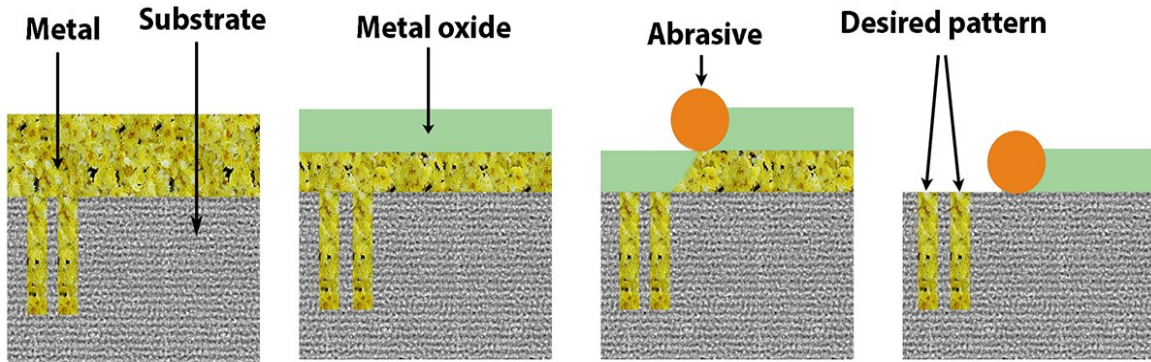


Figure 1-4. CMP mechanism of metals. The abrasives easily remove the soften oxide of metal. New oxide forms after it faces the slurry and the process continues.

1.2.2 Silicon dioxide

As mentioned earlier, polishing of hard materials such as silicon dioxide are based on mechanical buffing of the surface and solution pH contribution. The process of silicon dioxide material removal is known as chemical tooth and has been explained by Cook in 1990 [9]. In this sense, the oxide dissolution happens by breakage and hydration of siloxane (Si-O-Si) bonds. Therefore silica tetrahedron forms instead of fully network silica and the hydroxyl termination occurs on the oxide surface:



This reaction and presence of hydroxyl as a strong polarizer lead to weakening and breakage of siloxane bonds and hence the removal rate enhancement. After that abrasives such as silica or ceria remove the terminated surface by chemisorption of the silicon and lifting away from the surface. The abrasives will be washed away by the

slurry fluid afterwards and the surface removal will occur. This explains the influence of slurry pH and hydroxyl concentration on increasing the polish rate [9], [10].

1.2.3 *Polysilicon*

This thesis is focused on chemical mechanical polishing of polysilicon and heavily boron-doped silicon. Therefore polysilicon polishing will be discussed in more details in this section. Conductive polycrystalline silicon (polysilicon) is widely used as an alternative for metals and for fabrication steps in IC, MEMS and novel device fabrication process and where high thermal and mechanical stability are required [11], [12], [13]. Undoped polysilicon is used as a semiconductor for applications where insulation is required or where high conductivity is needed (doped polysilicon) [2], [14], [15], [16], [17]. The ability to change the conductivity by doping polysilicon provides a wide range of applications. Heavily doped polysilicon has been used extensively in applications such as a gate electrode in field effect transistors and as a fill material for TSVs. TSV technology is mainly used for front end of line and 3D packaging process and where interconnection between different layers is required. The via is usually filled by doped polysilicon since it has good thermal and mechanical stability at high temperatures while providing acceptable electrical conductivity [11], [13], [18]. Deposition technologies such as chemical vapor deposition (CVD) is used to fill the via. Since CVD is a conformal deposition process, the thickness of the deposited film and hence the overburden that must be removed is at least one half of the width of the narrowest cross-section of the via. This means that in some applications the polysilicon overburden can exceed 10 μm , demanding a high rate removal process (Figure 1-3).

1.2.3.1 Silicon as a semiconductor

Semiconductor materials provide a wide range of conductivities. They can be as conductive as metals or as resistive as insulators depending on the activated dopant concentration (doping level). Schematic illustration of n-type semiconductors such as phosphorous and p-type semiconductors such as boron is shown in Figure 1-5. In the presence of free electron or hole carrier inside the structure, the conductivity improves significantly. Active dopants must substitute for silicon atoms in the silicon lattice. In order to achieve this, annealing and proper cooling recipe must be developed. Polysilicon doping level directly affects the conductivity as shown in Figure 1-6 for silicon with boron and phosphorous as dopants. In our experiments heavily boron-doped polysilicon (p-type semiconductor) with high hole concentration is used with an expected low resistivity of $\sim 2\text{m}\Omega\cdot\text{cm}$.

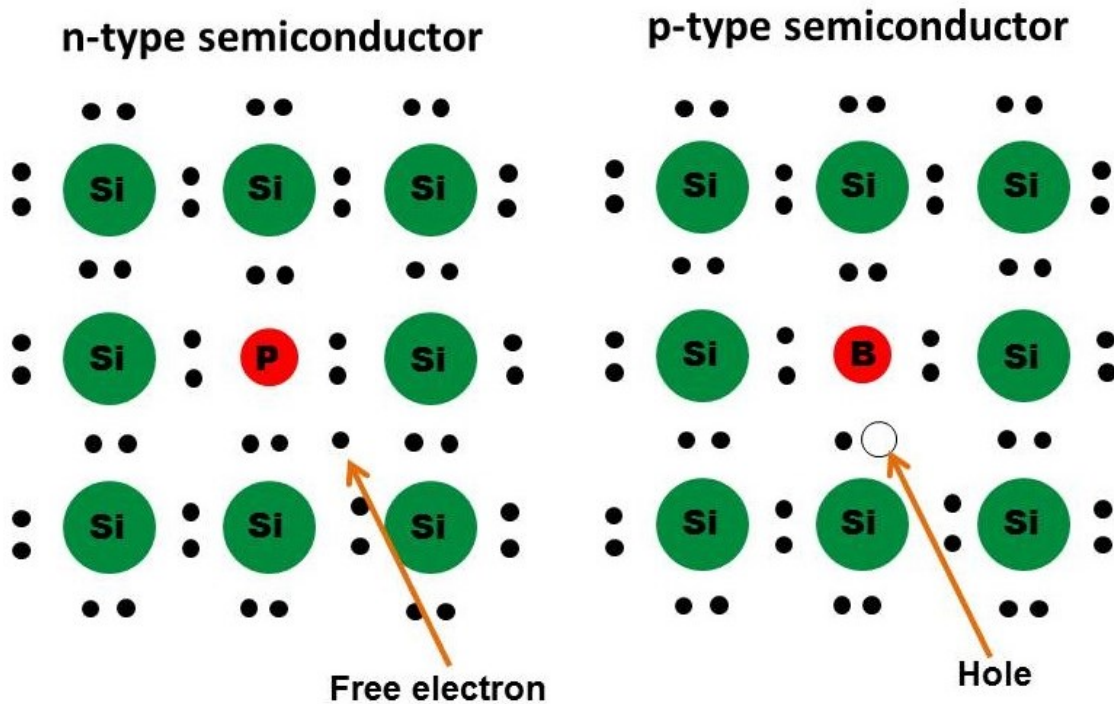


Figure 1-5. Atomic configuration of n-type (phosphorous) and p-type (boron) silicon based semiconductor.

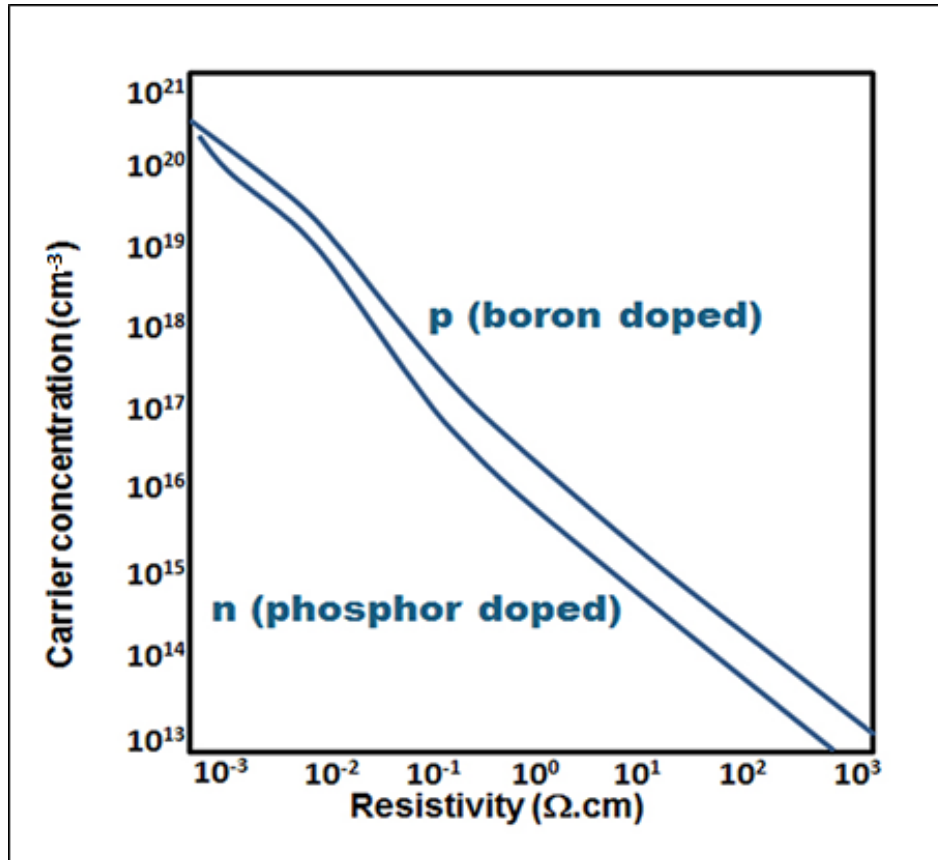


Figure 1-6. Relation between the carrier concentration and resistivity for phosphorous and boron doped polysilicon.

1.2.3.2 Polysilicon polishing mechanism:

Improving the polysilicon polish rate is impossible without understanding the polish mechanism. Pietsch *et al.* suggested that polysilicon polishing improves in the presence of hydroxyl anions as a strong polarizer [19], [20], [21], [22]. It has been shown that the polish rate strongly depends on the pH of the slurry and increasing the hydroxyl concentration and consequently pH increases the polish rate significantly. This is shown in Figure 1-7 by Pietsch *et al.* where the maximum polish rate is achieved at pH values $\sim 11-12$. The process of polysilicon polishing in an aqueous solution first happens by surface hydrogen termination. Hydroxyl anions weaken the

Si-Si and Si-H bonds and eventually breakage of the silicon bonds occurs. The dissolution occurs either by reaction of silicon atoms with the water or with the dissolved oxygen. In this process the Si-Si bonds break and react with oxygen or hydrogen and hydroxyl anions. This leads to the dissolution of silicon atoms in the solution as shown schematically in Figure 1-8. The silica abrasives help this process by mechanically removing the silicon atoms from the weakened bonds. The dissolution cycle is repeated until the desired amount of material is removed.

The rapid decrease in polish rates at $\text{pH} > 12$ can be attributed to the formation of hydrides with oxygen atom back bonds [19], [23]. At this pH, the surface is mostly covered by silicates and oxides. On the other hand at higher pH values the surface becomes more hydrophobic due to hydroxyl termination of the surface in the presence of excessive hydroxyls. Thus, increasing the hydrophobicity and consequently maximizing the cohesion over the adhesion leads to the surface removal rate reduction [21], [23].

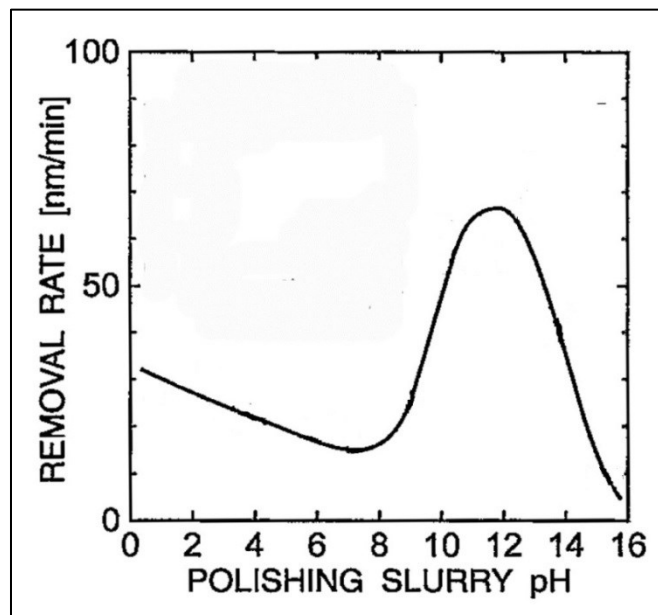


Figure 1-7. Effect of slurry pH on polish rate of polysilicon[19].

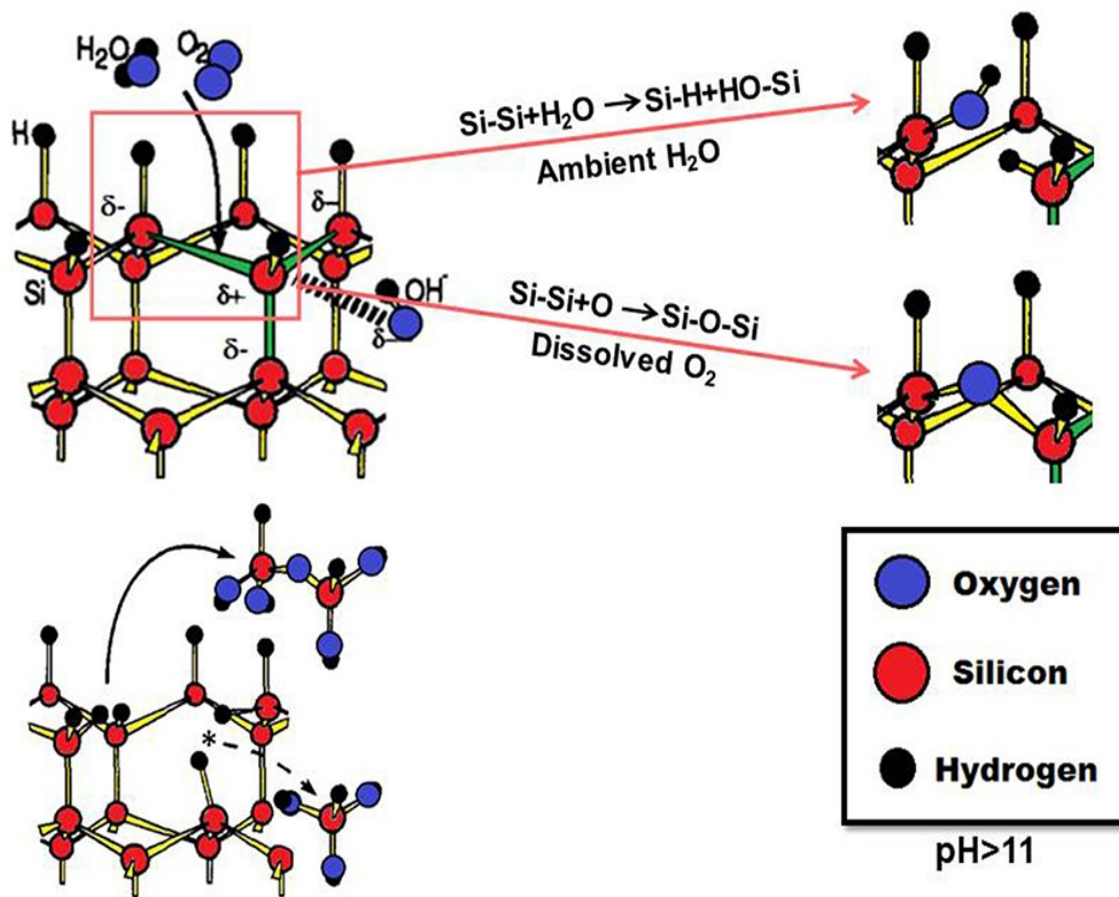


Figure 1-8. Polishing mechanism of polysilicon proposed by Pietsch *et al* [19].

1.2.3.3 Effect of doping on the polish behavior of polysilicon

Polysilicon is usually doped by phosphorous as n-type or boron as p-type semiconductor. Although both boron and phosphorous show acceptable conductivity, in-situ doping of silicon by phosphorous dramatically lowers the CVD deposition rate while a higher CVD deposition rate is obtained for boron doped polysilicon (Figure 1-9) [24]. This makes boron doping the preferred route for heavily doped polysilicon.

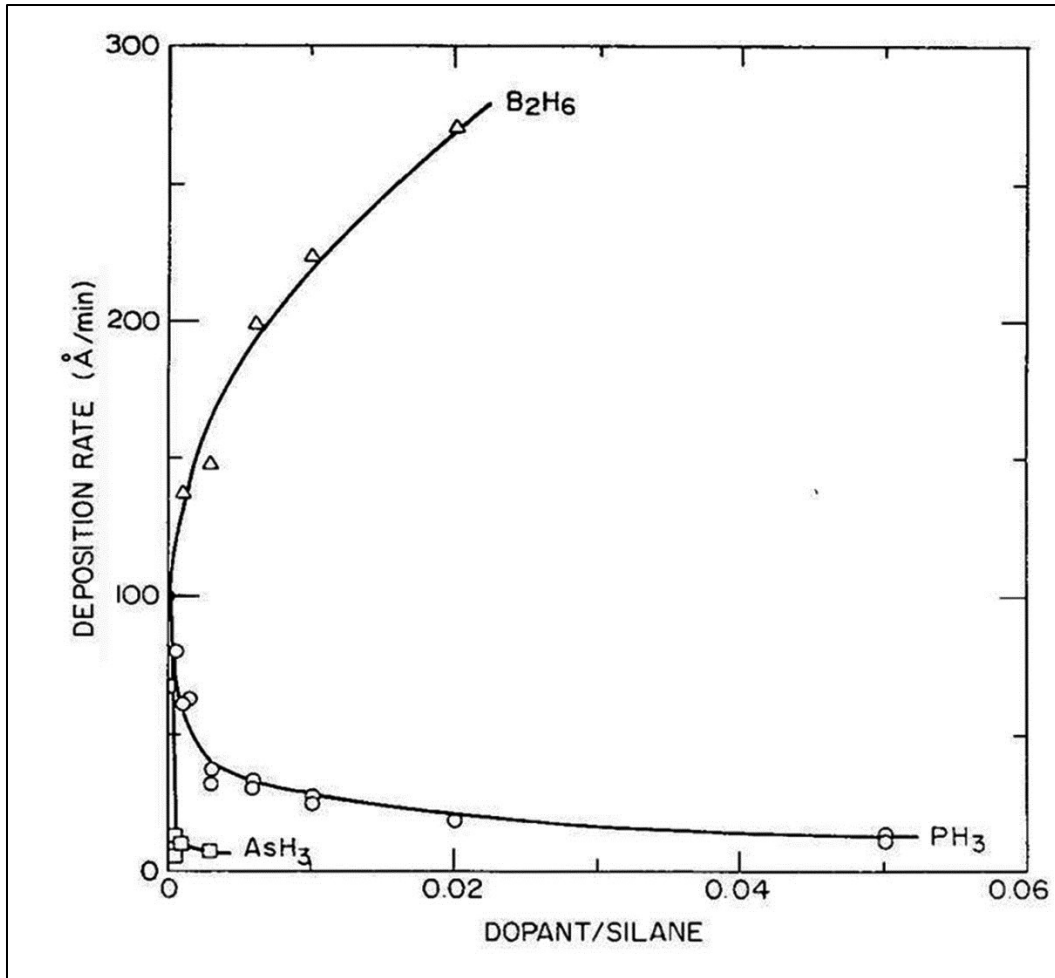


Figure 1-9. Deposition rate of arsenic, boron and phosphorous doped polysilicon in the CVD process [24]. Adding boron shows a significant increase of the deposition rate [24].

CMP of polysilicon has been studied within the last two decades and it has been shown that the doping can have a noticeable impact on the polysilicon polishing rate [8], [17], [25], [26]. Doping polysilicon with phosphorous can increase the removal rate ~50% while boron suppresses the rate significantly. In this study we focus on understanding the role of boron on the polish rate of polysilicon.

Several hypotheses have been proposed to explain the retardation of polysilicon polish rate. In one hypothesis it was proposed that the chemical behavior of boron is

responsible for this phenomenon [27], [28]. Here the boron dopant has more tendency to react with hydroxyl ions than silicon atoms and would reduce the Si-Si hydrolysis, thereby reducing the polish rate. However, the extremely low concentration of boron in the bulk silicon minimizes this effect. Another theory relates reduced CMP polish rate to the atomic size difference between silicon and boron and the stress generated which is trapped in the crystal structure. However, since the polish rate change was observed for different dopants such as phosphorous and arsenic, regardless of their atomic size, this effect can be neglected as well. The more acceptable model is shown schematically in Figure 1-10. This model postulates that the electric field formed by dopant in silicon is responsible for the polish rate change [8], [29]. As discussed earlier the presence of hydroxyl anions on the polysilicon surface causes the surface polishing during CMP. Hindering or assisting the transportation of these anions to the surface can affect the polish rate significantly. As shown in Figure 1-10, the dopants form a depleted layer on the surface depending on the type of dopant. The depleted layer forms because free electrons and holes can move freely inside the structure while the dopant anions are fixed and will remain in their lattice position after the carrier migration. For n-type dopants such as phosphorous, positive anions remain on the surface and for the p-type dopants such as boron, the wafer surface will be filled with negative ions. The attraction and the repulsion of hydroxyl anions on the surface can cause the polish rate change in the presence of dopants.

Since using of boron as dopant is more desirable than phosphorous, enhancing the boron-doped polysilicon polish rate improves chip fabrication costs and reduces polish

time significantly. In this study we intend to increase the boron-doped removal rate by understanding the nature of this retardation effect.

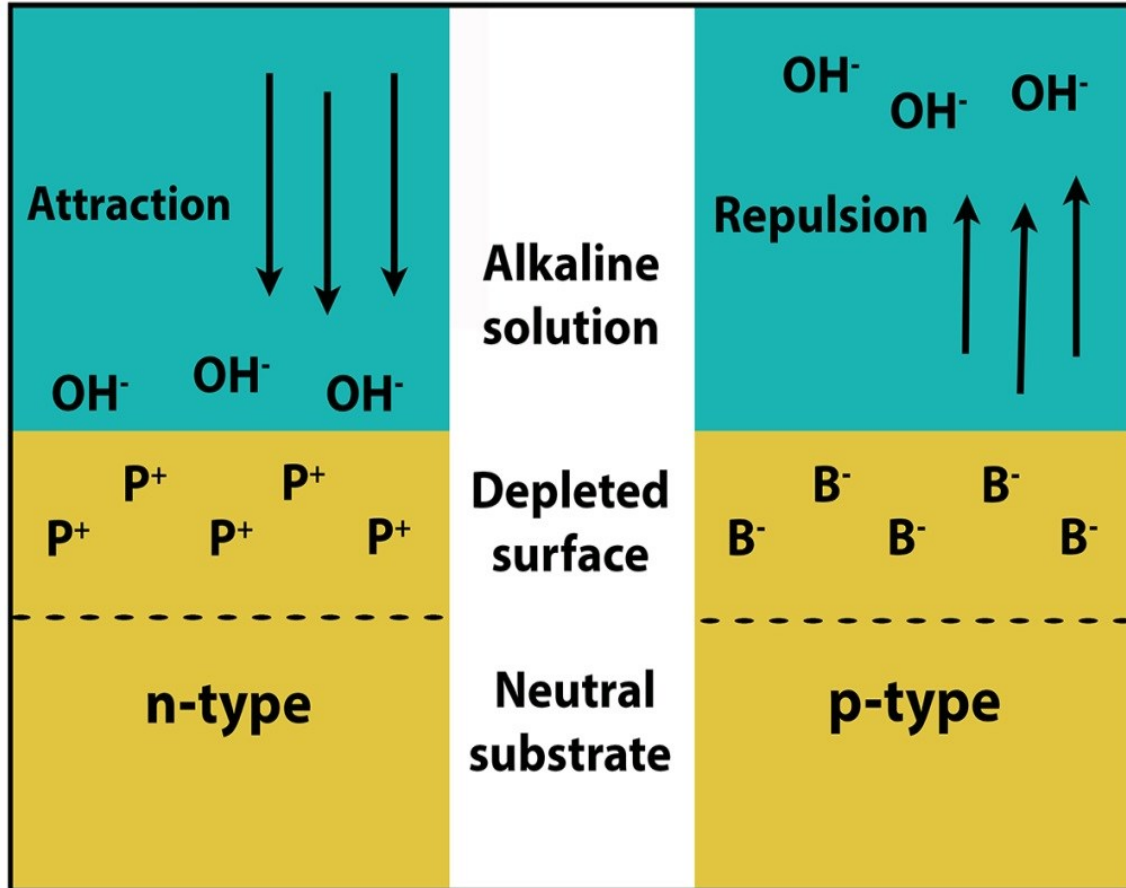


Figure 1-10. Electrical effects of dopants on CMP of doped polysilicon [29].

1.3 Literature review- CMP process

Chemical mechanical polishing is a planarization process which involves both chemical etching and mechanical buffing of the surface. The CMP process was first introduced by IBM in early 80s for SiO₂ polishing for planarization of interlayer dielectrics. It was then applied for shallow trench isolation (STI) and DRAM device manufacturing in Japan. Excellent surface quality and global planarization lead to the

quick growth of CMP and the first commercial CMP polishers was designed in 1988 by Westech and Cybeg [6], [8]. From the beginning, it was clear that there are many factors affecting the CMP process. Moreover, the cost of short term consumables such as slurry and long term consumables such as the polish pad make CMP a critical step for microelectronic production with significant influence on device production costs, time and defects. There have been many studies and models explaining the polish rate, surface quality and polish behavior and other aspects of CMP since it was introduced. Due to the nature of our research, we will mainly focus on CMP of polysilicon in the next section. It was mentioned before that CMP relies on the combination of chemical and mechanical forces. In general chemical forces help mechanical interactions by providing a softer surface.

1.3.1 *Chemical aspects of polysilicon CMP*

As discussed earlier, neglecting the chemical aspects of CMP minimizes the polish rate and might damage the wafer surface through abrasive scratching and gouging. Generally, the chemical components of CMP are related to the chemistry and the abrasives of the slurry. Increasing the slurry flow rate and increasing the slurry temperature are two important factors which can enhance the chemical etching of the thin film [30]. This effect is more evident in metals where different chemicals such as oxidizers and corrosion inhibitors are required for polishing. Polysilicon polishing has the greatest dependency on the pH of the slurry where the change in pH varies the polish rate significantly (more than 10X change) [3], [6], [19]. Other chemicals are usually added to the slurry for the purpose of increasing the selectivity of the slurry.

Selectivity is often important to control the stopping of polishing on an underlying material. Usually polish rate selectivity is defined by:

$$\text{Selectivity: } \frac{\text{Polish rate of overburden material}}{\text{Polish rate of material under the overburden}} \quad (1.1)$$

and values of more than 100 are desirable. There have been several studies trying to improve this selectivity by suppressing the polishing rate of the layer under the overburden. In polysilicon CMP this layer is usually silicon nitride for STI and silicon oxide for TSV [16], [31].

Polysilicon etch rate is directly a function of hydroxyl anion concentration. Another important parameter which has a decisive role on the etch rate is the hydroxyl anion transportation rate to the polysilicon surface. The transportation of hydroxyls can occur both by the solution and by abrasives [23]. The most common abrasive which is used for polysilicon polishing is colloidal silica. Silica can enhance the polysilicon etch rate by transporting the hydroxyl anions that attached on the particles surface.

The role of dopants such as boron and phosphorous on polysilicon polishing has been discussed earlier. The enhancement or hindrance of the removal rate is believed to be due to the effects of dopants on the hydroxyl transportation to the polysilicon surface. In other words, using phosphorous as dopant improves the polish rate by attracting the negative hydroxyl anion, increasing transportation and enhancing the chemical forces of CMP while boron has the opposite effect.

1.3.2 *Mechanical aspects of polysilicon CMP- Tribology*

Mechanical polishing of materials and especially metals has been conducted for many years. The basis of mechanical polishing relies on the mechanical interaction between two surfaces (usually solid) and the generation of a friction force. Harder abrasives and higher friction lead to a faster surface removal while increase the damage to the surface. In CMP, hard abrasives act as the nano-polishers on the wafer surface. In polysilicon polishing, abrasives such as silica help to planarize the surface by forming sub-nano scratches on the surface [6], [32].

Tribology- the science of surfaces- is the science which directly affects the mechanical interactions between surfaces. Tribology is used to explain many industrial applications such as bearings, lubricants and many other functions where the surface interaction is essential. Lubricants are traditionally used to reduce the friction between surfaces and facilitate the movement of two surfaces [33], [34], [35], [36], [37]. In CMP, the pad and the wafer are two engaged surfaces and the slurry between them acts as the lubricant. Determining different lubrication behaviors originated in the nineteenth century with the investigation of hydrodynamic lubrication behavior. The lubrication behavior depends on the coefficient of friction (COF) and operational parameters such as lubricant viscosity, relative speed between the two surfaces, pressure and the lubricant film thickness. The relation between lubrication behavior and above mentioned parameters is given by the Stribeck curve. This curve was first represented by Stribeck in 1902 and relates the COF to a lubricant film parameter which depends on the lubricant film thickness and the surface roughness [32], [33]. The Stribeck curve is usually represented with more practical parameters as shown

schematically in Figure 1-11. The operational parameters which are used in Figure 1-11 are defined as a dimensionless group called the Sommerfeld number, or in some references the Hersey number [3], [33], [38]:

$$S_o = \frac{\omega\mu}{P} \quad (1.2)$$

where ω is the rotational speed (in rpm), μ is the lubricant viscosity and P is the contact load. In CMP, ω is the rotational speed of polish pad and wafer carrier, μ is the slurry viscosity and P is the applied pressure on the wafer. When there is no significant lubricant between two solid surfaces dry lubrication occurs and the simple friction equations are used instead of the Stribeck curve. However in the presence of lubricants, there are three lubrication regimes as illustrated in Figure 1-11. These regions correspond to the thickness of the slurry film between the wafer and the pad [39].

1.3.2.1 Hydrodynamic lubrication: A familiar example of hydrodynamic lubrication and hydroplaning is the rotation of the automobile tires on a rainy road. Since there is no solid contact between the tires and the road and the water performs as a lubricant, increasing the speed can make the car lose control. In CMP when the slurry film thickness is more than the pad asperity height (\sim more than 1μ), the slurry separates the pad and the wafer completely and there is no solid contact between them. Due to the excessive amount of lubricant and no solid contact, the COF value is in a minimum range (usually less than 0.1). This is called the hydrodynamic lubrication regime and the lowest removal rates and surface damage occur when polishing in this lubrication region. Since there is no solid contact in this region the slurry mainly act as the the

chemical agent transporter in the slurry. There is also a very small mechanical polishing effect due to the shear stress from the slurry flow [33], [34].

1.3.2.2 *Mixed lubrication*: When the pressure increases or the velocity and viscosity decrease, the slurry film thickness is expected to reduce and a partial solid contact between the wafer and the pad occurs. This leads to an increase in the solid contact between the wafer and the pad. In the mixed lubrication regime friction is higher than hydrodynamic lubrication; therefore the polish rate is higher. Due to the combination of acceptable polish rate and surface quality, CMP processes mostly occur in this lubrication regime.

1.3.2.3 *Boundary lubrication*: When there is a complete solid-solid contact between the wafer and the pad the COF is usually higher than 0.3 and the surface removal and damage are high. Usually the film thickness in boundary lubrication is below 50nm which is smaller than the pad asperity height [33].

1.3.2.4 *Dry lubrication*: Practically, in this type of lubrication there is no notable lubricant between the surfaces and the film thickness is less than 10nm. Therefore there is complete solid-solid contact between the wafer and the pad and maximum mechanical interactions occur. Dry lubrication shows highest COF (close to 1), polish temperature and polish rates while the surface is strongly susceptible to damage [39]. In addition, the temperature between surfaces is maximized due to high friction force and absence of lubricants which can cool the surfaces.

As discussed earlier, altering the lubrication regime to higher frictional force regions increases the polish rate with the risk of damaging the surface. Thus, depending on the

hardness of the polished material the lubrication regime should be changed. In most cases mixed lubrication is used to control the surface damage while for harder materials such as oxides or ceramics higher friction forces can be used [17].

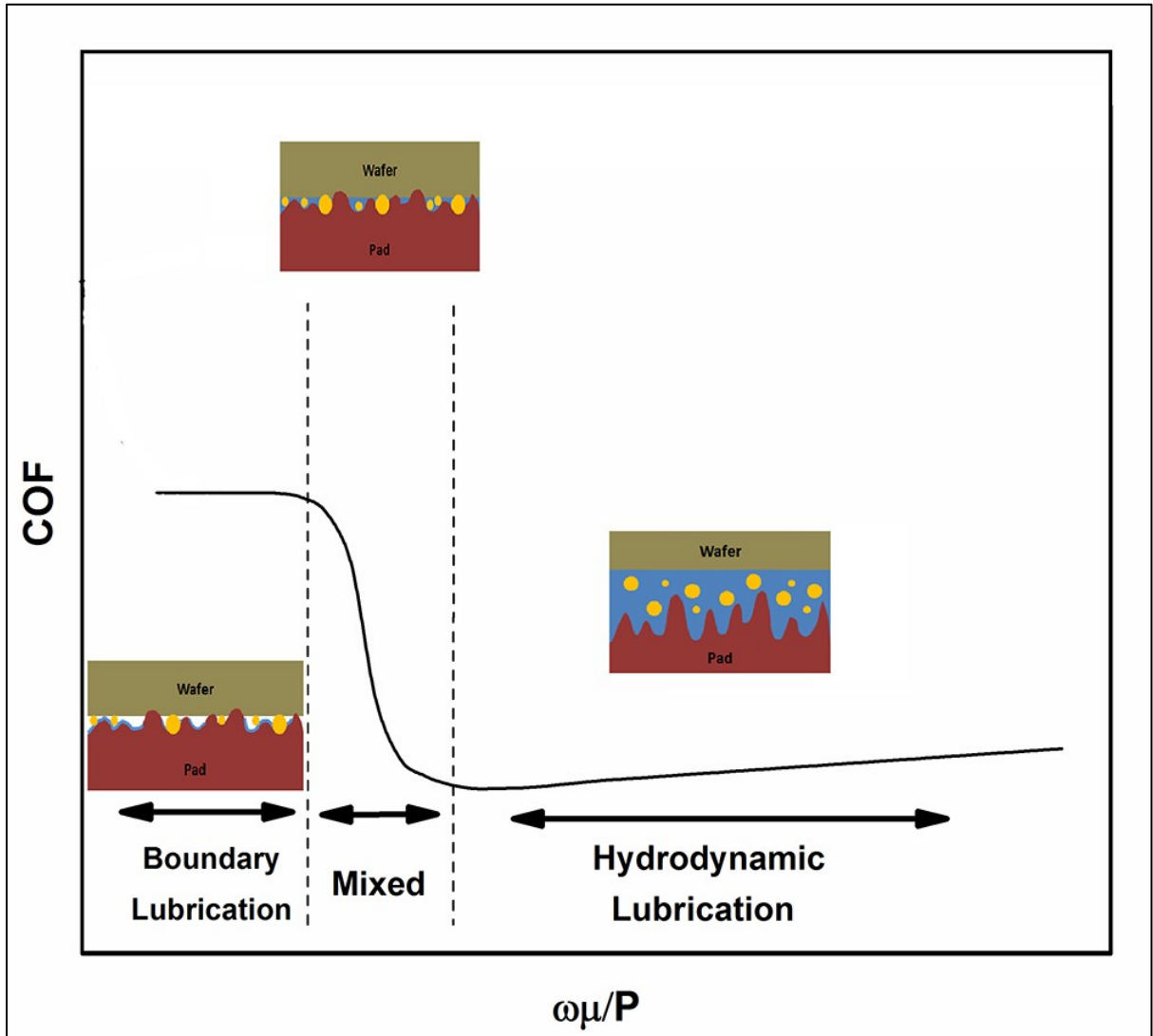


Figure 1-11. Stribeck curve and the relation between polish parameters and the COF.

1.3.3 *Effect of temperature on CMP*

Polish temperature change during CMP is a complicated process. It depends on both the mechanical and chemical forces of CMP. This relation is two-sided which means that while polish temperature is a function of friction, chemical reaction rates increases with temperature as well. In summary, temperature, mechanical and chemical effects are not independent and are strongly coupled [30], [40].

The temperature and generated heat energy between the wafer, slurry and pad strongly impact chemical etching and mechanical abrasion. Chemical etching is influenced by temperature because silicon atomic bonds are weaker and their breakage is easier at higher temperature. Besides, based on Arrhenius equation it is expected to increase the reaction rate by the increase of the temperature. This suggests that chemical etching of the polysilicon surface is strongly enhanced at higher temperatures [41], [42], [43]. On the other hand, polish temperature affects the mechanical forces by changing the pad hardness. In general, increasing the polish temperature reduces the pad hardness and consequently the mechanical interaction between the wafer, abrasives and the pad. Therefore the mechanical forces are expected to reduce at higher polish temperatures [44], [45]. In summary, while chemical etching increases with increasing temperature, the mechanical forces decrease. Depending on the amount of temperature change, the pad properties and the nature of the removal mechanism, a temperature rise can increase or decrease the polish rate.

The polish temperature can change depending on the enthalpy of the chemical reaction. The chemical dissolution of silicon in basic aqueous solutions is known to be

highly exothermic [46], [47]. The generated heat and the amount of local temperature increase depend on many factors such as the pH of the solvent and the slurry flow rate. It is also clear that the mechanical effects and specifically the friction force between the wafer and the pad also affects the polish temperature. High friction force leads to a significant increase in polish temperature.

As explained earlier, both chemical and mechanical forces increase the polish temperature during polysilicon CMP. During polishing the polish temperature increases until a steady state temperature. At steady state the heat generation is balanced by heat losses from slurry flow [48], [49], [50]. Usually polish temperatures of $\sim 40\text{-}50^\circ\text{C}$ are observed in the absence of platen cooling and after reaching the steady temperature.

1.3.4 *CMP models*

Some polish parameters are impossible or difficult to measure during polishing. It can be helpful to predict the polish behavior by understanding the theoretical basis of CMP mechanism. From this need many models have tried to link the process parameters such as pressure and velocity to polish parameters such as removal rate, temperature and slurry film thickness. Some of the most influential CMP models which mainly predict the material removal rate will be discussed here.

In 1927, Preston developed an empirical model which related mechanical forces of polish pressure and velocity to the material removal rate (MRR) [6], [33], [51]. This model was initially developed for glass polishing, however it showed an acceptable fit

for CMP of many materials. In this simple model MRR is a linear function of the pressure and the shear velocity between two surfaces.

$$MRR=KPV \quad (1.3)$$

where P is the actual pressure between the wafer and pad asperities, V is the linear velocity of the rotating wafer relative to the rotating pad and K is known as Preston's coefficient and is associated with the slurry and pad properties. Depending on the nature of the CMP process Preston's coefficient can be a function of pressure and velocity as well [17]. This model also suggests that under static conditions with no pressure or velocity, surface removal does not occur. However, in many cases under static condition chemical etching occurs and the removal rate is not zero [17], [52], thus Preston's equation has to be modified,

$$MRR=KPV + c \quad (1.4)$$

where c relates to the chemical interaction between the wafer and the slurry, regardless of the mechanical forces involved. In general it can be stated that the first term of Equation 1.4 is mainly attributed to the mechanical forces and the second term represents the chemical factors.

The Preston's model fits for systems where materials are removed mostly by abrasion. For more complicated cases, such as metal polishing more complex models have been suggested. Tseng and Wang modified Preston's equation by considering the shear stress of the slurry flow [52], [53], [54]:

$$MRR=MP^{5/6} V^{1/2} \quad (1.5)$$

where M is a constant related to the wafer and slurry properties. In this model the role of pressure is close to the Preston's equation while the velocity has a weaker effect on removal rate.

The above two models are widely used for material removal prediction. However there are many models for specific polish conditions that are more appropriate [55], [56], [57], [58]. Many of these models are based on the Hertzian contact model which predicts the amount of force applied at the wafer surface by a singular abrasive supported by an elastic pad [59], [60], [61], [62].

Another popular CMP modeling hypothesis is based on defining a critical pressure at which the polish rate behavior alters significantly [63], [64], [65], [66]. This model basically suggests that the polish rate variation with pressure is lower when the critical pressure is small. This is due to the lack of solid-solid contact at low pressures. In other words at pressures below the critical pressure the slurry separates the surface of wafer and pad and hydrodynamic lubrication occurs [17].

1.3.5 *CMP processing parts*

In this section, different parts of a CMP tool will be explained briefly. As mentioned earlier the CMP process seems a simple process at first sight but it is complicated due to numerous factors and parts which affect the polish behavior. Each of these parts is required for polishing a wafer and will be discussed below:

1.3.5.1 Wafer carrier

The wafer carrier has a critical role in providing a uniform, smooth surface after polishing. It prevents the wafer slipping out of the carrier due to shear stress between

the wafer and the pad. Controlling polish pressure during polishing is essential for a consistent polish process. The wafer is initially held in the carrier by vacuum at the back of wafer. After the wafer and pad are brought into contact, pneumatic pressure provides the applied force. To improve the uniformity especially at the edge of the wafer, a pneumatic back pressure is usually applied to the wafer [3], [67], [68].

1.3.5.2 Conditioner

The non-uniformity of the polish rate and the polish rate itself can also change depending on the shape of the pad asperities, referred to as the pad condition. Typically the pad condition changes during polishing and the asperities deform plastically and flatten, a phenomena called glazing. This can lead to the material removal rates close to zero. Glazing is shown in Figure 1-12 where the glazing effect can be inhibited by using small diamonds with a pointed shape to return the pad asperities to their initial condition. This pad conditioning process typically occurs simultaneously with polishing. The diamonds can have a regular or irregular pattern [3].

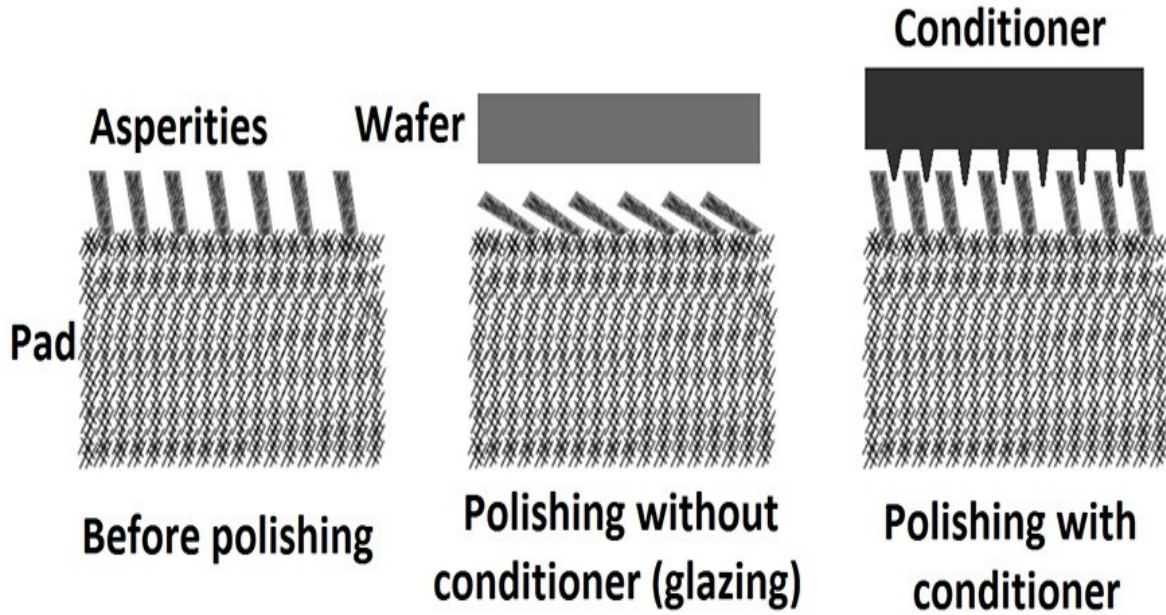


Figure 1-12. Role of conditioner in preventing the pad glazing effect during polishing.

1.3.5.3 Pad

The polish pad is made of elastic materials such as polyurethane polymer with balanced mechanical properties and excellent chemical and thermal stability. The pad structure can be cellular or fibrous as shown in Figure 1-13. Also the pad porosity and thickness can affect the polish behavior significantly [7], [69]. To have better slurry transportation, grooves with different patterns are formed on the surface of the pad. Pads are one of the most expensive CMP consumables and need to be used in optimum condition to reduce fabrication costs.

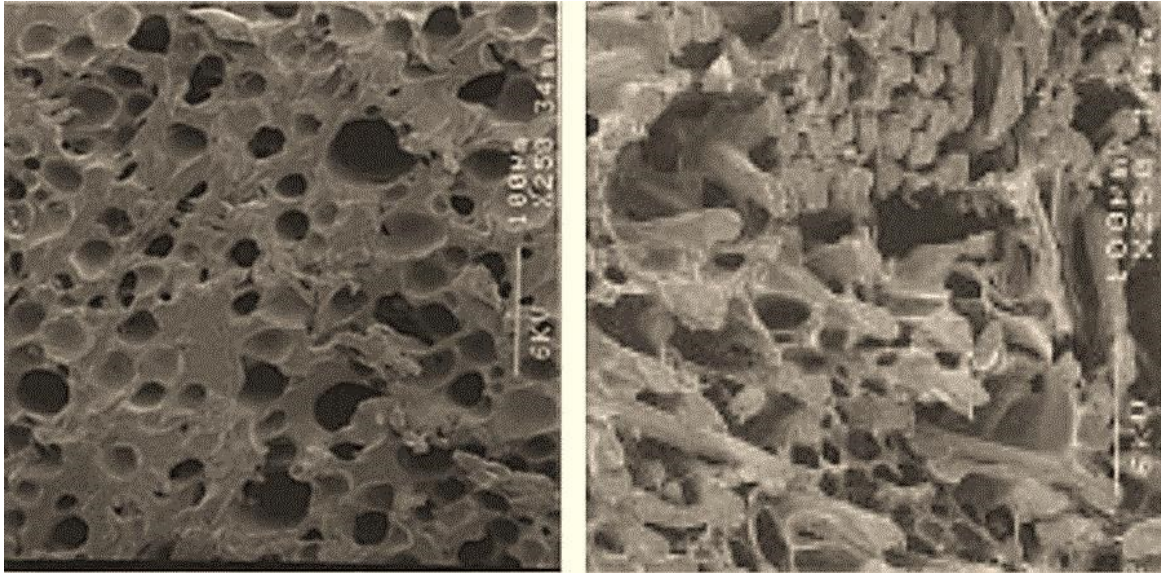


Figure 1-13. SEM micrograph of polymeric pads [70].

1.3.5.4 Slurry

In general the slurry is made of two major components [71], the abrasive and the chemistry. The abrasive is responsible for surface removal and chemical agent transportation. Abrasives are made from different materials and can have different shapes, depending on the wafer material properties such as hardness and zeta potential [72], [73]. Also the abrasive size and concentrations can significantly affect the polish behavior.

The material which is used for mechanical abrasion and its hardness is important for the CMP process. Abrasives usually improve the polish rate by forming sub-nano scratches on the wafer surface. Also they can act as the chemical agent carriers to the surface. To remove the polysilicon surface, the hardness of the abrasive is required to be equal to or higher than the wafer surface. In addition, the zeta potential of the abrasives in the colloid has notable influences on the slurry stability, polish rate and post-CMP cleaning [3], [72]. Due to the price, availability and material properties, the

most common material used for polysilicon polishing is silica. Silica is usually synthesized as fumed or colloidal form [10]. For polishing, colloidal silica is often used due to the large surface area range and stable structure in the solution. It has also been shown that the abrasive size can significantly impact the polish rate. This is attributed to the increase of surface area as the chemical carrier through the surface and the decrease of sub-nano scratch size when smaller particles are used. In addition, using larger abrasives can potentially damage the surface. Hence there is a tradeoff between polish rate and surface quality [72]. The slurry abrasive concentration is another polish parameter that influences the polish behavior and cost. Generally increasing the abrasive concentration raises the polish rate to the level where the wafer surface is saturated with sufficient abrasives then the rate levels off [72], [73].

Chemicals are responsible for the surface reactions such as chemical etching or oxidation. The chemistry of the solution directly depends on the wafer properties. For metals such as copper and tungsten, oxidizers and corrosion inhibitors are added to the solution. While for ceramics such as polysilicon, the solution is simpler and the high pH of the solution plays the key role in the surface etching.

Chapter 2. Experimental procedure

This chapter outlines the techniques used for fabricating, chemical mechanical polishing and characterizing boron-doped polysilicon wafers.

2.1 Wafer fabrication

All experiments were carried out on 6 inch polysilicon wafers. Heavily boron-doped polysilicon films were deposited on 2 μ m thick thermal silicon oxide grown on 6 inch [100] silicon wafers. The films were deposited by low pressure chemical vapor deposition with silane (SiH₄) and boron trichloride (BCl₃) precursors, at 612.5 °C and 675°C temperature and 325 millitorr pressure in the nanoFAB at University of Alberta. The deposition temperature and silane and boron trichloride flow rate were varied to achieve different doping levels and consequently resistivity. The silane and boron trichloride were used in the flow rate range of 87-200 and 10-30 standard cubic centimeters per minute (sccm) respectively. The undoped polysilicon wafer was deposited at 160 sccm silane flow rate. The deposition rate depended on the deposition temperature and showed an average of $\sim 0.5\mu$ /hr. Higher deposition temperature increased the deposition time while worsening of the surface quality was observed.

2.2 Wafer polishing

Polishing was conducted on an Axis 372 M instrument, picture in Figure 2-1. For polishing a polyurethane polishing pad (Nexplanar E7070-30S) was attached to the

polish platen (maximum rotation rate of 175rpm) with pressure sensitive adhesive. The pad contained both concentric and radial pad grooves to aid slurry distribution. To prevent pad glazing a diamond grit conditioner was used during polishing. The conditioner covered the pad surface during polishing by rotating and moving back and forth. A 6 inch wafer carrier (maximum of 125rpm speed and 6psi pressure) was used in this study. During polishing, the slurry was fed on the pad using peristaltic pumps with flow rates from 20 to 500ml/min. There were two pumps installed on the polisher for using *in situ* mixture of slurries. In our study only one of the pumps was used and the slurry was prepared prior to polishing.



Figure 2-1. Axis 372M polisher.

During the polish experiments the polish pressure was varied between 3 and 6psi, the flow rate between 50 and 500ml/min, and the pad rotation rate between 30 and 120rpm. The back pressure was one third of the polish pressure. In this work, the wafer rotation rate and direction were the same as the pad. All polishes were carried out for 1 minute. *In situ* measurement of pad temperature and wafer carrier power current was conducted in all experiments. A summary of the process conditions is given in Table 1 below.

Table 2-1. Summary of process conditions

Process condition	Range
Pressure	3-6 psi
Back pressure	1-2 psi
Slurry flow rate	50-500 ml/min
Pad rotation rate	30-120 rpm
Wafer carrier rotation rate	30-120 rpm

In the course of this work two types of slurry were used. A commercial Fujimi slurry (Planerlite 6103) with high polysilicon polish rates and polysilicon/oxide selectivity as high as 450 was used to study the nature of doping effects and mechanical interactions. The slurry contains 17.3wt% colloidal silica with a bimodal abrasive sizes distribution with peaks at 30-40 and 70-80nm. The slurry has a pH between 11-11.8 and the slurry is suggested to diluted 10:1 with deionized water. The slurry shows high stability with zeta potential of approximately -50mV. The slurry composition is a trade secret and was not disclose us by the vendor. However, it is expected to have organic chemical

additives and buffer compounds to increase the selectivity and to stabilize the pH. In order to study the nature of chemical etching during polishing, colloidal silica abrasives with different particle size and concentration were used. Bindzil 300/30 and 30/50 (Akzo Nobel) were used to study the silica size on polishing. The first number of the colloidal silica solution indicates the surface area of abrasives in m²/g and second number is the abrasive concentration. The slurry pH was controlled by adding KOH to increase and citric acid (C₆H₈O₇) to decrease the pH of the solution. In order to confirm the colloid stability and the abrasive size, the particle size and zeta potential of these slurries have been explored.

2.3 Polish measurements

2.3.1 Pad and wafer rotational velocity

The relative linear velocity between the wafer and the pad is a function of wafer carrier and pad speed and the offset between their centers. In our experiments, the pad and wafer were rotating at same rpm and in the same direction. The relative velocity of point A shown in Figure 2-2 on the wafer surface with respect to the pad can be calculated using the following equations:

$$\overrightarrow{V_{P/W}} = \overrightarrow{V_P} - \overrightarrow{V_W} \quad (2.1)$$

$$\overrightarrow{V_P} = \overrightarrow{\omega_P} \times \vec{e} \quad , \quad \overrightarrow{V_W} = \overrightarrow{\omega_P} \times \vec{r} - \overrightarrow{\omega_W} \times \vec{r} \quad (2.2)$$

$$\overrightarrow{V_{P/W}} = \overrightarrow{\omega_P} \times \vec{e} + (\overrightarrow{\omega_P} - \overrightarrow{\omega_W}) \times \vec{r} \quad (2.3)$$

where $\overrightarrow{V_{P/W}}$ is the relative velocity, $\overrightarrow{V_P}$ and $\overrightarrow{V_W}$ are the linear velocities of pad and wafer (m/s) and $\overrightarrow{\omega_P}$ and $\overrightarrow{\omega_W}$ are rotational speeds of pad and wafer respectively

(rad/s). If the wafer and the pad have the same rotational speed, the second term of Equation 2.3 is zero and the relative velocity will be the same for any position on the wafer surface. Thus, the relative velocity between the wafer and the pad is constant at all points across the wafer surface if they have the same rpm [74], [75], [76]. This indicates that in our experiments, the relative velocity on the wafer surface with respect to the pad is a function of offset between the pad and the wafer surface and the rotational speed. The offset oscillated between 0.15-0.19 m with a speed of 7mm/s during polishing. Therefore the relative velocity changed during polishing on the wafer surface. The average center position of 0.17m was used to report the mean velocity. The pad diameter was 0.5m.

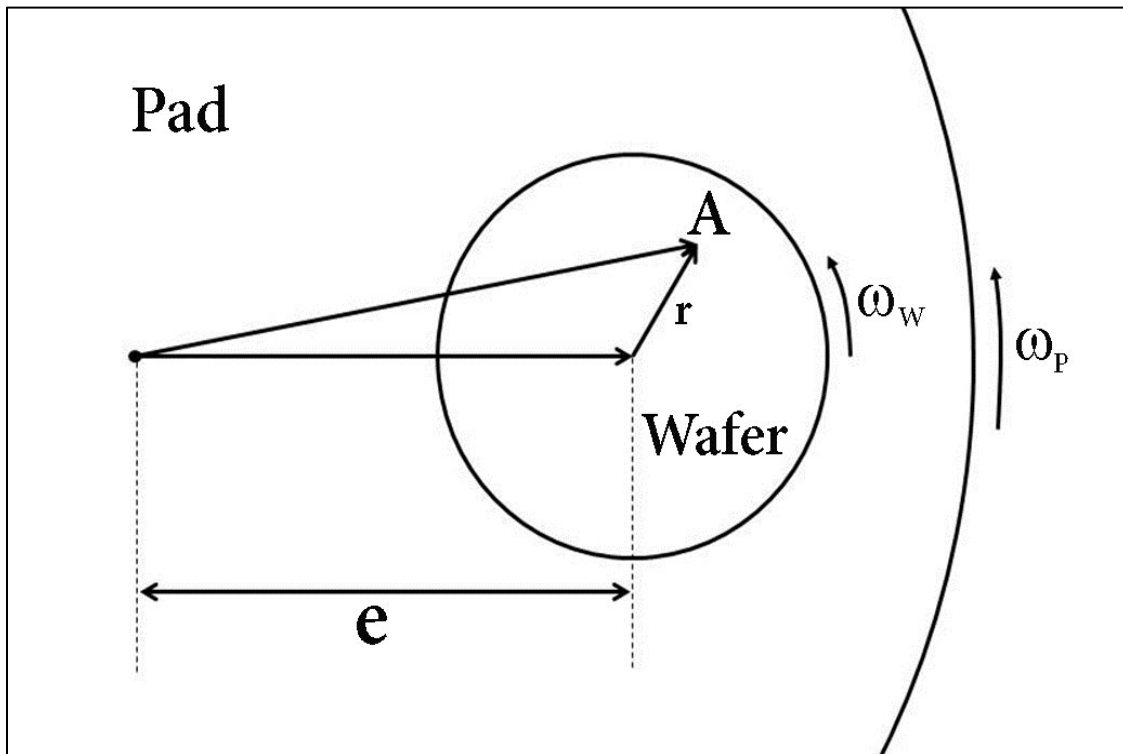


Figure 2-2. Relative velocity of point A on the rotating wafer with respect to the rotating pad.

2.3.2 Friction force

To investigate the mechanical components involved in CMP, measuring the friction force between the wafer and the pad during polishing is essential. A few methods have been published to quantify the friction force *in situ* [77], [78]. One common technique is to measure the lateral force applied on the carrier [35], [79]. This relies on the fact that friction force is equal and in the opposite direction of lateral force and linear relative velocity as shown schematically in Figure 2-3. In this process the lateral force in the relative velocity direction and is measured with a strain gauge to measure the lateral force and displacement. The results are then transferred to a data acquisition system by a force transducer. For larger polish tools such as the one used in this work, this approach is not practicable. In this case friction force can be obtained indirectly by methods such as measuring the platen and/or the carrier motor current and the power. It has been shown that the platen and the carrier current are functions of friction force [80], [81], [82].

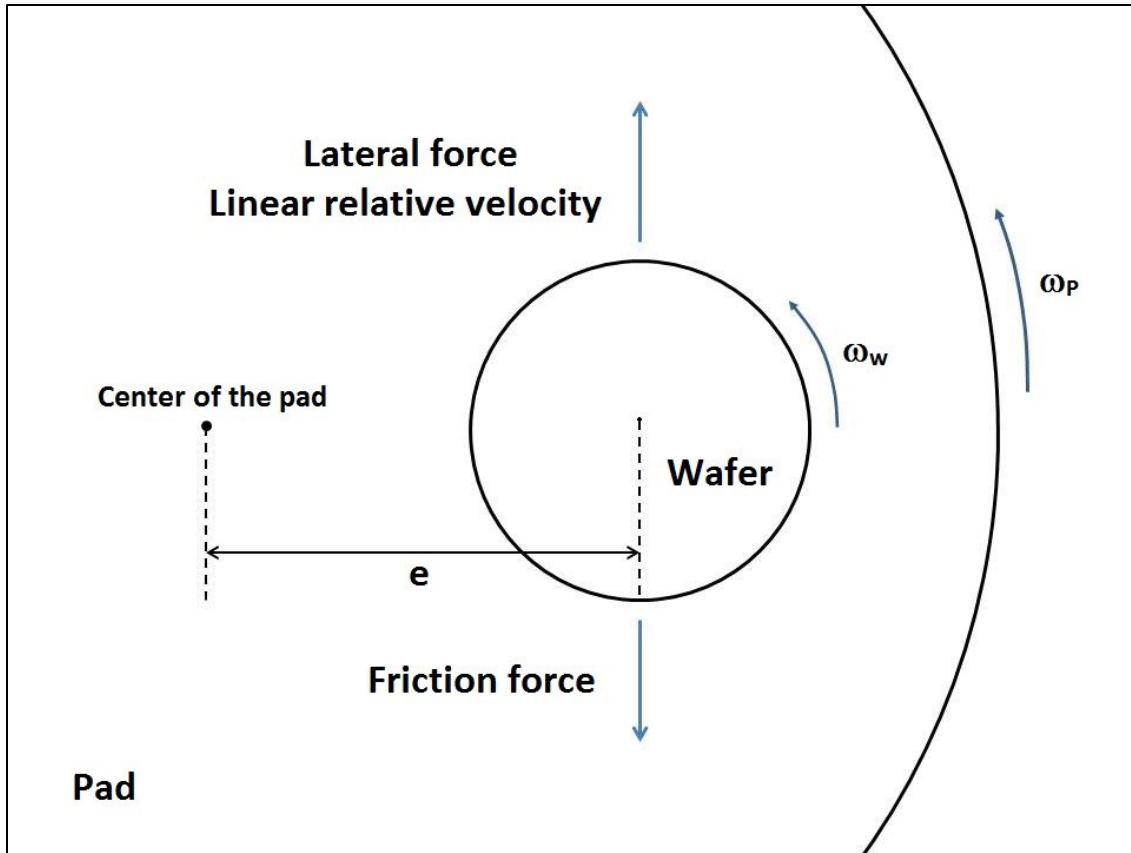


Figure 2-3. Direction of lateral force, linear velocity and friction force of the wafer when pad and carrier have the same speed.

In this work and on the Axis 372M tool, the friction force measurement was achieved by measuring the current via the motor power of the wafer carrier. In general friction tends to promote the rotation of the carrier; therefore less supply power is needed to rotate the carrier in the presence of friction. To quantify this, the carrier power is measured when the carrier raise off the pad (disengaged) and when the carrier and pad are in contact (engaged). Polishing occurs is the engaged condition. Since the speed is set during polishing, the motor has a feedback loop in order to keep the speed constant by reducing or increasing the power. The feedback loop incorporates a 10A shunt resistor and a voltage range of 0- 100mV. An acquisition system was designed by the

Department of Chemical and Materials Engineering instrument shop to record this voltage and the current drawn by the motor. Since the pad and the wafer rotate in the same direction, the friction force between the wafer and the pad helps the carrier to move and reduces the power required by the motor to maintain the set speed. Hence, the motor power difference between the engaged and disengaged conditions can be related to the friction force between the wafer and the pad. This relation can be represented by:

$$P=Vi=\omega T \quad (2.4)$$

where P is the motor power required to rotate the wafer, V is the motor voltage (set as 90V for all polishes as specified by the manufacturer), i is the motor current measured *in situ*, ω is the carrier rotational speed and T is the produced torque. By measuring the motor current and knowing the rotational speed the torque can be calculated. The friction can be calculated by collecting the difference of disengaged and engaged power and torque:

$$P_{eng}=Vi_{eng}=\omega_{eng}T_{eng} \quad , \quad P_{dis}=Vi_{dis}=\omega_{dis}T_{dis} \quad (2.5)$$

$$\Delta T=T_{dis}-T_{eng}=V\left(\frac{i_{dis}}{\omega_{dis}}-\frac{i_{eng}}{\omega_{eng}}\right) \quad (2.6)$$

where P_{eng} , i_{eng} , ω_{eng} and T_{eng} are the power, current, rotational speed and torque of the engaged case, and P_{dis} , i_{dis} , ω_{dis} and T_{dis} are the power, current, rotational speed and torque of the disengaged case respectively. Eventually the friction force between the wafer and the pad can be calculated by:

$$F = \frac{\Delta T}{e} \quad (2.7)$$

where e is the eccentricity which is the offset distance between the center of the pad and the carrier (which is 0.17m in our experiments as mentioned before).

In Equations 2.5 and 2.6, ω_{dis} is the equivalent rotational speed during polishing and needs to be calculated separately. As the friction force assists the wafer rotation, the current at engaged case is less than disengaged case. Thus, the carrier motor current was measured during polishing (engaged) and before polishing (disengaged) separately. To do this for the disengaged case, the current was recorded for 10 speeds (30-120rpm, 30 seconds each) and the polynomial relation between the current and rotational speed was extracted. This was used to calculate the equivalent rotational speed at which the carrier would rotate if powered with the same current of the disengaged case. Finally, the root mean square average values of the currents (i_{eng} , i_{dis}) were calculated by the LabView software.

The carrier motor is a DC electric permanent magnet motor with a constant operating voltage of 90V (Leesonr model number C42D17FK7), connected to the carrier shaft by a gearbox (MorseLeesonr model number 18SF15) that reduces its output speed by a factor of 15. In order to measure the torque, the gearbox ratio was also included in Equation 2.6.

2.3.3 Polish temperature

As mentioned before polish temperature significantly influences the polish behavior. In this study the polish temperature was defined as the maximum temperature of the

pad after one minute of polishing. The pad temperature was measured *in-situ* by pointing an IR-gun thermometer at the surface of the pad and close to the wafer carrier during polishing and at one minute of polishing.

2.4 Wafer characterization

To study the wafer properties and material removal rate, different material and electrical characterization techniques were used.

2.4.1 Film conductivity

Measuring the wafer sheet resistance is required in order to calculate the film resistivity and conductive boron-doped polysilicon film thickness (if the resistivity is known). Sheet resistance measurement is a non-destructive method of measuring conductive film thicknesses. After measuring the film resistivity as an intrinsic material property, the thickness of the wafer could be simply measured by:

$$\rho=R.t \quad (2.8)$$

where ρ is the film resistivity, R is the sheet resistance and t is the film thickness. In general, by measuring the film thickness and resistance of one wafer, the resistivity can be measured. Therefore, the film thickness of other samples can be measured indirectly by measuring R . A 4-point probe was used to measure the sheet resistance of the wafer, the film thickness before and after polishing and study the conductivity of the deposited film. In the 4-point probe technique a constant current is applied across two outer electrodes and the voltage is measured across two inner electrodes, hence there are four point in contact with the surface of the conductive material [83]. The

probe measures the sheet resistance following this relationship when the film thickness is negligible compared to sheet area:

$$R = \frac{V}{I} \frac{\pi}{\ln(2)} \quad (2.9)$$

where V and I are measured voltage and applied constant current. The term $\frac{\pi}{\ln(2)}$ is the correction factor that shows that the film is not infinite. All the measurements in this work were accomplished using either a Jandel probe with a Keithley Sourcemeter (model 2400), or a Veeco (model FPP-5000) probe, both with probe spacings of 1mm. The sheet resistance of the wafers was measured at 13 points of each wafer with 5mm distance and 45° rotation as shown in Figure 2-4. The probe was placed manually on the wafer and all the tested points were far enough from the edges to prevent measurement inaccuracy.

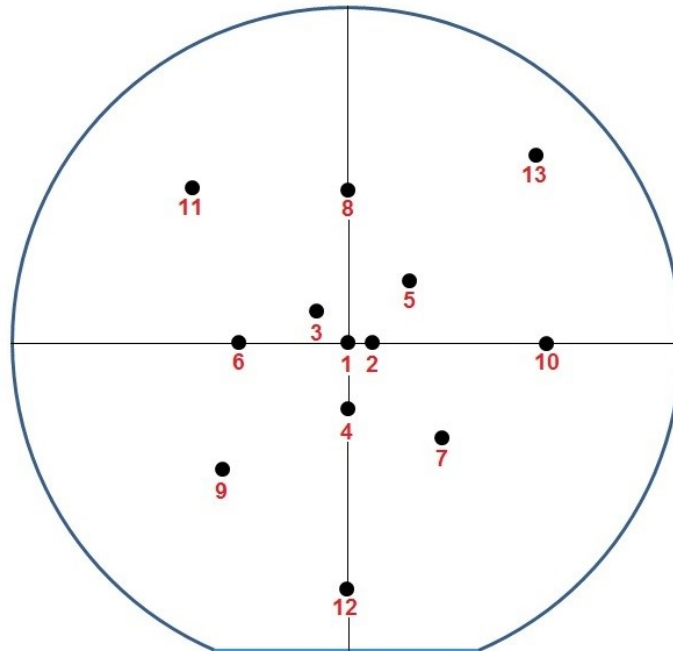


Figure 2-4. Schematic of the 13 points measurement with 4-point probe.

2.4.2 Film thickness

A Filmetrics dielectric thickness mapping system was used to measure the film thickness non-destructively. In this technique a light is reflected through the wafer surface over a range of wavelengths. By knowing the refractive index of the tested material and the reflected wavelengths, the film thickness can be calculated. Scanning electron microscopy (SEM) was also used to measure the film thickness measuring the cross sectional thickness of a wafer that had been cleaved through the wafer center. SEM was used on a few wafers to confirm the Filmetrics results and examine the microstructure of the doped polysilicon. An example of the SEM image, taken in the secondary electron mode, is shown in Figure 2-5 where the conductive boron-doped polysilicon is deposited on the $2\mu\text{m}$ silicon dioxide and the bottom layer is the single crystal silicon substrate.

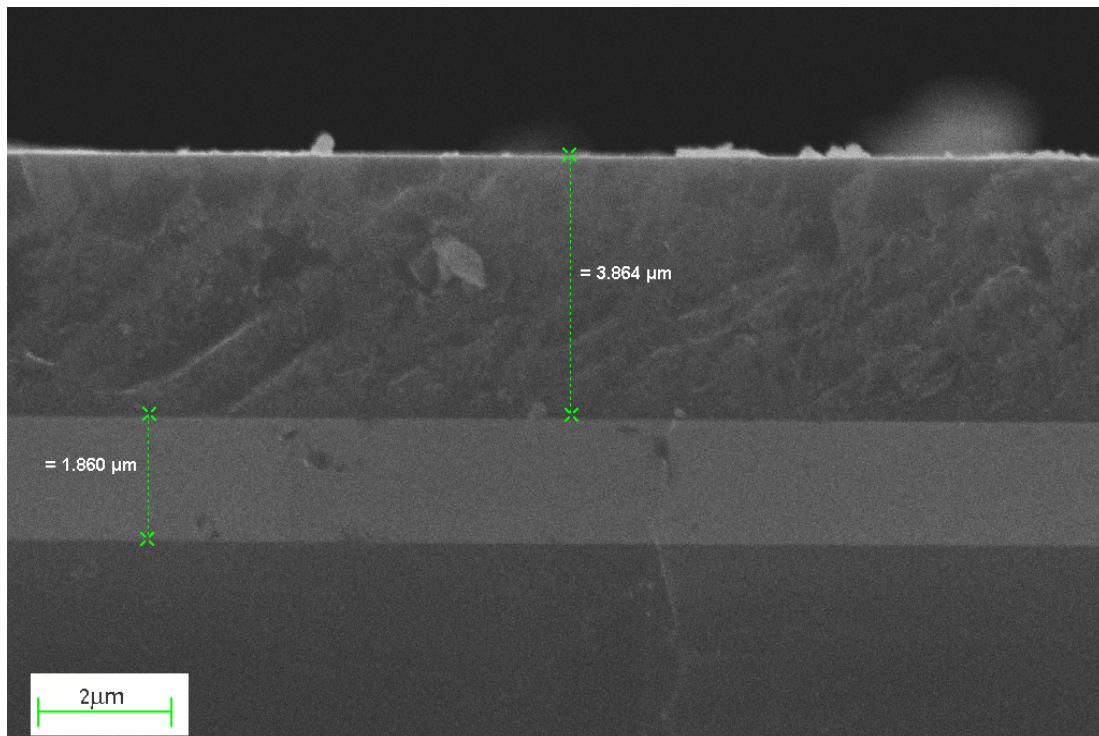


Figure 2-5. Cross-sectional SEM micrograph of wafers. The top layer is boron-doped polysilicon, second one is thermal oxide film and the bottom layer is single crystal silicon.

2.4.3 Surface characterization

In order to study the surface topography before and after polishing, atomic force microscopy (AFM) was used. AFM (Veeco Dimension 3100 AFM) was carried out using the tapping mode at 0.8 Hz frequency with a scan area of $1\mu\text{m}^2$. The surface quality was reported by measuring the roughness of six areas on the wafer surface and averaging them. Arithmetic average value (R_a) and root mean square (R_q) were used to calculate the surface roughness:

$$R_a = \frac{1}{n} \sum_{i=1}^n |Z| \quad (2.10)$$

$$R_q = \sqrt{\frac{1}{n} \sum_{i=1}^n Z^2} \quad (2.11)$$

where n is the number of points scanned on each surface and Z is the distance of each point from the center line. R_q is most widely used for 2-dimensional and R_a for 1-dimensional measurements. The surface roughness is expected to decrease considerably after polishing.

2.4.4 Dopant concentration

The chemical concentration and the concentration depth profile of boron dopant were analyzed by secondary ion mass spectrometry (SIMS). In this method the thin film surface is bombarded by ion beam and the ejected secondary ion masses are analyzed by a mass spectrometer. In our study the SIMS analysis was carried out on one sample of each LPCVD condition and on each thin film resistivity.

2.4.4.1 *Hole carrier concentration*

Normally not all dopants are activated after deposition. This can be due to the precipitation of dopants at grain boundaries or placement of boron atoms in interstitial sites instead of substitutional sites in the Si crystal structure [84]. The hole concentration in boron doped polysilicon is equal to the activated boron concentration, since each activated boron donates one hole to the silicon lattice. SIMS measures the chemical (total) concentration of boron in the Si lattice, while electrical measurements such as resistivity measure the activated boron concentration. Concentration depth profile of activated boron was measured using spreading resistance profiling (SRP). SRP was carried out on one sample of each LPCVD condition. In this method the resistance between two probes with distances below 50 μm on the thin film surface is measured. The thin film surface will be beveled in a shallow angle with respect to the film surface to accomplish the depth profiling. The probes are then moved to the next location where the measurement corresponds to a deeper layer of the sample [85].

2.5 Slurry characterization

To study the effect of slurry chemistry on polish rate, both slurry and abrasive properties were investigated. The average particle size was measured using a Brookhaven ZetaPALS instrument that based on dynamic light scattering (DLS). The refractive index of silica is 1.45. In the DLS technique the particles are suspended and a laser beam is passed through the solution. The beam is then diffracted and forms patterned rings with respect to the size of particles. In general larger particles form rings with stronger intensity and wider angle. Transmission electron microscope

(TEM) was also used to get a direct measurement of particle size. A JEOL 2010 TEM, with a LaB6 electron gun) was used to image the abrasives. The samples were prepared by placing a small diluted silica colloid (20:1) on a 200 mesh size copper grid.

Zeta potential measurements (Brookhaven ZetaPALS) was used to measure the charge on the abrasive particles. Particle zeta potential and surface charge is calculated by measuring the electrophoretic mobility of particles in an electric field applied in the solution. This charge is critical to determine if the slurry is stable enough.

Increasing the slurry pH accelerates the dissolution of the silica abrasives. The dissolution rate was studied by measuring the dissolved silicon atoms in the solution. In order to measure the dissolved atoms, abrasives were separated from the solution using a Beckman Coulter centrifuge (Avanti J-30I) for 2hrs and 5000rpm. After separating the abrasives from the solution, the clear solution was analyzed by atomic absorption spectroscopy (AAS).

Chapter 3. Lubrication behavior of boron doped polysilicon

This chapter is based on the H. Pirayesh and K. Cadien paper published in ECS journal of Solid State Science and Technology [17].

The tribology of polishing has been studied and it has been shown that mechanical interaction between the wafer, slurry and pad can significantly influence the polish rate [86], [87]. Increasing the friction and mechanical forces aid the wafer surface removal rate due to abrasion and buffing of the surface via solid contact between the wafer, pad and abrasives. In this chapter the lubrication behavior of boron-doped polysilicon CMP is investigated. Friction forces are compared to clarify the lubrication regimes and then surface quality of polished wafers under different lubrication regimes will be studied. All wafers used in this study have a resistivity of 3.5m Ω .cm. The commercial Fujimi slurry (Planerlite 6103) was consumed for all experiments.

3.1 Polish rate study

Changing the polish parameters such as pressure and velocity affects the polish properties and the polish rate. The relation between the polish rate and PV product is expected to be linear as suggested by Preston's equation. The removal rate results are illustrated in Figure 3-1 and Figure 3-2 where the removal rate is shown as function of the pressure and velocity product for three different slurry flow rates (100, 200, and 350 ml/min). The slope of the curves (Preston's constant) is related to the polish parameters such as the slurry chemistry, the abrasive size and composition, and the

pad properties. Higher slopes mean that these polish parameters have a greater effect on the polish rate. Preston's constants for different polish regimes are shown in Table 3-1. By comparing the Preston's constants it is evident that highest K values were achieved at high pressure and low flow rates while the lowest Preston's constant was measured for the highest polish velocity and the lowest pressure cases where hydroplaning is expected to happen. During polishing at low pressure (3psi), PV has a smaller effect on the polish rate than at higher pressures, 4.5 and 6 psi. This behavior can also be related to the lubrication regimes. Lower dependency of the removal rate on PV at lower pressures is attributed to the fact that at this pressure there is no solid contact between the wafer pad/abrasives and therefore the polish rate is minimized. At high values of PV , 110rpm, and high flow rates (negative slopes in Figure 3-1 and Figure 3-2), a removal rate reduction was observed depending on the polish pressure and slurry flow rate. This is due to the changing lubrication regime at higher velocities, according to the Stribeck curve. This effect is more evident at higher flow rates since there a slurry film between the pad and the wafer causing hydroplaning to occur. At 100ml/min flow rate and high pressures this effect was not observed because there was no enough slurry at high velocities to cause hydroplaning. Unlike Preston's equation, the intercept values of the curves shown in Figure 3-2 are greater than zero; which means that at zero pressure or velocity polishing still occurs. This can be explained by the chemical static etching of the silicon at high PH values[3], [10], [66]. The intercept for all the experiments is in the range of 0.1-0.2 μ /min which is close to the silicon etch rate at room temperature at pH=11.4 [43], [88].

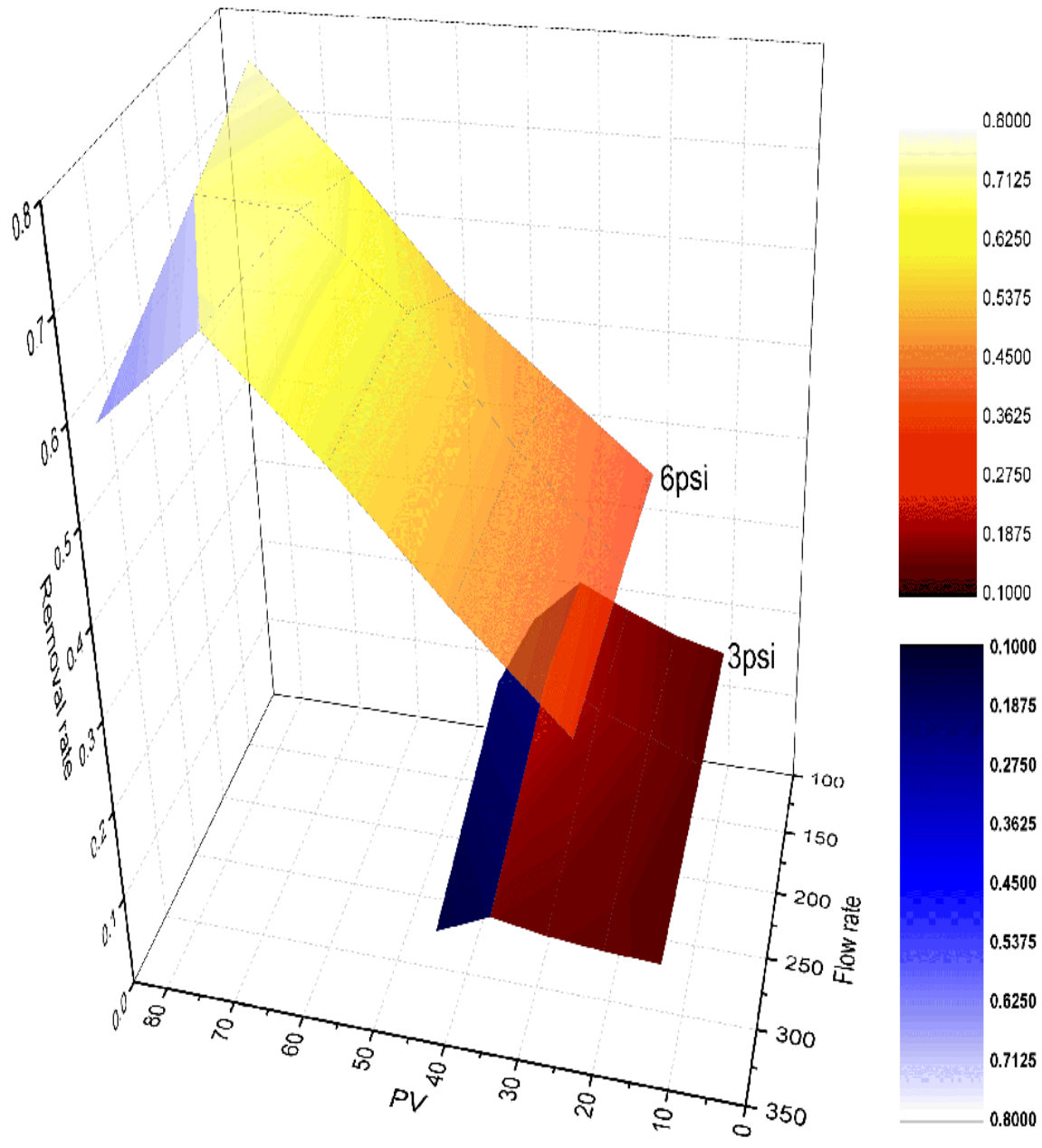


Figure 3-1. Polish rate as a function of PV and flow rate. The negative slope of the graph is due to hydroplaning at high polish velocities. The 4.5 psi polish data is not shown for clarity.

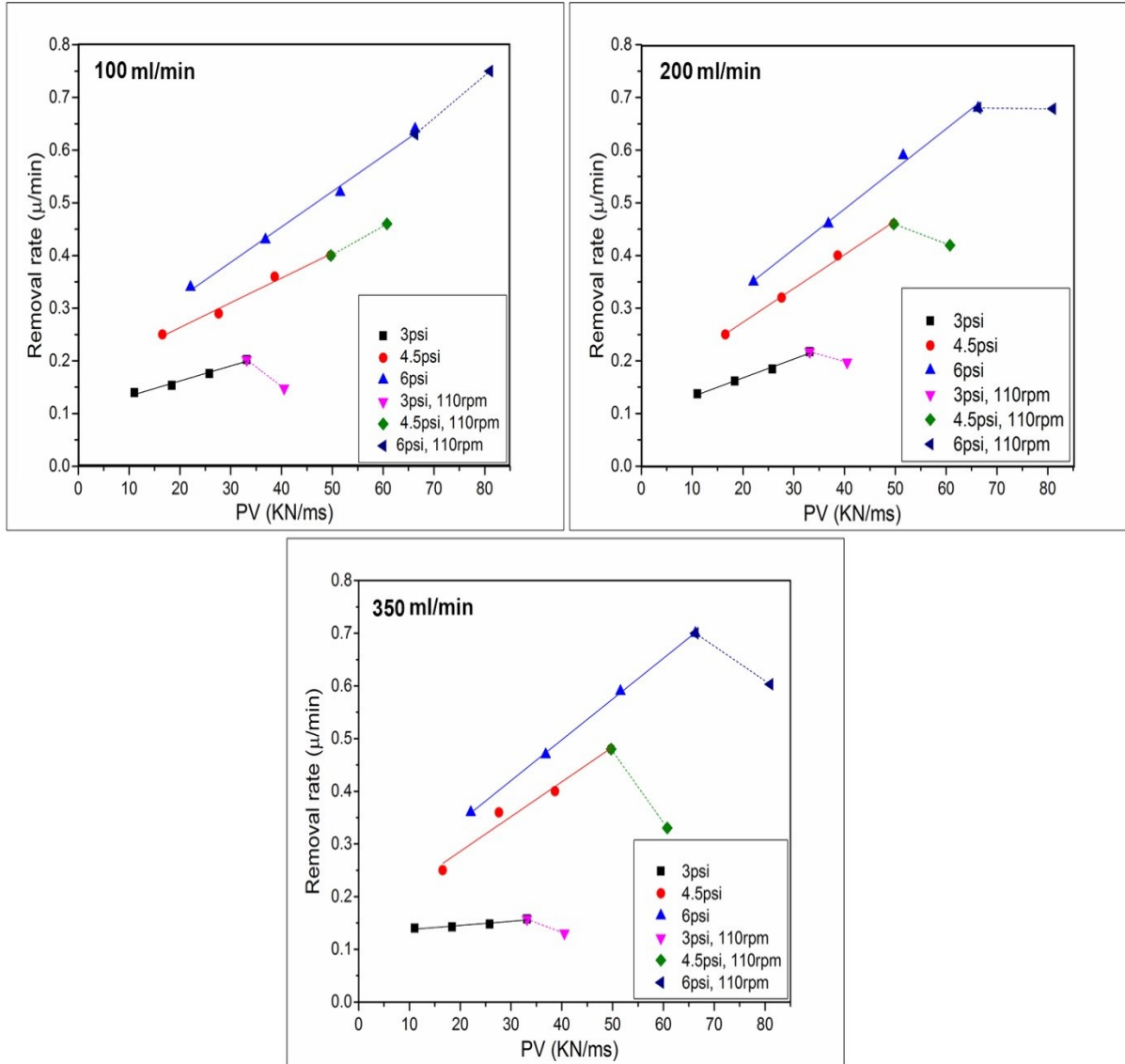


Figure 3-2. Relationship of removal rate to the pressure velocity product at different flow rates for highly boron doped wafers. The dashed lines represent the hydrodynamic lubrication with reducing the polish rate.

The optimum polish rate is achieved at 200ml/min slurry flow rate. Increasing the flow rate to 350ml/min did not show a significant change in the polish rate. This can be explained by comparing the dependency of chemical and mechanical forces on the flow rate. In polysilicon polishing, hydroxyl anions in the solution play a major role in chemical etching of the surface [20]. A high pH slurry is required to complete the

chemical reactions on the wafer surface. Increasing the slurry flow increases the number of hydroxyl ions on the pad and therefore the polish rate is expected to increase. However, the increase of the flow rate to the optimum value (~200ml/min) means that the wafer surface is saturated with the required chemical agents and the dissolution of silicon and reduction of hydroxyls in the form of silicic acid are in equilibrium. Polishing with higher flow rates (350 ml/min) does not change the chemical component of the polish rate since it was saturated at 200 ml/min[19], [89]. In addition, increasing the flow rate to 350ml/min diminishes the mechanical forces by flooding the pad and thereby reducing the friction and increasing the role of lubrication. On the other hand, at 100ml/min flow rate the chemical factors (hydroxyl anions) are not abundant enough to maximize the polish rate while the friction force is expected to increase due to more contact between the wafer and the pad/abrasives (Figure 3-3).

Table 3-1. Preston’s coefficient for various polish conditions.

	Flow rate (ml/min)	Preston’s coefficient (K) at low and moderate velocities	Preston’s coefficient (K) at high velocities
3psi	100	0.0029	-0.0074
	200	0.0036	-0.0027
	350	0.0008	-0.0037
4.5psi	100	0.0047	0.0054
	200	0.0064	-0.0036
	350	0.0066	-0.0136
6psi	100	0.0067	0.0075
	200	0.0064	0.0001
	350	0.0077	-0.0066

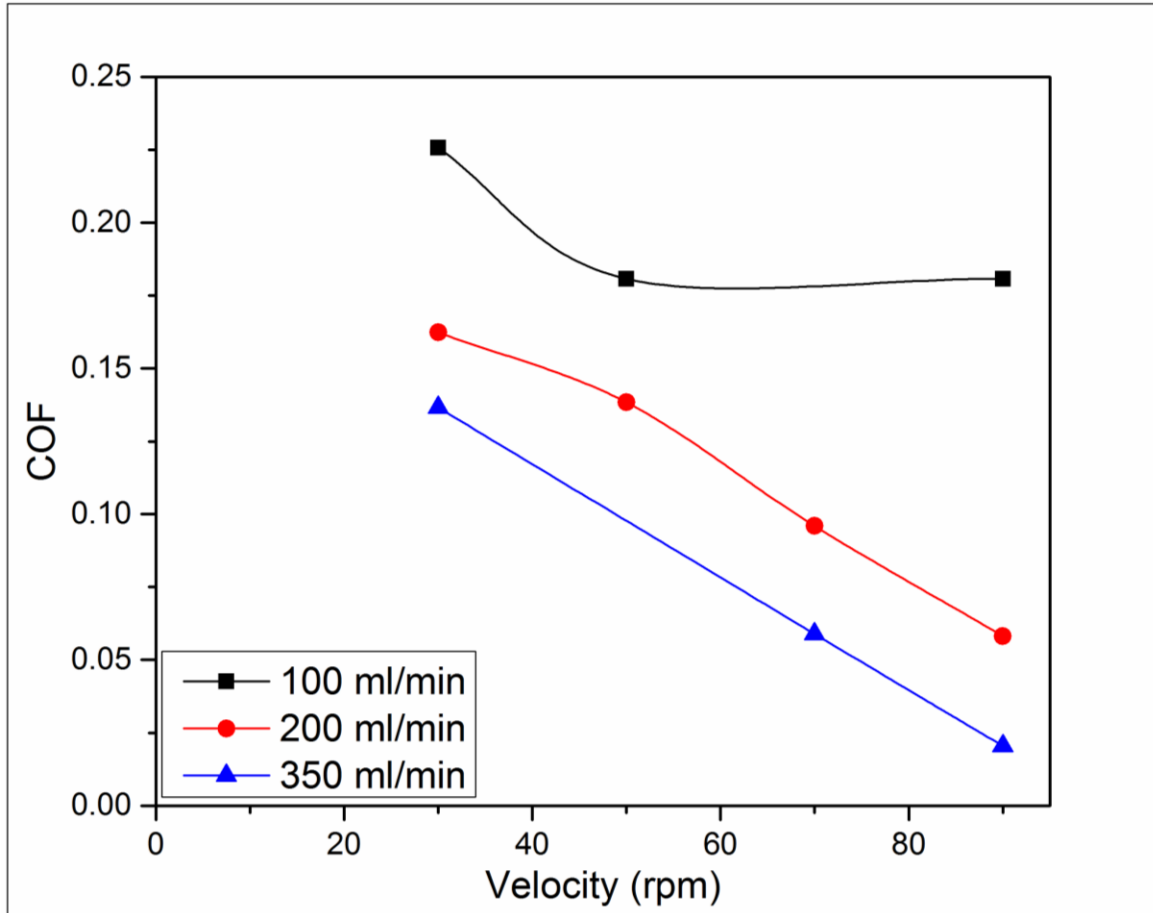


Figure 3-3. COF as function of velocity for low polish pressure (3psi), hydrodynamic lubrication regime.

There have been different models proposed to relate the polish rate to the polish parameters such as pressure, velocity and slurry chemistry. For silicon polishing, Preston's equation fits the experimental results the best[51]. However, operating in different lubrication regimes can affect polish behavior. As mentioned earlier, comparing the COF and the polish rate at different polish conditions showed that three lubrication regimes and therefore polish behaviors are observed. The polish behavior under each of these lubrication regimes is discussed below.

Case 1: Hydrodynamic to partial lubrication (3psi pressure)

In this regime solid contact does not occur between the wafer and the pad, and the slurry forms a thick boundary ($\sim 50\mu$) between the surfaces which reduces the friction force significantly[3], [33]. If the slurry thickness is greater than the maximum pad asperity height then polishing occurs in the hydrodynamic lubrication regime. From the Stribeck curve, it is clear that reducing the pressure and increasing the velocity decreases friction[34]. The variation of the coefficient of friction with velocity at low polish pressures is shown in Figure 3-3. Generally the COF value in the hydrodynamic lubrication regime is expected to be below 0.1[77], which agrees with our experimental results.

The critical pressure, P_c , is the pressure below which the lubrication regime changes from boundary to hydrodynamic. It has been shown that below P_c there is minimum contact of pad and wafer. However, there have been only a few studies focusing on value of P_c [66]. In our study the P_c is between 3psi and 4.5psi as shown in Figure 3-2.

Due to the nature of the tribology in hydrodynamic regime the mechanical component of the polish rate is minimal and the chemical component and the fluid shear stress have the dominant role in determining the polish rate[90]. Only minor surface polish occurs by hydrodynamic lubrication because polishing occurs mainly due to solid-solid contact[61], [91]. This leads to a minor dependency of the polish rate on mechanical factors such as pressure and velocity with the resulting much lower Preston's constant compared with the higher polish pressures (4.5 and 6 psi).

Comparing the slope of the 3psi polish pressure curves (Preston's constant) in Table 3-1 agrees with the hypothesized optimum polish flow rate discussed earlier and shows that the highest dependency is achieved at 200ml/min flow rate. At 200ml/min a change in PV has more effect on the polish rate which suggests the importance of other polish factors at the optimum flow rate. At 350ml/min flow rate hydroplaning is more evident and the slope is at a minimum.

Case 2: Partial to boundary lubrication (4.5, 6 psi) at low and moderate velocities

In most CMP applications polishing occurs at pressures higher than P_c and in the boundary or partial lubrication regime where the polish rate is higher due to the higher friction and mechanical forces [33], [92]. In this lubrication regime there is a solid-solid contact between the wafer, pad and abrasives which enables removal from the wafer surface by increasing the friction force and providing nano scratches on the surface. The film thickness in this lubrication regime is expected to be less than in the hydrodynamic region and less than the pad asperity height. Due to the solid-solid contact the polished surface is susceptible to surface damage [34]. Therefore, there is a tradeoff between the low polish rate but good surface quality of hydrodynamic lubrication and the high polish rate and poor surface quality of the boundary lubrication. Comparison of the slope of the 4.5psi and 6psi at each flow rate in Table 3-1 shows that the slope is slightly increased at 6psi. This suggests that the polish rate and the Preston's constant depends more on the pressure than the velocity. By increasing the pressure from 4.5psi to 6psi, it is expected to change the lubrication regime from mixed lubrication to boundary lubrication.

The COF values of high and low flow rates at high polish pressure are shown in Figure 3-4 as an example. At low flow rates the COF value is >0.25 which is higher than other polish experiments. This is explained by the Stribeck curve where the lower velocities keep the polish process completely in the boundary lubrication regime.

Comparison of the slopes on the three flow rate curves in Figure 3-1 and Figure 3-2 shows that the slope and the removal rate did not change significantly by increasing the flow rate from 200ml/min to 350ml/min, similar to what happened 3psi pressure. Higher flow rates reduce the mechanical forces and lower flow rates reduce the chemical activity leading to the highest Preston's constant being achieved at 200ml/min.

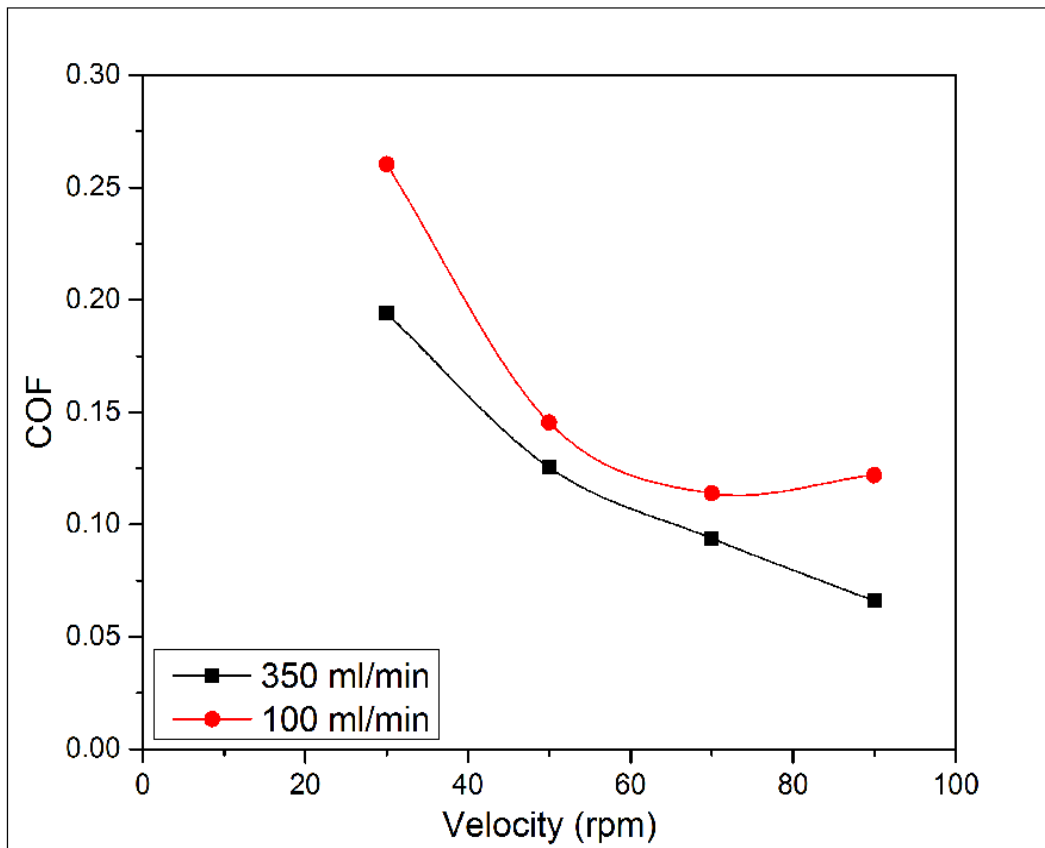


Figure 3-4. COF as function of velocity for high polish pressure (6psi), boundary lubrication regime.

Case 3: Hydrodynamic lubrication at high flow rates and dry lubrication at low flow rates for the high velocity (110 rpm)

From the Stribeck curve it can be understood that hydroplaning occurs even at high pressures if the velocity is high enough. In this study, at high velocities, such as 110 rpm, the polish rate does not follow the linear relationship discussed earlier and the polish rate decreases. The relation between removal rate and PV at 110rpm is shown by blue color surfaces in Figure 2 and by dashed lines in Figure 3 where the slope of the curve is negative. It is clear that there is a slope change in the graphs by increasing the velocity and the slope change also varies with the flow rate. At 100 ml/min and high PV , the removal rate and Preston's constant is higher at 110 rpm. This can be explained by considering the fact that at extremely high velocities and low flow rates the lubrication regime varies from the boundary lubrication to the dry lubrication regime[39]. This occurs because at high velocity and low flow rates there is not enough slurry to cover the interface between the wafer and the pad. There is contact between the pad asperities and the wafer. The highest polish rates were achieved in this lubrication regime. At higher flow rates, such as 200 and 350 ml/min, a removal rate drop can be observed in Figure 3. At higher flow rates there is sufficient slurry and higher polish velocities changes the lubrication regime to the hydrodynamic regime. As discussed earlier, polishing in the hydrodynamic lubrication region reduces the polish rate due to the lack of solid-solid contact between the wafer and the pad. This effect is more evident at 350 ml/min flow rate than at 200 ml/min and at 3psi than at higher pressures, as expected. Comparison of polish rate results at different conditions, leads to the observation that increasing the flow rate and the velocity do not necessarily increase the removal rate. The key factors that control the polish rate

are (a) increasing the friction force (and down force), (b) staying in the boundary lubrication regime, and (c) using sufficient slurry to saturate the chemical reactions.

From the above discussion a diagram of the lubrication regime versus the COF can be estimated. The suggested lubrication regimes for polishing conditions is shown in Figure 3-5, where hydrodynamic lubrication is expected to be the dominant lubrication regime at high flow rates and low PV . Increasing the PV and reducing the flow rate results in a change in the lubrication behavior to the mixed and boundary lubrication regime. At high PV and low flow rates dry lubrication was observed which leads to an increase of the polish rate.

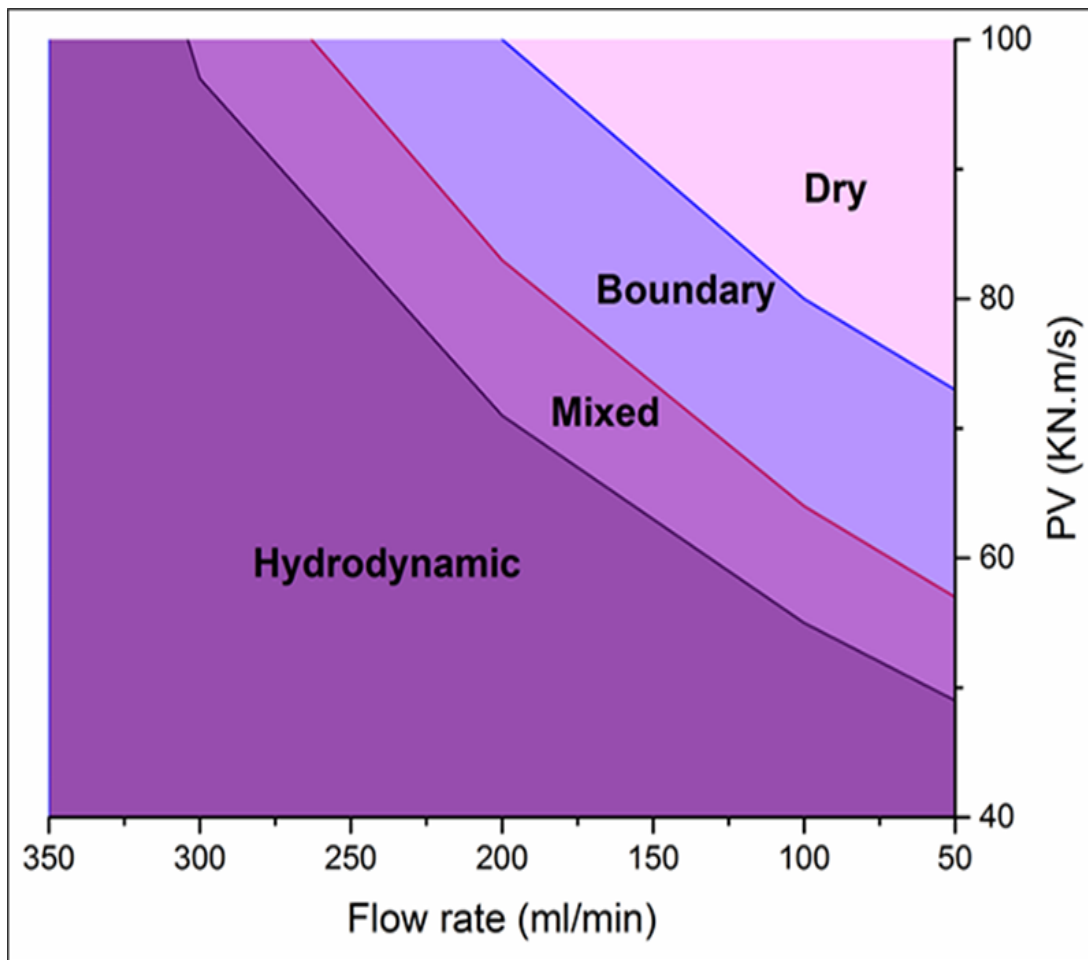


Figure 3-5. Phase diagram representing the lubrication behavior as function of PV and flow rate.

3.2 The influence of polish temperature

Energy losses due to friction manifest itself as an increase in temperature. Therefore, CMP conditions with high COF will also have higher temperature at the wafer pad interface. To study the polish temperature at different tribology regimes, the highest pad temperature during polishing was recorded. The polish temperature results as function of PV is shown in Figure 3-6. A linear relation was achieved for different flow rates. The intercept shows the pad temperature at room temperature is between 15-20°C and by increasing the polish pressure and velocity it reaches to the maximum value of 53°C.

There are several factors which affect the polish temperature such as the slurry chemistry, friction, pressure and velocity. Since the slurry chemistry is the same for all experiments, it is neglected. As discussed earlier there is a large COF change with changes in the lubrication regime. The temperature dependence on PV implies that unlike polish rate, the temperature has approximately the same slope for both hydrodynamic and boundary lubrication. Therefore it can be concluded that the COF has a minor effect on the slope of the curve shown in Figure 3-6. On the other hand, velocity and pressure have linear relationships to the temperature. It seems that increasing the velocity leads to increase of the rate of contact between the wafer, pad and slurry per unit time. Increasing the contact raises the interactions per unit time thus the temperature increases linearly. The same statement can be used for the role of the pressure. The effect of the number of solid-solid contacts per unit of time on the pad temperature is more dominant than the lubrication and contact nature.

Comparing the slope of curves at different flow rates in Figure 3-6 shows that by decreasing the flow rate and transferring the lubrication regime from hydrodynamic to boundary lubrication the slopes slightly increase as expected. This means that at a constant P.V, the lower flow rate leads to the higher pad temperature. This difference is not significant due to the minor role of lubrication regime and friction forces on the temperature, as discussed earlier. On the other hand, slurry acts as coolant of the pad and the wafer. Therefore increasing the flow rate and coolant agents helps reducing the polish temperature.

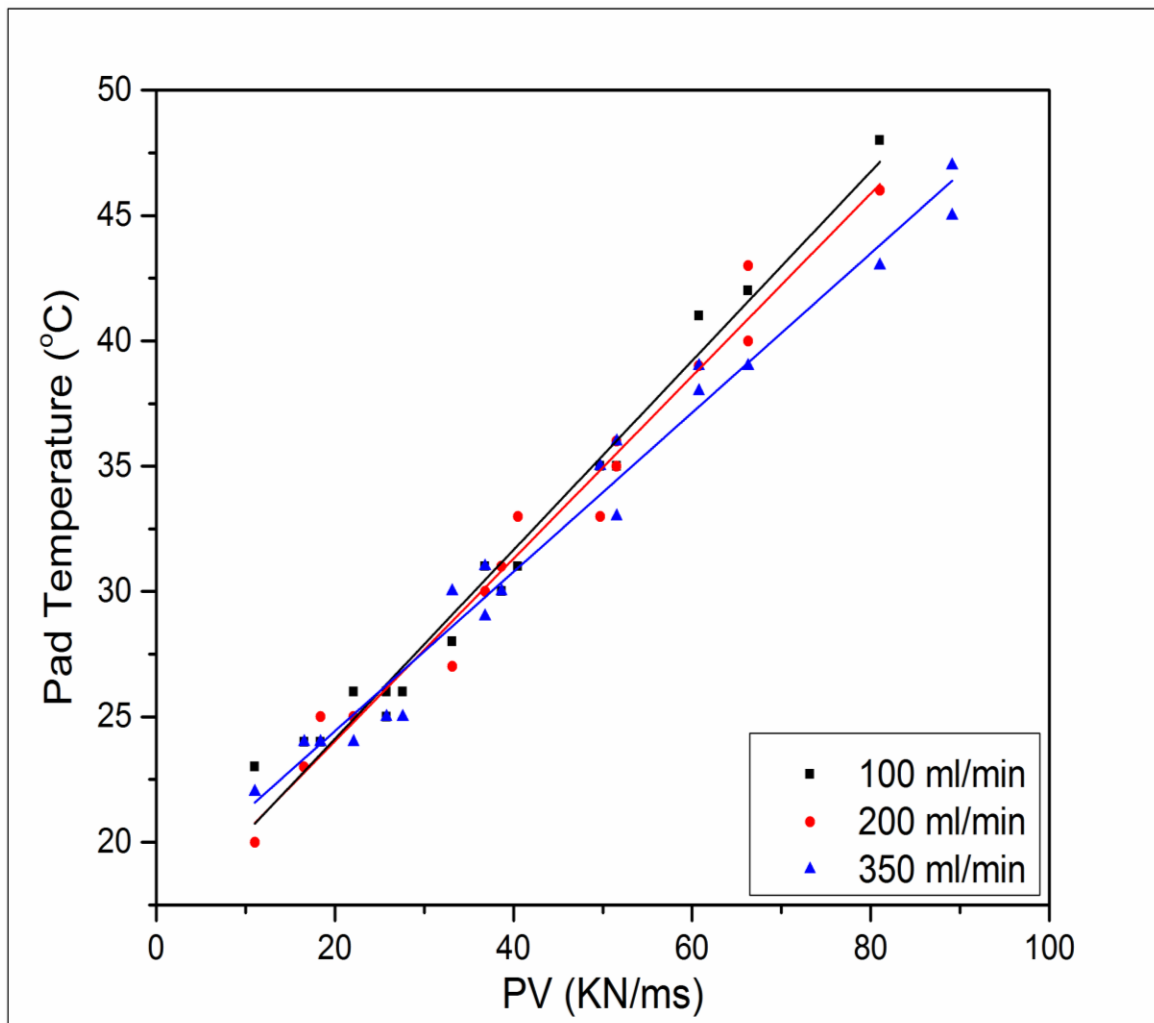


Figure 3-6. Effect of PV on the maximum polish temperature, after 1 minute of polishing.

3.3 Surface quality (AFM)

As shown in Figure 3-1 and Figure 3-2, increasing friction and changing the lubrication regime increases the polish rate. This is due to the solid contact between the wafer, abrasives and the pad. High friction force and solid contact may damage the wafer surface. To evaluate the effect of solid contact on the surface quality and topography of wafers atomic force microscopy (AFM) was performed before and after CMP. AFM images before and after polishing wafers are shown in Figure 3-7 and the results show that the surface roughness before polishing is approximately 120\AA and after polishing the maximum measured R_q was 2.6\AA . The surface roughness is the average of six R_q (root mean square) values for each wafer. The AFM results show that the polished wafers were smooth after polishing and the polish condition has an undetectable effect on the surface quality. This is due to the high hardness of silicon compared to other polished materials such as copper. The hardness of the polysilicon prevents any damage occurring on the wafer surface.

3.4 Conclusions

In this study, the polish behavior of highly boron-doped polysilicon was studied during CMP. A direct relation of polish properties such as pressure, velocity and flow rate to the lubrication behavior and polish rate was observed. During the mixed lubrication regime from the Stribeck curve, the polish rate showed a linear relation with the PV product (Preston's equation). It was shown that by changing the lubrication behavior to dry lubrication the COF and polish rate were increased significantly while increasing the flow rate and velocity did not necessarily increase the polish rate. Unlike Preston's equation the y-intercept was not zero in our experiments. This

suggests that the chemical etching is also responsible for polysilicon polishing. Increasing the COF and mechanical forces caused no damage to the polysilicon surface due to its hardness. Optimum polish behavior was achieved at 200ml/min flow rate, 6psi pressure and 90rpm with $\sim 0.7\mu/\text{min}$ polish rate.

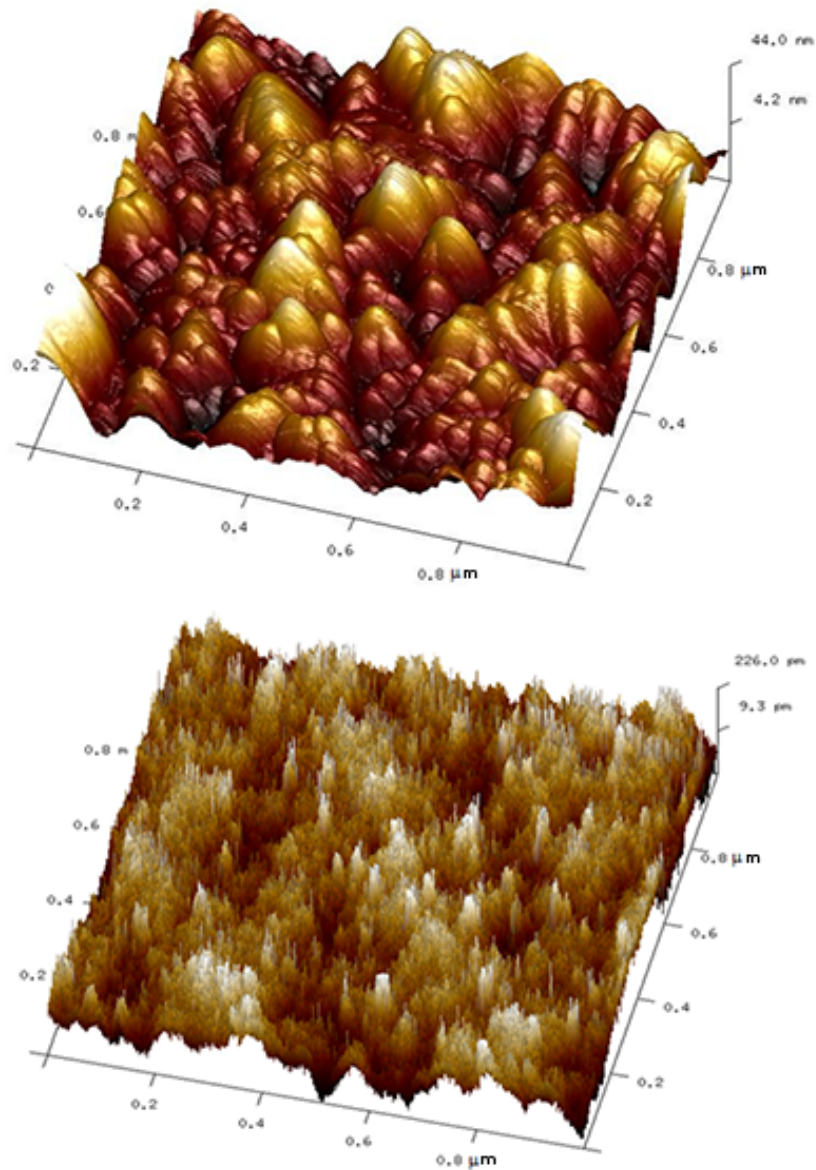


Figure 3-7. AFM images of wafers before and after polishing.

Chapter 4. Effect of chemical and mechanical components on high rate CMP of boron-doped polysilicon

This chapter is based on the H. Pirayesh, K. Cadien paper submitted on Journal of Materials Processing Technology.

Earlier work [17] and the previous chapter have shown that boron-doped polysilicon with resistivity of 3.5 m Ω .cm has a polish rate of ~ 0.7 $\mu\text{m}/\text{min}$ at 6 psi, 80 rpm, and 200 ml/min slurry flow rate. In this chapter the same slurry and pad is used while the heavily boron-doped polysilicon films had a resistivity of 2.2 ± 0.1 m Ω .cm indicating an even higher carrier concentration than previous chapter samples [84]. It is expected that the polish rate of heavily boron-doped polysilicon thin films in this work will be somewhat lower due to the chemical effect of the boron. The commercial Fujimi slurry (Planerlite 6103) was used for all experiments. In this chapter, improving the polish rate was investigated by suppressing the chemical effects and increasing the mechanical forces by using high friction conditions during polishing. In the following sections these experiments will be presented and discussed.

4.1 The effect of slurry flow rate and velocity on polish rate and temperature.

The polish rate was measured for various slurry flow rates at each polish velocity. At higher flow rates a thicker slurry film is expected to form which lowers the COF. The effect of slurry flow rate on polish rate at high velocities and high pressure (6psi) is

shown in Figure 4-1 where, at moderate velocities (80 and 90 rpm), a positive slope is detected and at higher velocities (≥ 100 rpm) the polish rate drops significantly with increasing flow rate. Under conditions comparable to the earlier work, the 2.2 m Ω .cm polysilicon removal rate is ~ 0.2 mm/min, $>3X$ lower than the 3.5 m Ω .cm polysilicon.

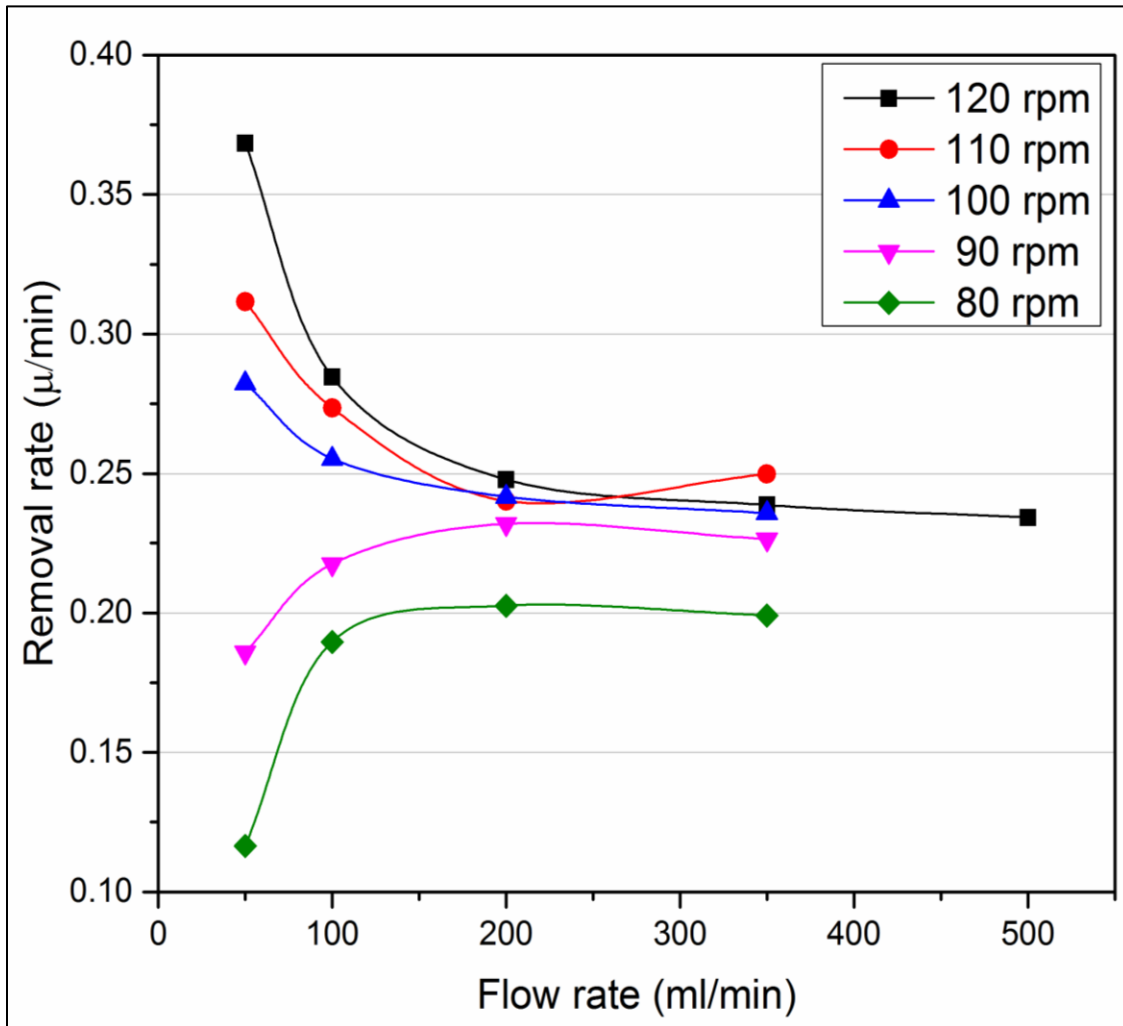


Figure 4-1. Effect of flow rate and polish velocity on polish rate at 6psi pressure for 2.2 m Ω .cm resistivity films.

At moderate velocities (80-90 rpm) and increasing slurry flow rates, the removal rate increases and reaches a steady state at 200 ml/min, the transition point. Clearly, at low flow rates the removal is limited by the supply of chemical reactants, while above 200

ml/min the wafer surface is saturated with reactants and the removal rate does not increase. This phenomena has been observed in other CMP processes [93], [94]. In case of polysilicon polish the chemical reactant is the hydroxyl anion (OH^-) which softens the polysilicon surface by weakening the Si-Si bond [19], [20]. At flow rates close to the transition point, the rate of softening due to hydroxyl anions is equal to the rate of removal, that is, the surface reaction rate is equal to the surface polishing rate. At moderate velocities the chemical force is dominant and by increasing the slurry flow rate and thus the chemical factors, the polish rate increases.

Polishing at moderate velocities and pressure occurs in the mixed or boundary lubrication regime [95] where there is solid contact between the pad, abrasives and the wafer. This results in the removal of polysilicon which has been softened by OH^- . While the relationship between removal rate and flow rate at moderate velocities appears to be easily explained, this explanation is confounded by the fact that slurry flow rate and velocity also affect the temperature at the wafer/pad interface, the polish temperature. This temperature will affect the chemical reaction rate. Polish velocity, pressure and slurry composition (chemistry, particles) affect friction, while the flow rate acts to remove heat. Generally it is expected that higher friction results in higher polish temperatures [79], [96]. Furthermore, increasing the velocity and pressure at constant friction rises the temperature. This is due to higher interaction between the wafer, the pad and the slurry per increment of time. In this study, the maximum pad temperature after 1 minute polishing was recorded for both moderate and high velocities, and is shown in Figure 4-2. With increasing velocity the pad temperature increases, and with increasing slurry flow rate the temperature decreases. All curves

have a similar shape, with a lower rate of temperature increase at low and high rpm, separated by a region of higher rate of temperature increase.

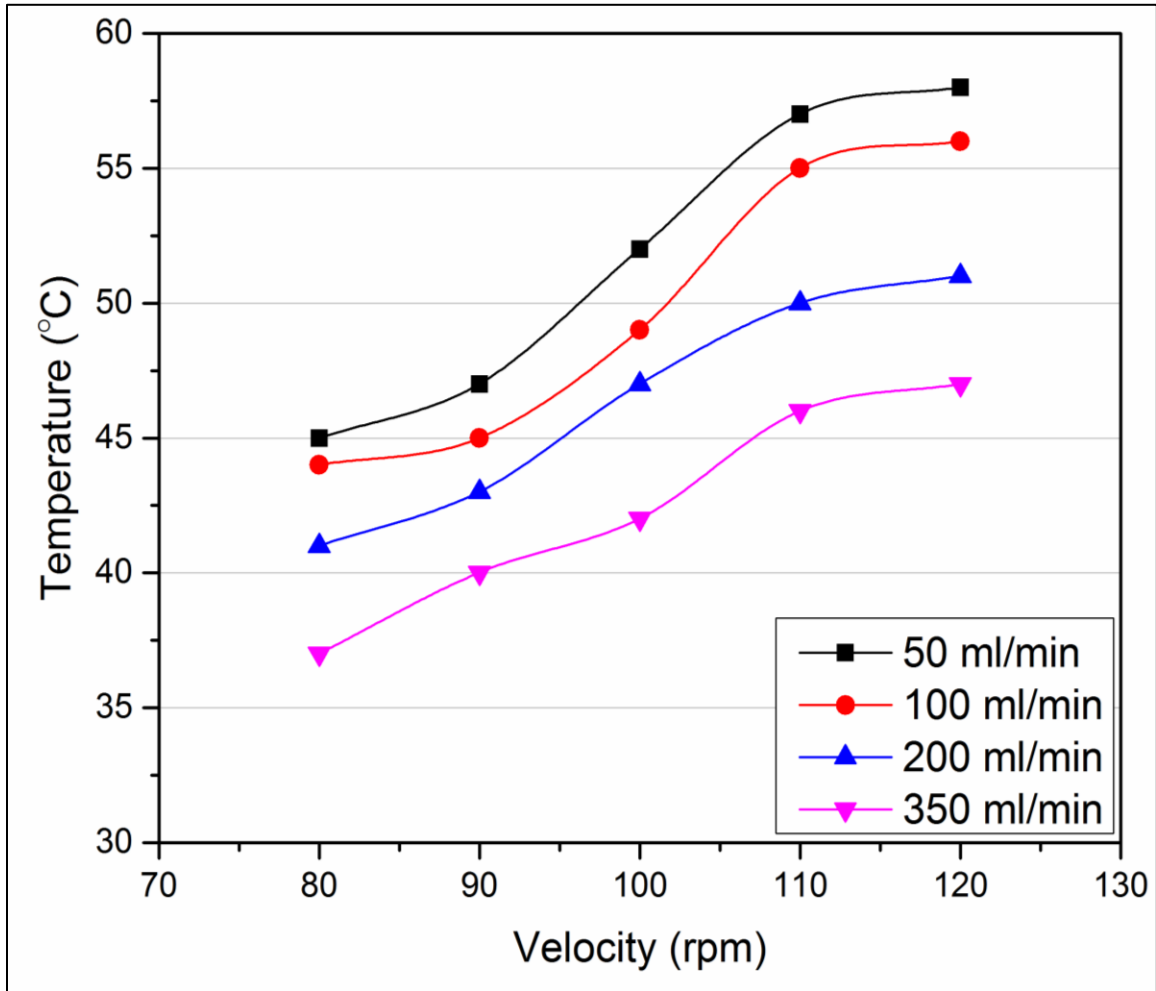


Figure 4-2. The pad temperature during polishing of boron doped polysilicon at 6psi pressure and various flow rates and velocities.

Polysilicon removal rate at high velocities (100-120rpm) and low slurry flow rates (<200 ml/min) is fundamentally different from that at moderate velocities as discussed earlier (Figure 4-1). In order to understand this behavior, the effect of rpm on the mechanical forces on the slurry and on the lubrication regime will be discussed. As the

velocity is increased the centripetal force on the slurry increases which acts to remove the slurry from the pad at an increasing rate. Therefore at high velocities, a higher slurry flow rate is required to maintain slurry between the wafer and the pad. At high velocities and low slurry flow rates, the wafer is starved of slurry and it is expected that the lubrication regime be dry. This occurs because more slurry is needed per unit time at higher velocities to have a similar friction to polishing at lower velocities. This is due to the relationship between the pad rpm and the time slurry needs to escape from the pad surface,

$$a_r = \omega^2 r \quad (2)$$

$$V_r = \omega(r^2 - r_o^2)^{0.5} \quad (3)$$

$$t = \text{Ln}(2(R^2 - r_o^2) + R) \quad (4)$$

where a_r and V_r are radial acceleration and velocity respectively, ω is the pad rotational speed and r and r_o are the instant and initial positions of the slurry on the pad respectively, R is the pad radius and t is the time that slurry needs to escape from the pad surface. Equation 4 shows that the time that the slurry stays on the pad surface is directly related to the rotational speed and increasing the speed reduces the time considerably. Thus, at low flow rates and high velocities the wafer pad surface becomes dry and the friction force and the pad temperature increase.

The influence of rpm at low slurry flow rates and flow rate at high rpms on the coefficient of friction, COF, is shown in Figure 4-3. In Figure 4-3a, at a slurry flow rate of 50 ml/min, increasing the polish velocity raises the COF. The curve has two regimes, between 80 and 90 rpm the COF increases rapidly, while at 100 rpm and above the COF increases slowly. From the Stribeck curve in the boundary lubrication regime, it is

expected that the COF would decrease with increasing velocity. This indicates that at low flow rates the polish is not in the boundary lubrication regime. The lack of slurry at high velocities and low flow rates lead to the formation of a semi-dry surface between the wafer and the pad; therefore the frictional force and pad temperature increase significantly. Figure 4-1 clearly shows that at high polish velocities the effect of slurry flow rate is unlike moderate and low velocities. A sharp increase of the polish rate was observed for low flow rates and high velocities which can be attributed to the transition of the lubrication regime from boundary to the dry region. At low flow rates, the slope of the curves in Figure 4-1 changes from positive to negative by increasing or decreasing the velocity. At high velocities and low flow rates mechanical and frictional forces dominate the polishing. Figure 4-3b shows the effect of flow rate on COF at high polish velocities (110rpm). As expected, the COF is increased significantly (0.27 to 0.44) by flow rate reduction. This can only be explained by the lubrication regime moving from boundary lubrication to dry lubrication. Therefore, by reducing the slurry flow rate and increasing friction the polish rate improves significantly. In this region there is not enough slurry to cool the pad and lubricate the wafer/pad interface; therefore the temperature shows a stronger dependency on the flow rate. Figure 4-2 shows that reducing the flow rate from 350ml/min to 50ml/min results in $\sim 20^{\circ}\text{C}$ increase in the temperature at 120 rpm.

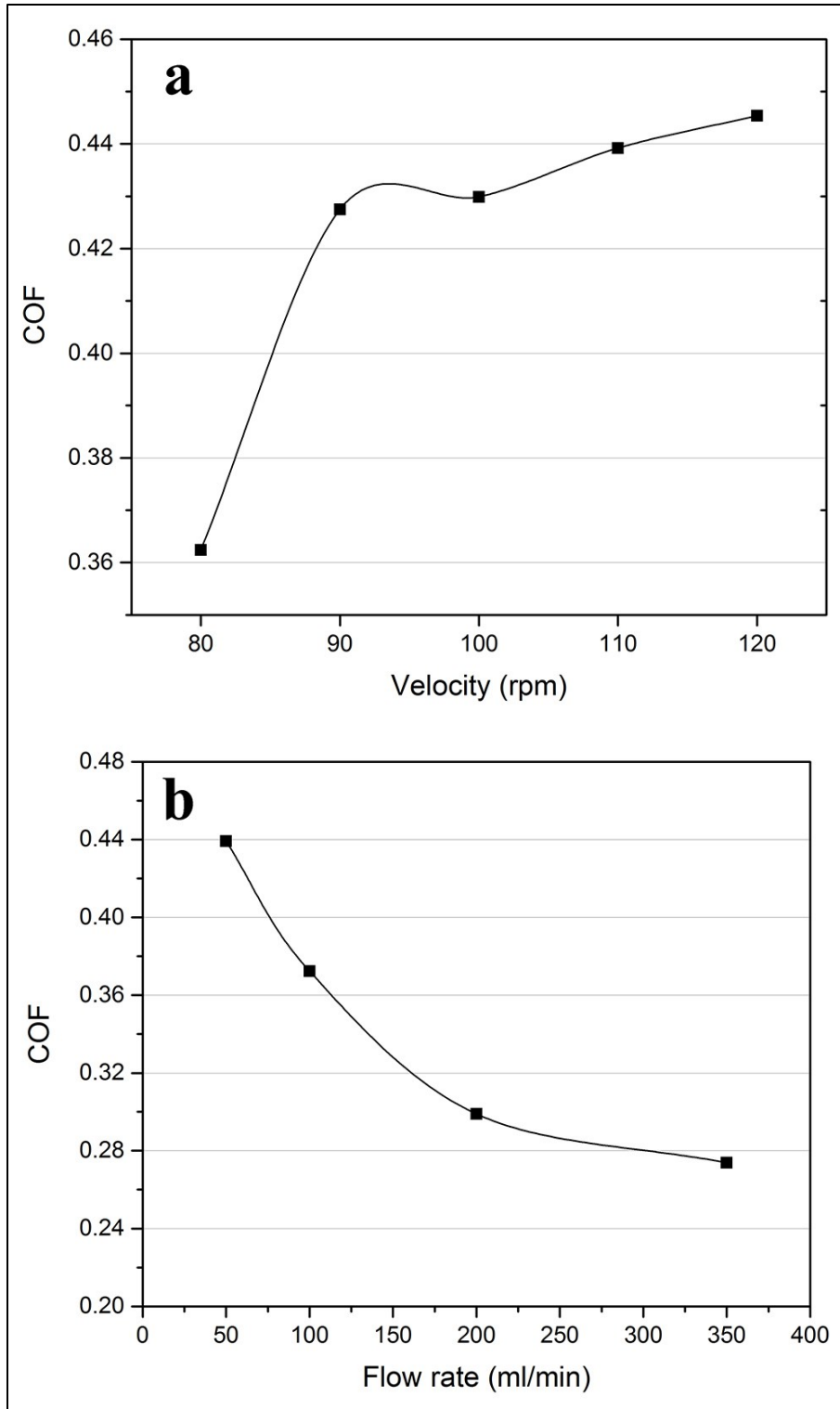


Figure 4-3. Coefficient of friction versus a) pad/wafer velocity at low slurry flow rates (50ml/min), b) flow rate for high pad/wafer velocity (110rpm). All experiments at 6psi pressure and for 2.2 m Ω .cm resistivity films.

4.2 The effect of slurry temperature of polish rate behavior

To investigate the effect of slurry temperature on the polish rate independent of the polish parameters, the slurry was heated 70°C prior to polishing. To differentiate between the two slurries we will use HT to refer to slurry preheated to 70°C prior to polish, and RT to refer to slurry that was not preheated. Increasing the slurry temperature, pad softening and etch rate improvement are expected to occur simultaneously. Figure 4-4 shows the effect of temperature on the pad hardness measured by NexPlanar Corporation. As shown, increasing the pad temperature from 25°C to 85°C reduces the hardness ~ 25%. There are few publications in the literature on the effect of temperature on polish behavior and it seems that the effects depend on the system being studied [86], [96]. Investigating the dominant factors that control polish rate removal during high temperature polishing is essential for this study.

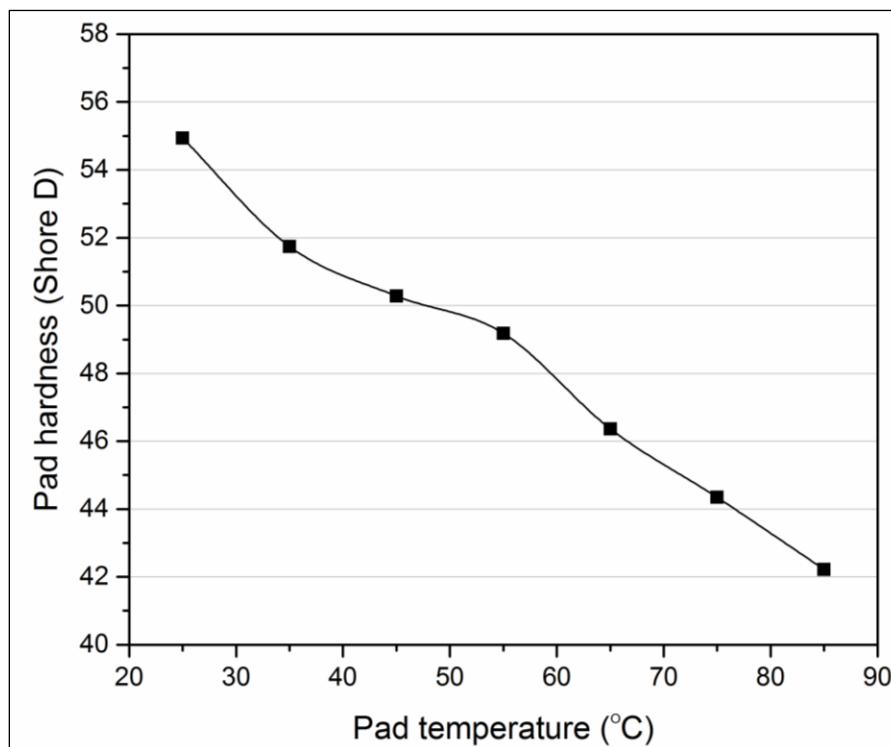


Figure 4-4. Pad hardness as a function of temperature (Courtesy of NexPlanar Inc.)

The HT slurry CMP polish rate as function of flow rate and polish velocity is illustrated in Figure 4-5 where the polish behavior with HT slurry is completely different from what was observed for RT slurry polishing (Figure 4-1). In addition, the polish temperature trend is different when Figure 4-2 is compared to Figure 4-6. The observed differences between HT slurry polishing and RT slurry polishing include: 1) Unlike RT slurry polishing, for HT slurry the polish rate decreases with increasing polish velocity; 2) The dependency of the polish rate on the polish velocity is much lower than for RT slurry polishing; 3) The polish rate increases with increasing flow rate while RT slurry polishing showed a twofold behavior depending on the polish velocity; 4) The polish rate dependency on the polish velocity increases with increasing flow rate while the opposite occurs for RT polishing; 5) The polish temperature is almost independent from the polish velocity; 6) Unlike RT slurry polishing, the polish temperature increases with slurry flow rate; and, 7) The polish rate in general is slightly lower than RT slurry polishing. All of these phenomena can be explained by considering the effect of HT slurry on the pad and the wafer. As mentioned earlier, increasing the slurry temperature to 70°C reduces the hardness of the pad which minimizes the mechanical forces, while increasing the chemical forces and polysilicon etching. It is evident from Figure 4-5 and Figure 4-6 that at high flow rates the chemical factors are dominant and mechanical forces are minimized. This occurs because the HT slurry increases the chemical etching while simultaneously reduces the mechanical interaction of pad asperities with the wafer due to pad softening. This also minimizes the low dependency of the polish rate on the polish velocity. The slight higher polish rates at low polish velocities and high flow rates

(unlike RT slurry polishing) is due to the fact that there is more HT slurry in contact with the wafer per unit time. Higher surface etching and reaction with the slurry mean that there is more slurry required to saturate the wafer surface with hydroxyl anion. Thus the optimum point for the slurry flow rate is higher than the RT slurry optimum (~200ml/min). In other words, using HT slurry leads to more chemical etching of the surface while the softened surface is not completely mechanically abraded. The increase in the polish rate with increasing slurry flow rate is also related to the fact that higher polish temperatures are maintained with higher HT slurry flow rates. This increases the role of chemical forces during polishing, while diminishing the effect of mechanical forces. The decrease in mechanical forces with the HT slurry is more evident at low slurry flow rates. As shown in Figure 4-1 for RT slurry, at extremely low flow rates and high polish velocities the polish rate and temperature increase significantly due to the interaction between the pad asperities and the wafer. The HT slurry reduces the mechanical interactions by weakening the pad asperities. Therefore both mechanical and chemical forces become minimized at low flow rates and the polish rate becomes lower than other polish conditions. This can also explain the low dependency of polish temperature and polish rate on the pad velocity.

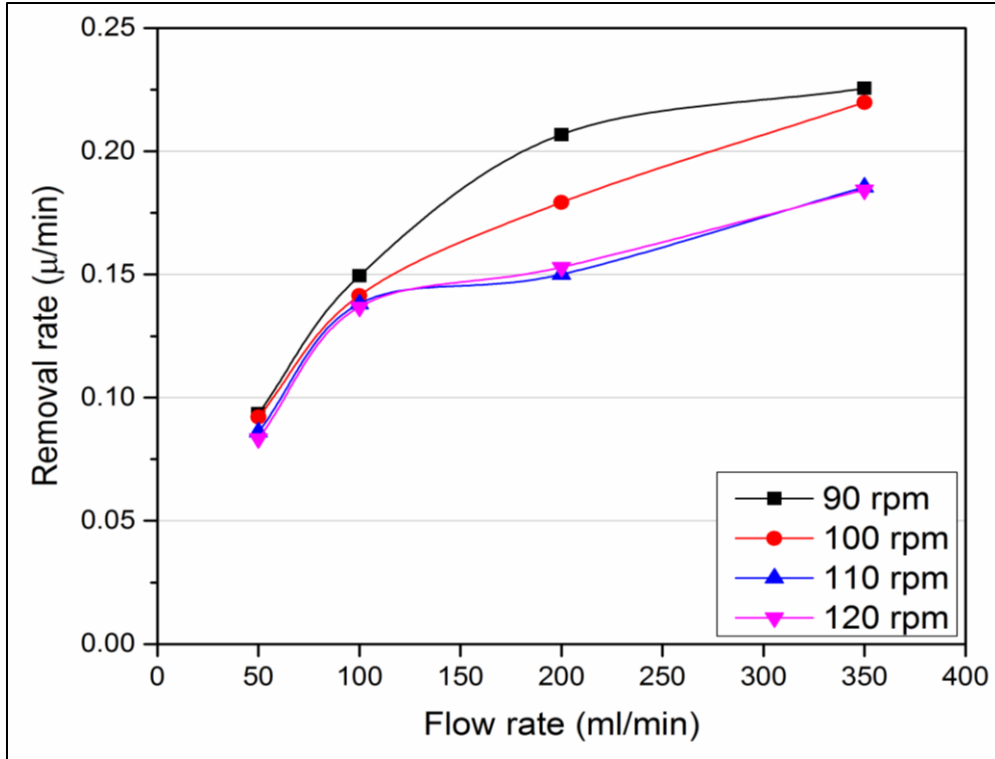


Figure 4-5. The effect of flow rate and polish velocity on the removal rate of polishing with HT slurry (70°C) and high pressure (6psi) for $2.2 \text{ m}\Omega\cdot\text{cm}$ resistivity films.

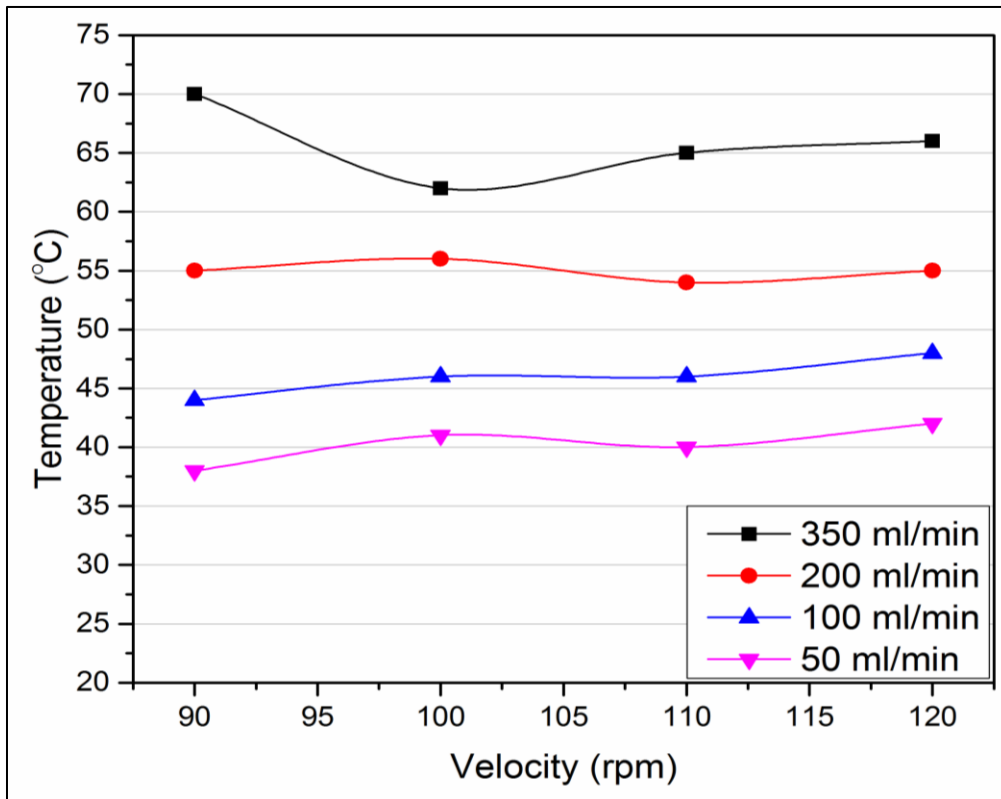


Figure 4-6. The pad temperature during the polishing of boron doped polysilicon ($2.2 \text{ m}\Omega\cdot\text{cm}$ resistivity films) at 6psi pressure with HT (70°C) and various flow rates and velocities.

4.3 The effect of chemical and mechanical forces on the polish rate model

Figure 4-1 suggests that in order to achieve high polish rates, extremely low flow rates and high pad/wafer velocities should be used. This is due to the chemical and mechanical forces which affect the surface polishing during CMP. Chemical forces can be defined as the effective hydroxyl anion concentration in slurry. It was shown earlier that chemical forces improve with increasing flow rate up to the optimum flow rate where the pad/wafer surface is saturated with hydroxyl ions. As discussed earlier the chemical force effects are not significantly affected by the polish velocity and can be kept constant in this model (Figure 4-5). On the other hand the mechanical forces are directly proportional to both slurry flow rate and polish velocity. Generally altering the lubrication regime and slurry film thickness affect the mechanical forces on the wafer surface. In this model the chemical and mechanical forces as the two critical factors that determine CMP behavior. Since all of the polish parameters can be categorized as mechanical or chemical forces and both components are force vectors, it is assumed that they can be added to achieve the normalized removal rate. Figure 4-7 schematically shows the role of mechanical and chemical factors in CMP and their effect on removal rate as function of flow rate. As mentioned earlier, changing the velocity does not have a significant effect on the chemical forces of CMP. The chemical effects increase with flow rate up to the saturated point, where there is equilibrium between dissolving silicon and forming silicic acid. Therefore, above this point the chemical etching mechanism is not a function of flow rate. Furthermore, mechanical forces such as friction have a strong dependency on polish velocity. As discussed earlier, changing the friction behavior from boundary

lubrication to dry lubrication increases the friction. This relationship is clearly shown in Figure 4-3 where at higher velocities and low flow rates a strong increase in the friction is observed. At higher flow rates this effect is reduced with the lubrication regime moving to boundary lubrication where the flow rate does not show a notable effect on friction. For moderate velocity cases, there is no dry lubrication and all the mechanical interaction occurs in the boundary lubrication regime. The results of low polish velocity have been shown elsewhere [17] and it was suggested that the polish with low velocity occurs in mixed or hydrodynamic lubrication. Finally, the combination of chemical and mechanical forces helps planarize the surface. This is shown in the third curve (RR curves) on Figure 4-7 by adding the chemical and mechanical factors. The RR curve axis with length/time unit is shown in the right hand y-axis. The RR curve resembles the curves shown in Figure 4-1 and represents that the highest polish rates that can be achieved at high velocity and low flow rate. This is important since it shows that by reducing the amount of slurry used (and therefore reducing waste) a higher polish rate can be achieved.

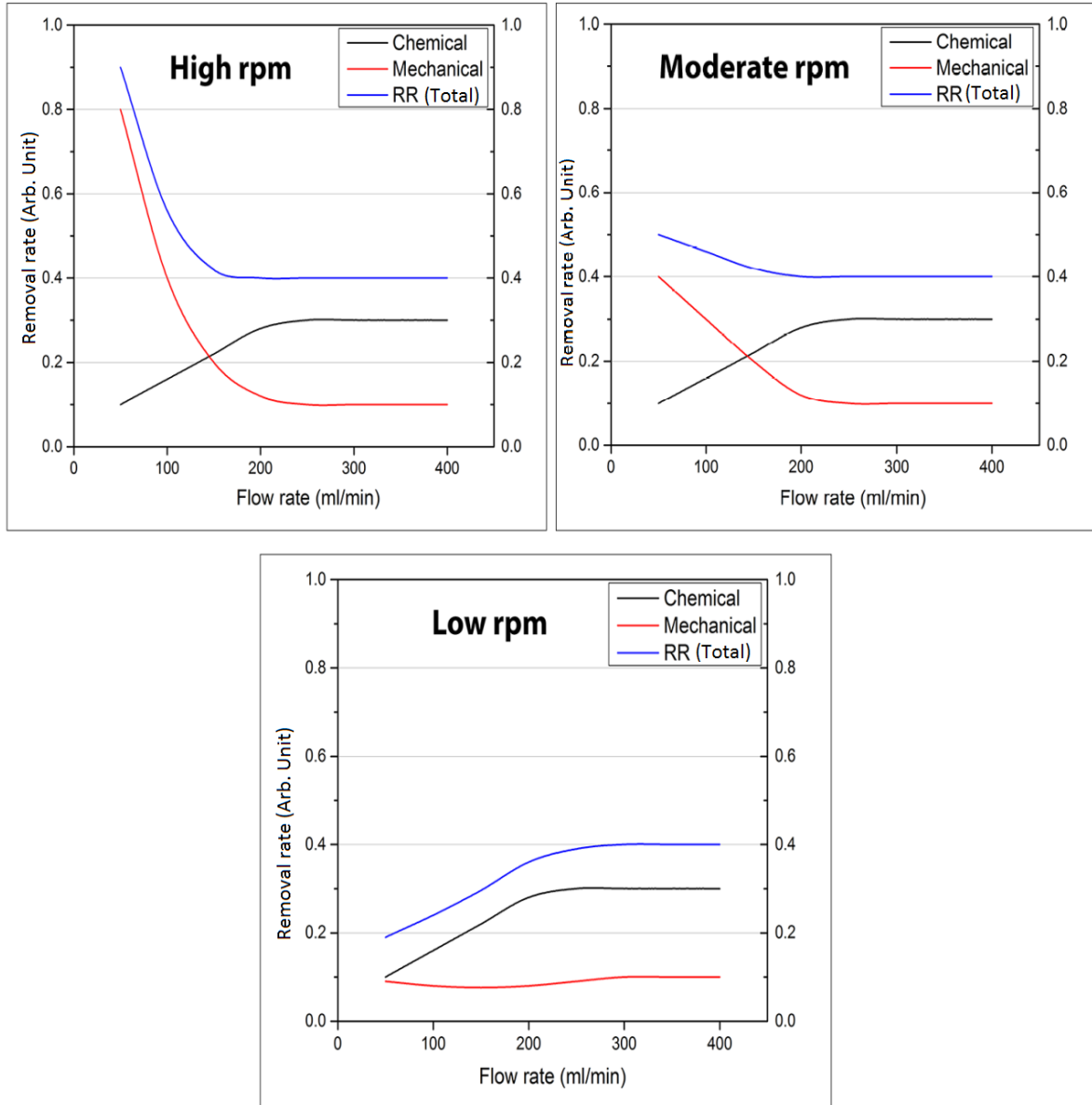


Figure 4-7. Schematic illustration of the effect of mechanical and chemical factors on removal rate for low, moderate and high pad/wafer velocities.

4.4 Effect of optimized high rate polish on surface quality

One of the potential drawbacks of polishing in the dry lubrication region is nano-scale damage which might occur on the wafer surface [3], [33]. In this study, all polishes occurred at 6 psi and moderate to high velocities leading to high mechanical conditions so it is essential to evaluate the surface topography after polishing. AFM

images of wafers before and after polishing are shown in Figure 4-8. As expected, the surface roughness before polishing is high, $\sim 10\text{nm}$, due to the columnar, polycrystalline grain structure. After polishing the roughness is in the sub-nanometer range. The average of six R_a (center line average) and R_q (root mean square) measurements for each polishing condition is shown in Table 4-1. The results show that for all three extremely high mechanical force cases (50ml/min flow rate and 110rpm), moderate mechanical forces (200ml/min flow rate and 90 rpm) and high slurry temperature, the surface roughness is in the acceptable range ($<3\text{\AA}$) and is independent of the polish process. The AFM results and surface roughness measurements indicate that polishing under the dry lubrication regime does not have significant adverse effects on the polysilicon surface quality which we attribute to the hardness of polysilicon.

Table 4-1. Surface roughness measurement of a few polish conditions. The results are the average of six measurements, including the standard deviation (SD).

	Before polish		6psi, 110rpm, 50ml/min		6psi, 90rpm, 200ml/min		HT polish 6psi, 110rpm, 50ml/min	
	Average	SD	Average	SD	Average	SD	Average	SD
R_a (\AA)	95.06	8.42	2.04	0.02	2.17	0.31	1.97	0.05
R_q (\AA)	122.29	8.98	2.58	0.03	2.78	0.43	2.50	0.08

Conclusions

In this study the tribological behavior of as-deposited boron-doped polysilicon (2.2 m Ω .cm) during CMP was studied. Due to the presence of boron ions on the polysilicon surface, the chemical effects of polishing were suppressed and the polish

rate was lower. In order to overcome this retardation effect and increase the polish rate the mechanical forces such as friction were increased. High temperature polishing mimicked chemically dominant polish behavior and showed that chemical forces have less effect on polishing boron-doped polysilicon than mechanical forces. Finally, an AFM study was used to study the surface quality of wafers after polishing and show that polishing under high mechanical forces did not damage the surface quality which was attributed to the hardness of silicon. The optimum polish outcome with maximum polish rate, $\sim 0.37 \mu\text{m}/\text{min}$, minimum slurry used and acceptable surface quality was achieved under maximum mechanical forces which is dry friction polishing at 120 rpm, 6 psi and 50 ml/min.

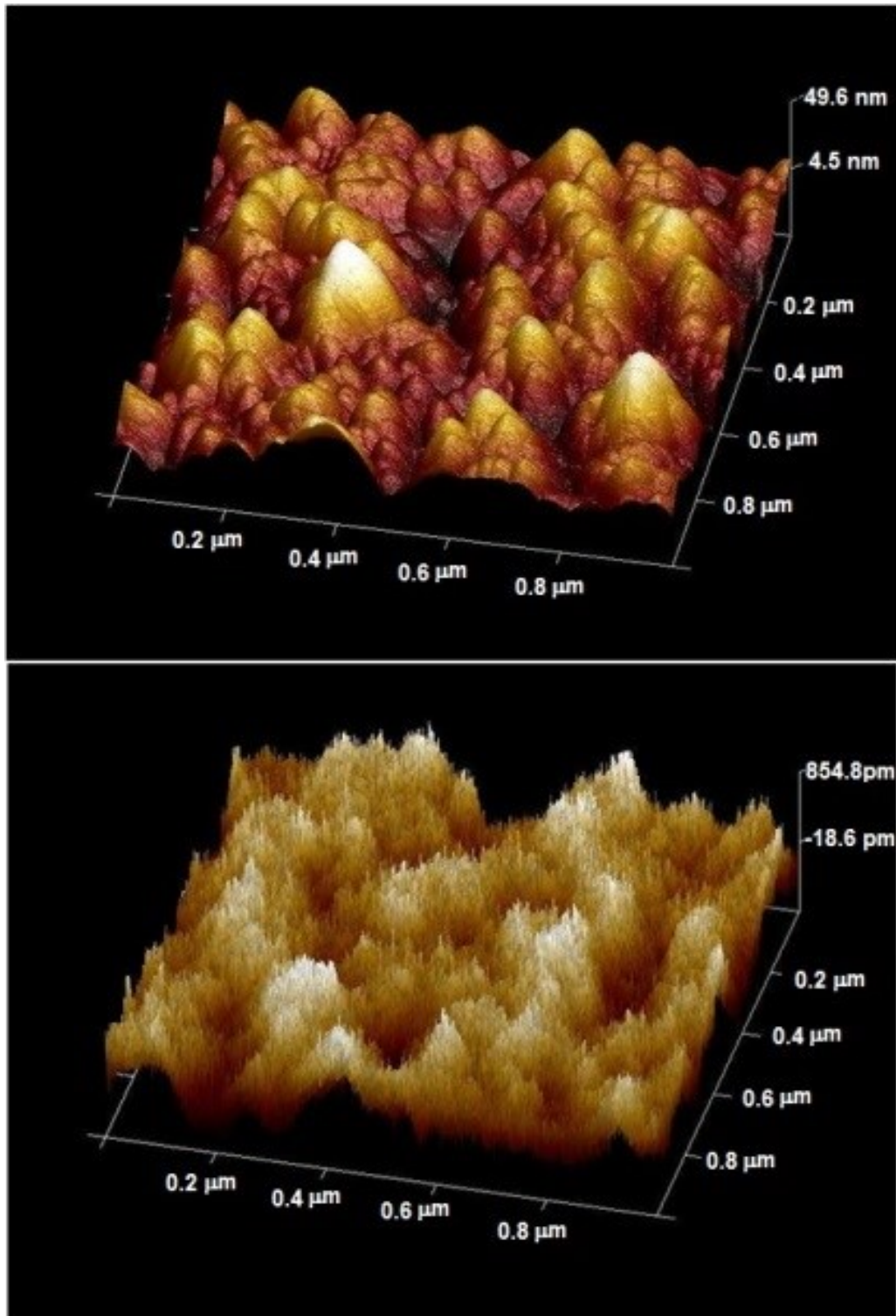


Figure 4-8. AFM images of sample, a) before polishing; b) after polishing at 6psi and 90rpm and 200ml/min.

Chapter 5. Effect of slurry chemistry and abrasive properties on boron-doped polysilicon CMP

This chapter is based on the H.Pirayesh, K. Cadien paper prepared to submit to Journal of Electrochemical Society.

As discussed earlier slurry properties such as slurry chemistry and abrasive properties play a key role in the CMP behavior. Polysilicon polishing is usually carried out by basic solutions and silica abrasives. There has been several studies in the literature on the chemistry of silica slurries and the role of the chemistry on polish behavior [21], [22], [72]. It has been shown that the highest removal rates occurs between the pH of 11 and 12 [20]. Two types of colloidal abrasive silica (Bindzil 300/30 and Bindzil 30/50) with different particle size range were used in this work.

In this chapter the effect of slurry pH and abrasive size and concentration on the CMP of boron-doped polysilicon is investigated. Two of the highest removal rate polish conditions were chosen for polishing. Case 1: 6psi pressure, 90rpm velocity, 200ml/min flow rate (chemical effects dominant) and Case 2: 6psi pressure, 110rpm velocity, and 50ml/min flow rate (mechanical effects dominant). Case 1 is expected to be more dependent on the slurry condition due to higher flow rate and lower polish speed than Case 2. In all experiments, heavily boron-doped polysilicon with 2.2m Ω .cm resistivity was used.

5.1 Colloidal silica abrasive

TEM micrographs of colloidal silica abrasives (Bindzil 30/50 and Bindzil 300/30) are shown in Figure 5-1. The particle size of Bindzil 30/50 was $>60\text{nm}$ while for Bindzil 300/30 it was $>5\text{nm}$ for most measurements. It was difficult to find single particles in the 300/30 solution since most particles were agglomerated.

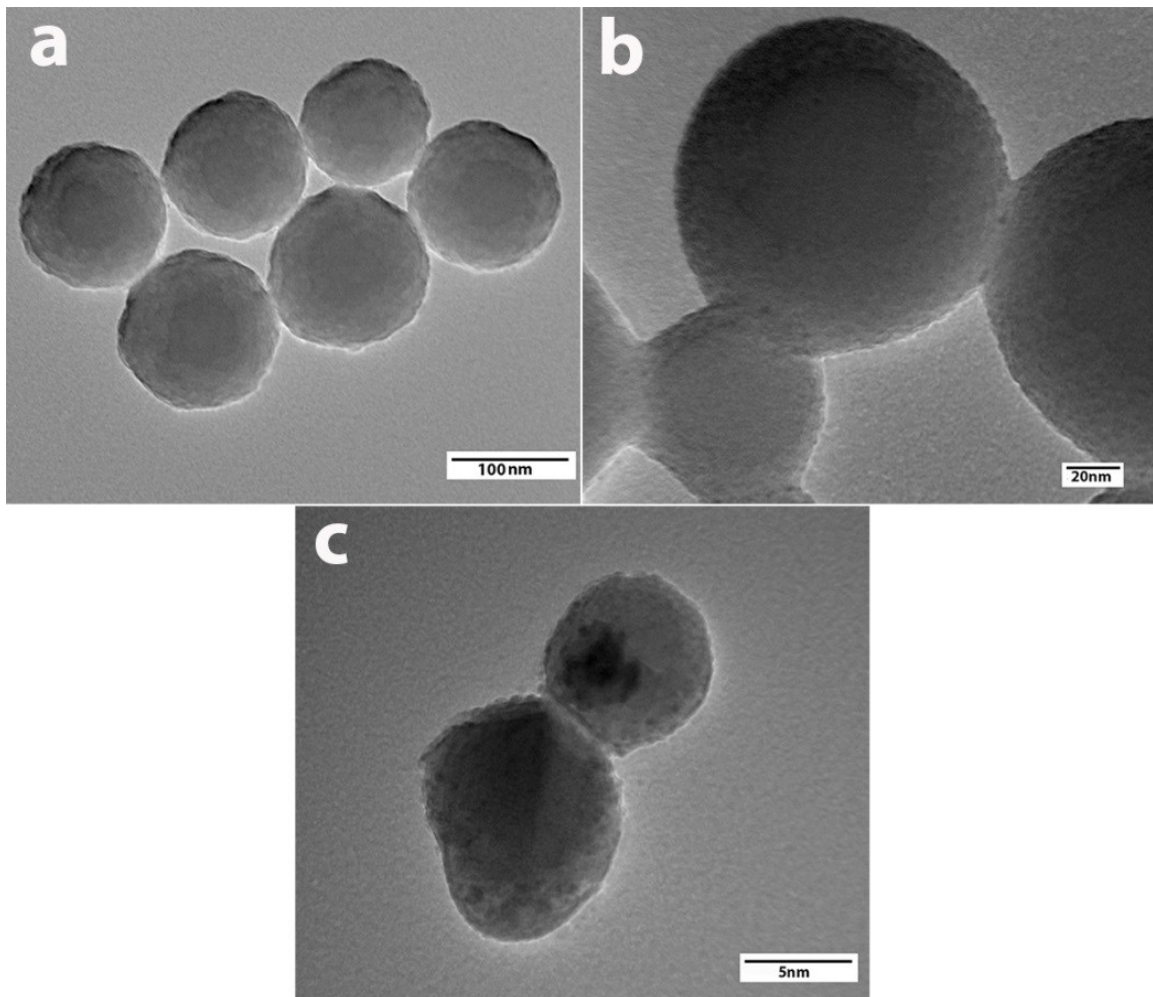


Figure 5-1. TEM micrograph of silica abrasives used in our experiment. 5-1a and 5-1b are 30/50 and c is 300/30 slurry.

5.2 Zeta potential

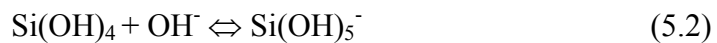
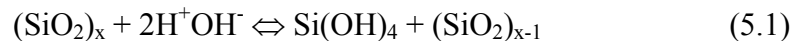
In order to study the colloidal stability of tested slurries, the zeta potential was measured and is shown in Table 5-1. The results show that the change of pH from the initial solution pH (~9-10) to the high pH values (~13) did not change the zeta potential significantly. High negative values of measured zeta potential suggest that the colloid is stable enough in all solution concentrations and pH values.

Table 5-1. Zeta potential of colloidal silica at different pH values.

	300/30	30/50
9.5	-33.06	-37.22
11	-30.12	-31.8
13	-28.73	-30.41

5.3 Silica abrasive dissolution

Silica is known to dissolve in aqueous solutions at various pH values. By increasing the pH and OH⁻ concentration above pH~10, the solubility increases exponentially [10]. This can be explained by the following equilibrium reactions:



In Equation 5.1 the hydroxyl anion acts as a catalyst for the dissolution process by weakening the oxygen-silicon bonds. This leads to the dissolution of silicon in the form of silicic acid (Si(OH)₄) which is in equilibrium with the silica abrasive. At higher pH values, Equation 5.2 occurs in addition to Equation 5.1. Here the silicate ion

is formed in the presence of hydroxyl anion, and the silica abrasive is in solubility equilibrium with both silicic acid and silicate anion.

Dissolution of silica in the slurry solution alters the chemistry and pH of the solution and also the particle size of silica abrasives. The AAS results for the dissolution of 6wt% silica abrasives in high pH solutions after 24 hours are shown in Table 5-2. The dissolution rate is increased by increasing the pH from 12 to 13 as expected. In addition, the particle size had a significant effect on the dissolution rate, the 300 m²/g surface area particles had a 50X increase in solubility compared to the 30 m²/g particles.

Table 5-2. Atomic absorption results (in ppm) for colloidal silica with different particle size and 6wt% concentration, remaining in pH 12 and 13 solutions for 24 hrs.

pH	300/30 Colloidal Si	30/50 Colloidal Si
12	399	22060
13	580.25	30125

To confirm the dissolution of particles in high pH solutions, the particle size was measured before and after exposure to the high pH solutions as shown in Table 5-3. The particle size of larger abrasive (30/50) was reduced ~50% after soaking in the pH solution for 24 hours. Higher silica concentration (12wt%) showed slightly lower particle size reduction compared to the lower concentration (6wt%). This is due to the fact that at higher silica concentration there is not sufficient hydroxyl ions in solution. The smaller abrasive (300/30) showed a different trend. The initial particle size showed two particle size ranges, the smaller particle size is due to single silica particles, while the larger range is due to the agglomeration of these particles. After

increasing the pH, single particles dissolve similar to larger abrasives (30/50). However, the agglomerated particles showed an increase in the size. The negative radius of the curvature between agglomerated particles results in the extremely slow silica dissolution in these regions [10]. This gives enough time to the dissolved silica to redeposit around the curvature and increase the agglomerated particle size.

Table 5-3. Particle size measurement of solutions before and after remained in the high pH solution for 24 hrs (in nm).

	300/30 Colloidal Si	30/50 Colloidal Si
Initial	3.1, 15.19	64.29
pH=12, 6wt%	0.7021, 46.21	40.48
pH=12, 12wt%	0.8969, 29.58	42.95

It is clear that dissolution of silica happens by consumption of hydroxyl anions and formation of silicic acid, thus the pH of the slurry is expected to be reduced over time. The change of pH versus time for two particle size abrasives and different concentrations is shown in Figure 5-2. After about 24 hours, the pH becomes stable in most cases which mean that the solution is saturated with silicic acid and the hydroxyl and silicic acid are in the equilibrium. The only exception is at high pH, low silica concentration and low surface area where the rate of pH decrease and the slope of the curve is less than other cases and equilibrium did not happened during the experiment. This effect is shown more clearly in Figure 5-3 where most conditions follow a linear trend between the initial solution pH and the pH after 24 hours except the condition mentioned above. At high pH, low silica concentration and low surface area there is not enough total surface area for the silica to react with the hydroxyl ions of the

solution. Therefore pH reduction occur slower and other conditions and it takes a very long time to reach equilibrium.

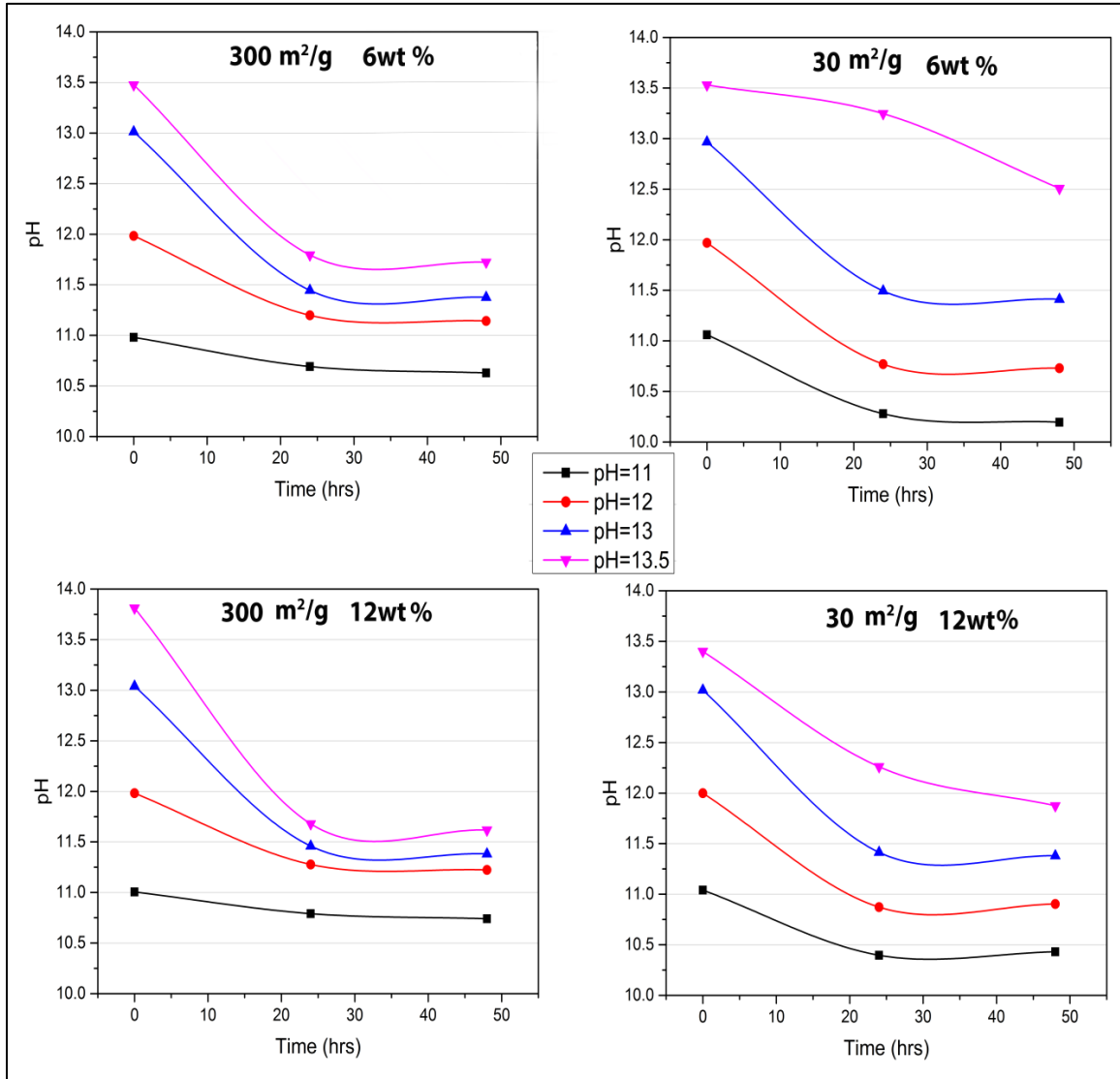


Figure 5-2. pH change of colloidal silica as function of time.

It has been shown that it takes approximately 24 hours for the slurry to become stable. In order to use the above slurry commercially, buffer solutions such as potassium bicarbonate might be required. To reduce the number of parameters affecting the

polish rate, no buffer solution was added in this study and the pH of the solutions was measured after one day.

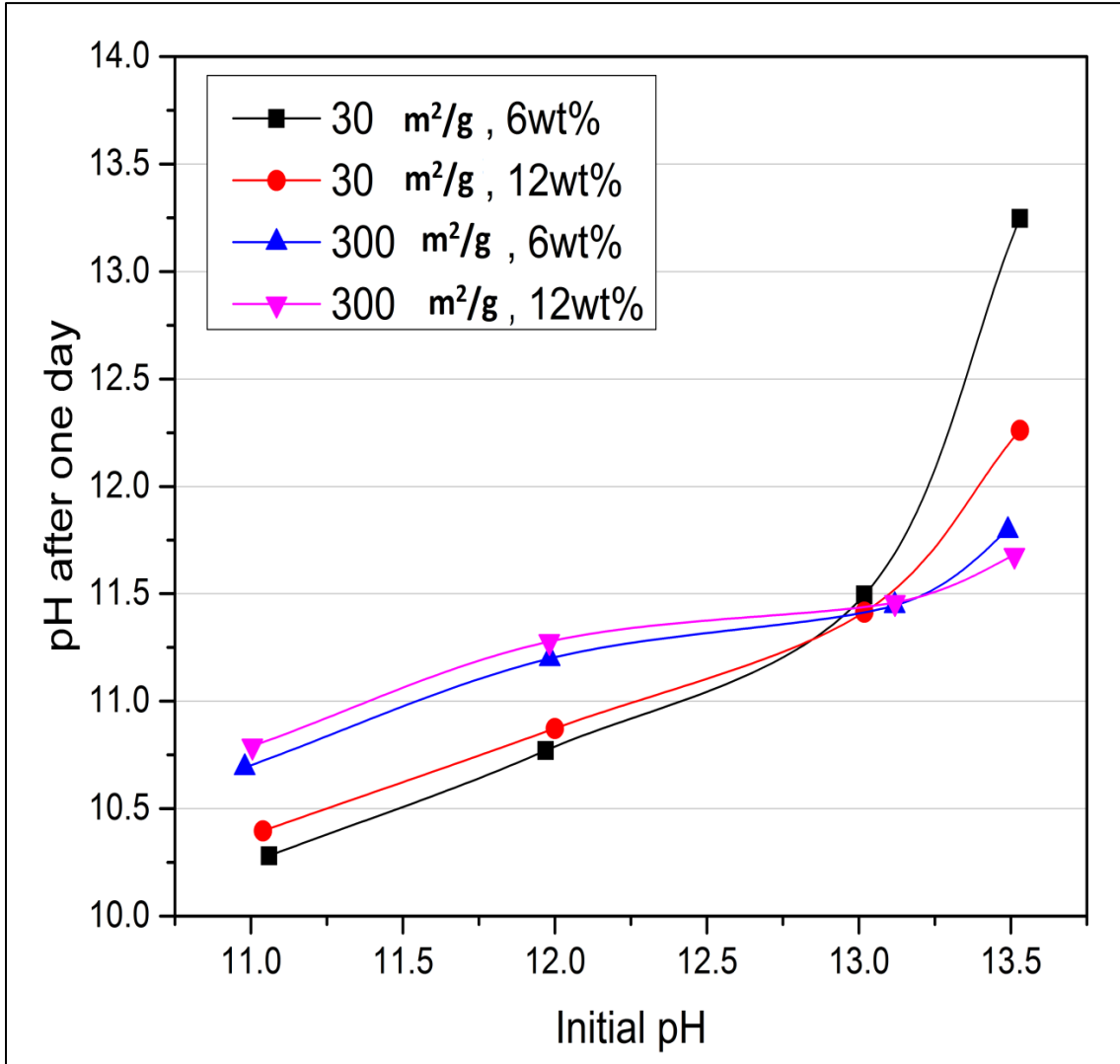


Figure 5-3. The colloidal silica pH change after 24 hours as function of initial pH.

5.4 Polish rate as function of pH and silica abrasives

To understand the effect of slurry pH and silica abrasives on CMP, polishing was carried out at different pH values, silica particle size and concentrations. The results

are shown in Figure 5-4 where the polish rate of high surface area abrasives ($\sim 300\text{m}^2/\text{g}$) was compared to low surface area ($\sim 30\text{m}^2/\text{g}$) abrasives at various concentrations. The polished wafers had a resistivity of approximately $2.2\text{m}\Omega\cdot\text{cm}$, which is expected to have a low polish rate.

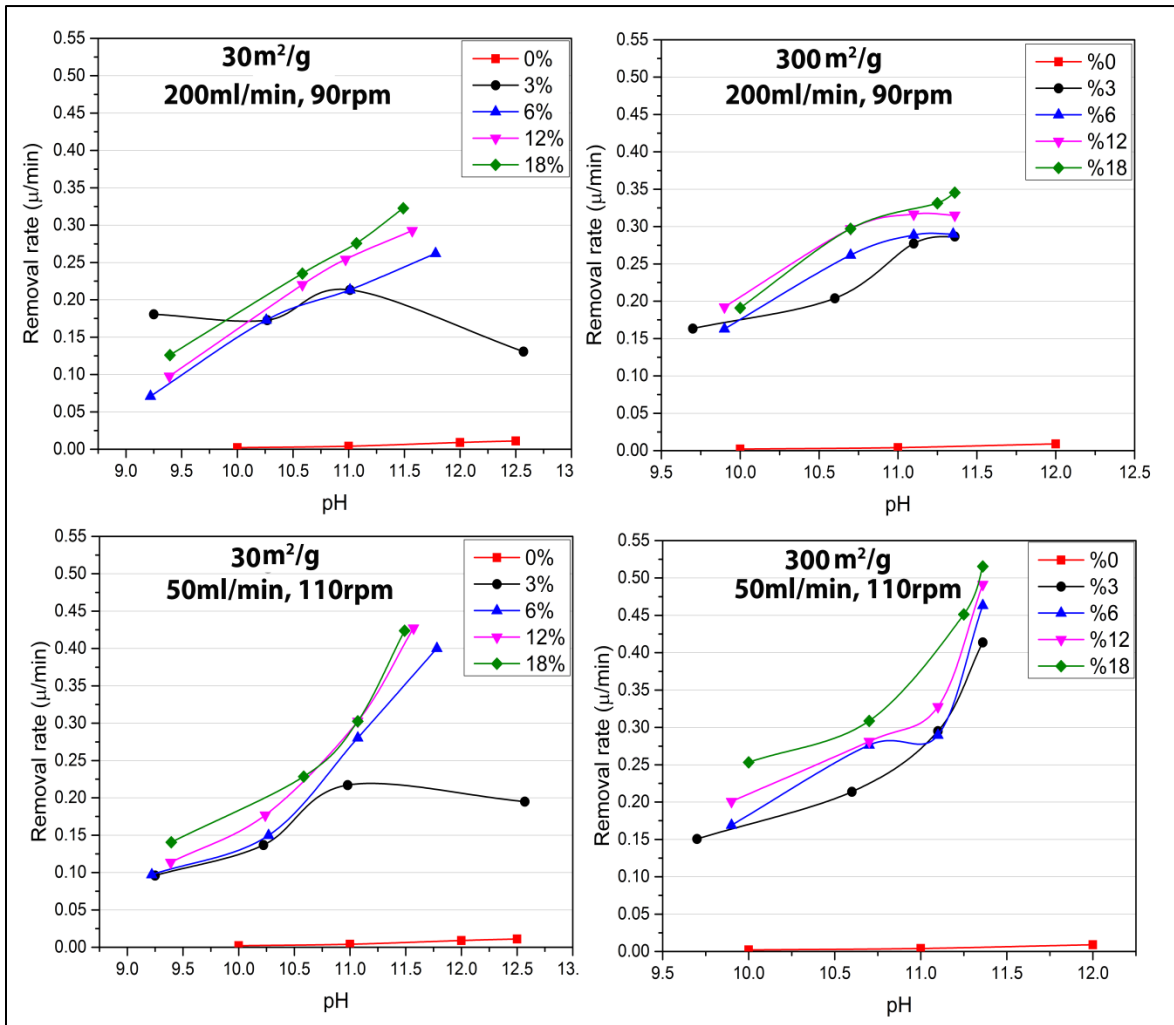


Figure 5-4. Polish rate as function of pH for different polish conditions and slurries.

As shown in Figure 5-4 increasing pH improves the polish rate with one exception, larger abrasives ($30\text{m}^2/\text{g}$) and at 3wt% silica. The polish rate increases with pH due to the increase of hydroxyl anions as a strong polarizer and the main agent of silicon

etching. In the case of larger abrasives ($30\text{m}^2/\text{g}$) and at 3wt% silica at the lower pH, the silica dissolution rate for abrasives with small surface area is low, thus the actual abrasive concentration is greater than other slurries evaluated at this pH. Therefore the polish rate is higher than expected. For 3 wt %, with increasing pH most of the silica is dissolved and there is hardly any abrasive in the slurry. This leads to the reduction of polish rate to levels observed for 0 wt% abrasives. This effect is more evident for Case 1 with higher flow rate (200 ml/min) since the role of slurry is more dominant than Case 2 with lower flow rate (50 ml/min).

It is also clear that in general increasing the abrasive concentration from 3-6 wt% enhances the polish rate. Higher concentrations of abrasives increase the interaction of hard solid particles with the surface both as the hydroxyl anion carrier and the sub-nano wafer surface scratcher. The role of abrasives in wafer planarization can be understood by comparing the polish rate of 0wt% abrasive with other curves. The polish rate of slurry without abrasive is almost zero and it seems that the chemical effects (surface etching at room temperature) at high pH cannot polish the silicon surface solely. However, it appears in Figure 5-4 that there is a saturation limit for the abrasive concentration and above 6 wt% silica there is no significant change in the polish rate. This is due to the fact that above the saturation limit the wafer surface is already covered with abrasives and more abrasives cannot change the polish rate. It is also clear that because of the increase of interaction between abrasives, at higher concentrations they are more susceptible to agglomeration. Due to the agglomeration effect and the higher costs of higher concentrated slurries, it is more desirable to

optimize the abrasive concentration. This means that the silica concentration of 6wt% is optimum with respect to removal rate, cost and colloidal stability.

Particle size is another important factor which affects the polish behavior. Comparing polish rate of high surface area abrasives (particle size ~3nm), with low surface area (particle size ~60nm), shows an increase of about 15% polish rate as shown in Figure 5-5. Increasing the surface area and the interaction of silica abrasives with the polysilicon surface is the key factor of this phenomenon.

Comparison between Cases 1 and 2 for different abrasive sizes and two optimum silica concentrations is shown in Figure 5-5, where Case 2 shows higher polish rates at high pH than Case 1. As discussed earlier, reaction of hydroxyl anions and formation of silicic acid reduced the pH of the slurry during polishing. This can be clearly observed in Figure 5-5 and using buffers can minimize this effect. On the other hand, Case 2 is expected to show higher polish rates due to the increase of mechanical forces during polishing. This means that at high slurry pH and low resistivity of the wafer, the mechanical factor is dominant. This can be an evidence to prove the role of high doping level on the hydroxyl anion transportation through the surface of the wafer. Since this effect is more evident at lower resistivities, mechanical factors are dominant in high doping level silicon wafer. It can be concluded that at wafers with extremely low resistivity, Case 2 with dominant mechanical force is favorable.

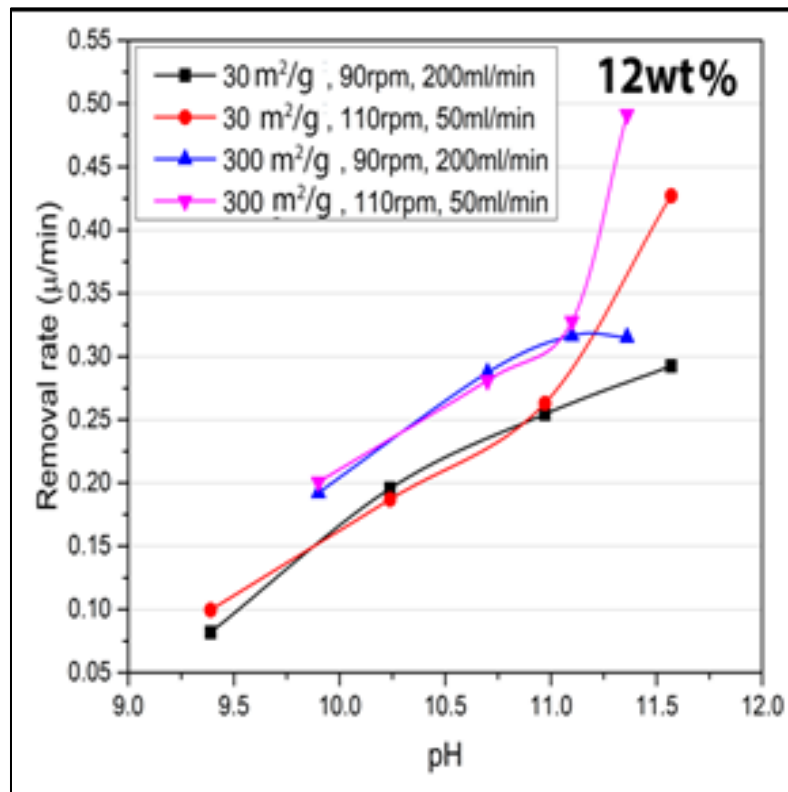
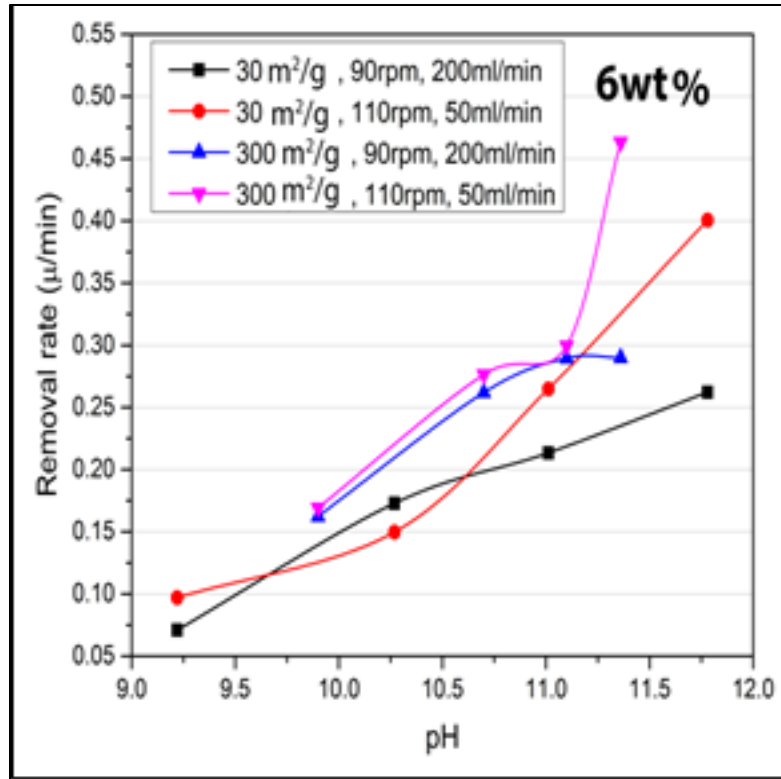


Figure 5-5. Effect of polish condition and particle size on the polish rate at 6psi pressure and with 6 and 12wt.% of silica abrasive. Case 1 is 90rpm and 200ml/min, Case 2 is 110rpm and 50ml/min.

By increasing the pH of the solution for Case 2, a sudden increase of polish rate was observed unlike Case 1. This can be attributed to the mechanical interactions on the wafer surface. For Case 2 with high mechanical forces, a minimum amount of slurry is expected to exist between the wafer and the pad [17]. Therefore the friction force and the polish temperature are higher than case 1 as illustrated in Figure 5-6. Since silicon etching is an exothermic process [46], [47], by increasing pH the polish temperature is expected to increase further. However, the slurry can act as the coolant during polishing and for Case 1 with higher flow rate the increase of temperature with pH was not observed. For Case 2 with low flow rate, there is not enough slurry to reduce the polish temperature sufficiently. Therefore, a notable increase of polish temperature is observed for Case 2. On the other hand, increasing the temperature can increase the etch rate significantly. In general, a 10°C increase in the temperature could double the etch rate [88]. This indicates that the polish temperature can directly affect the polish rate and for Case 2 higher polish rates were observed at higher pH values.

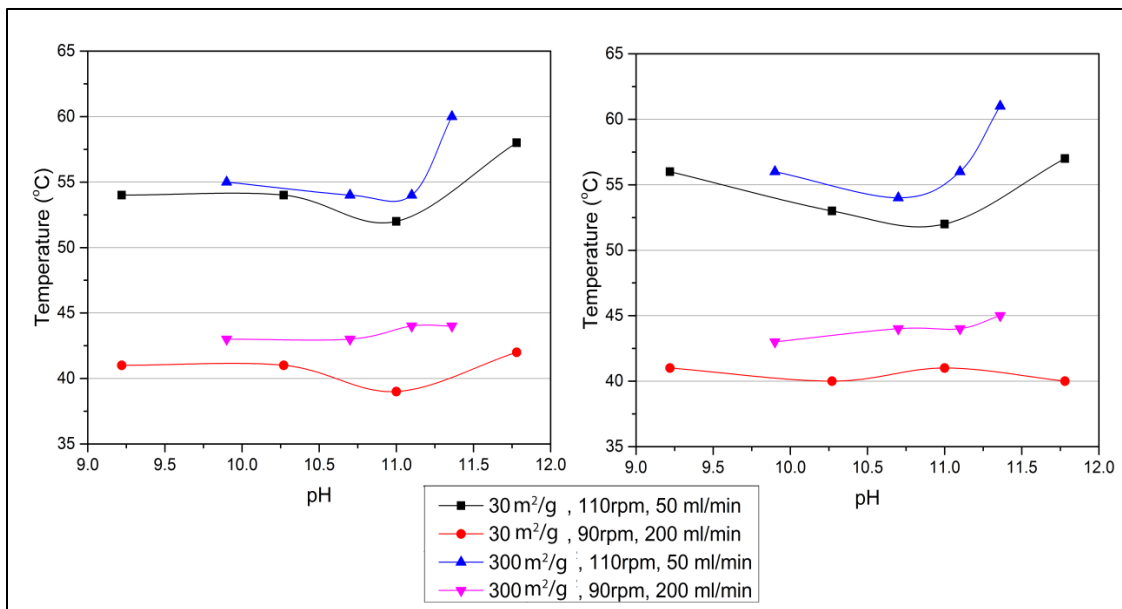


Figure 5-6. Effect of slurry chemistry, silica abrasive properties and polish condition on polish temperature.

5.5 Conclusion

In this chapter the influence of the slurry characteristics (slurry chemistry and abrasive properties) on the CMP of heavily boron-doped polysilicon were studied. The effect of slurry pH on silica abrasive size and colloidal stability was also investigated. High slurry pH showed a significant dissolution of slurry with rates depended on the silica concentration and size, and slurry pH. While the effect of slurry chemistry on polish rate showed that in most cases increasing the pH can improve the removal rate, abrasive properties had a more complicated behavior. Optimum abrasive concentration was observed at ~6wt% and higher concentrations did not improve the polish rate due to the saturation of the slurry on the wafer surface. The effect of abrasive size was more dominant and it was shown that smaller particles with 10 time higher surface area improved the polish rate ~20%. Finally polish conditions with mechanical and chemical dominance were compared and high mechanical polishing showed a superior polish rate.

Chapter 6. Boron doping effects on polysilicon CMP

The doping of polysilicon has a notable influence on the polish rate. As shown in Figure 1-10, the depleted layer of ions on the surface of the thin polysilicon films strongly impacts the hydroxyl anion migration through the wafer surface. The hydroxyl repulsion by negative anions such as boron and attraction by positive anions such as phosphorous cause this significant change in polish rate. This effect is more evident on p-type semiconductors. Liu *et al.* suggested that in the n-type wafers, the removal is limited by the surface reaction instead of hydroxyl transportation. The effect of dopant type on removal rate is schematically shown for phosphorous and boron doped polysilicon in Figure 6-1. Since boron shows higher deposition rate and slightly higher maximum doping level and conductivity (due to smaller atomic size) than phosphorous, it is considered the best candidate for the fabrication processes. From Liu *et al.* model and our results in Chapter 4, it can be concluded that the boron as a dopant mainly affects the polish rate by hindering the chemical aspects of CMP. In this chapter we will investigate the above statement by comparing different boron-doping level polishes and under different CMP conditions. By varying the polish conditions such as flow rate and polish speed the lubrication behavior and mechanical forces is expected to be altered.

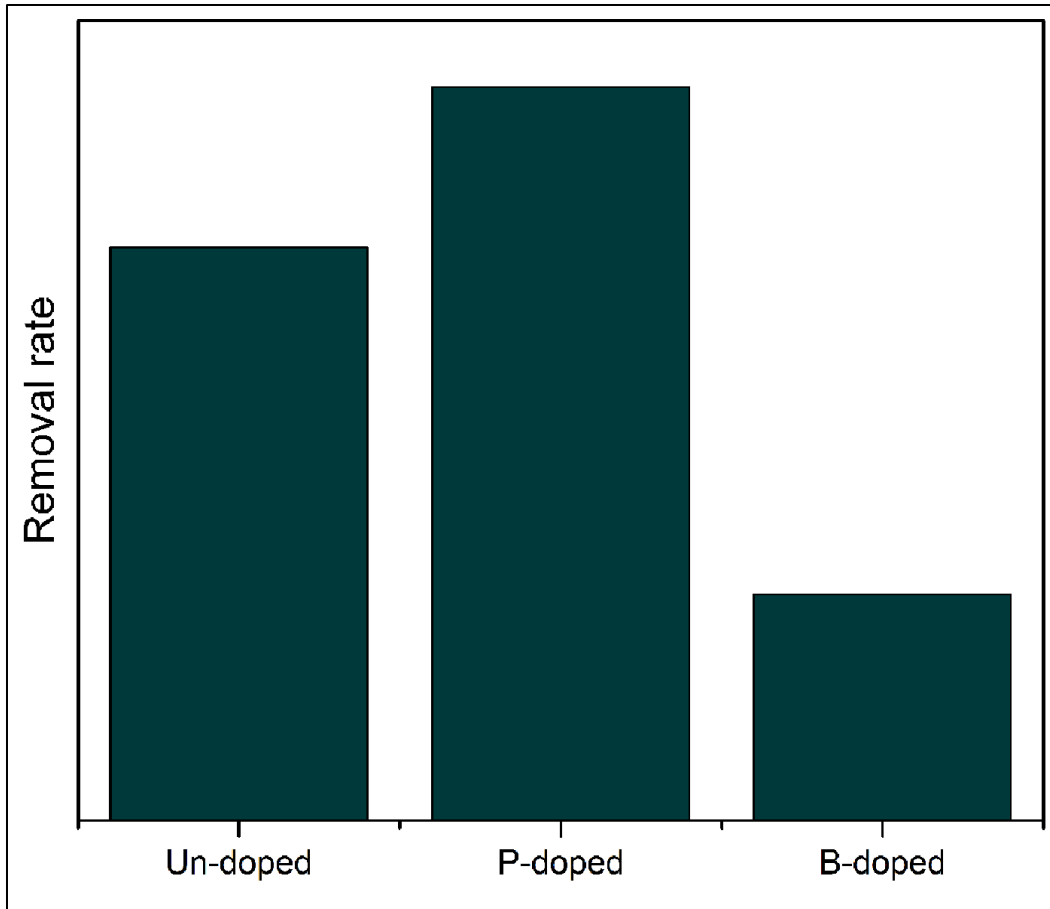


Figure 6-1. Effect of dopants on the polysilicon CMP rate [28].

In this work the polish behavior of boron doped polysilicon with 2.2 mΩ.cm (wafer A) and 3.5 mΩ.cm (wafer B) was compared to the un-doped (wafer C) thin film. The carrier and boron-concentration measurement of wafer A was conducted by SRP and SIMS analysis respectively and is shown in Figure 6-2. The SRP results were close to the data in Figure 1-6 and are expected to have $6.02 \times 10^{19} \text{ cm}^{-3}$ carrier concentration for wafer A and $3.1 \times 10^{19} \text{ cm}^{-3}$ for wafer B. This indicates a ~100% increase of activated boron atoms in the polysilicon structure of wafer A. Increasing the conductivity and carrier hole concentration is desirable since a smaller via can be used to achieve the

expected resistance. As illustrated in Figure 6-2, there is a difference between the carrier and boron concentration in wafer A. While the carrier concentration is $\sim 4.6 \times 10^{19}$ atoms/cm³ the boron concentration was more than 7.35×10^{20} atoms/cm³. This indicates that only a small portion of boron atoms (<10%) have been activated in the silicon structure. This may be due to the change in boron solid solubility going from the deposition temperature (885.5 K) to room temperature (295 K). It has been shown that the solid solubility of boron in silicon at 885.5 K is more than 10^{20} atoms/cm³ (which agrees with the SIMS data) while at room temperature it decreases to below 10^{19} atoms/cm³ [84]. This means that the excess boron inhabits non-substitutional sites such as non-silicon interstitial sites or precipitates at grain boundaries.

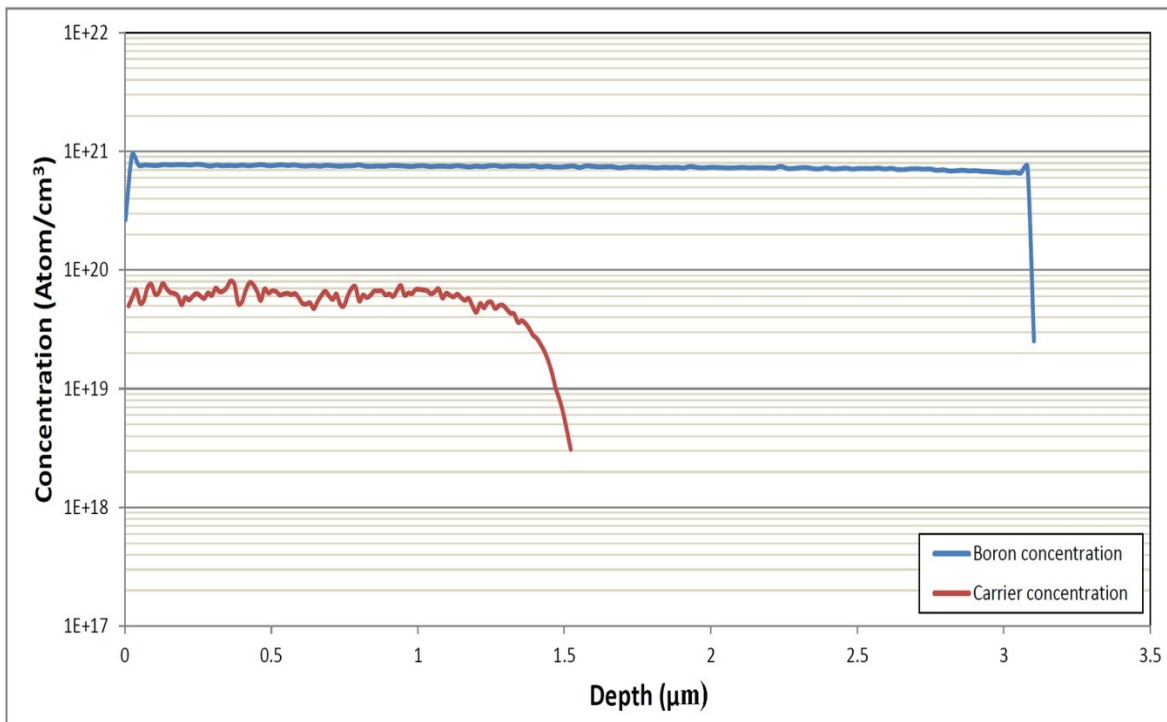
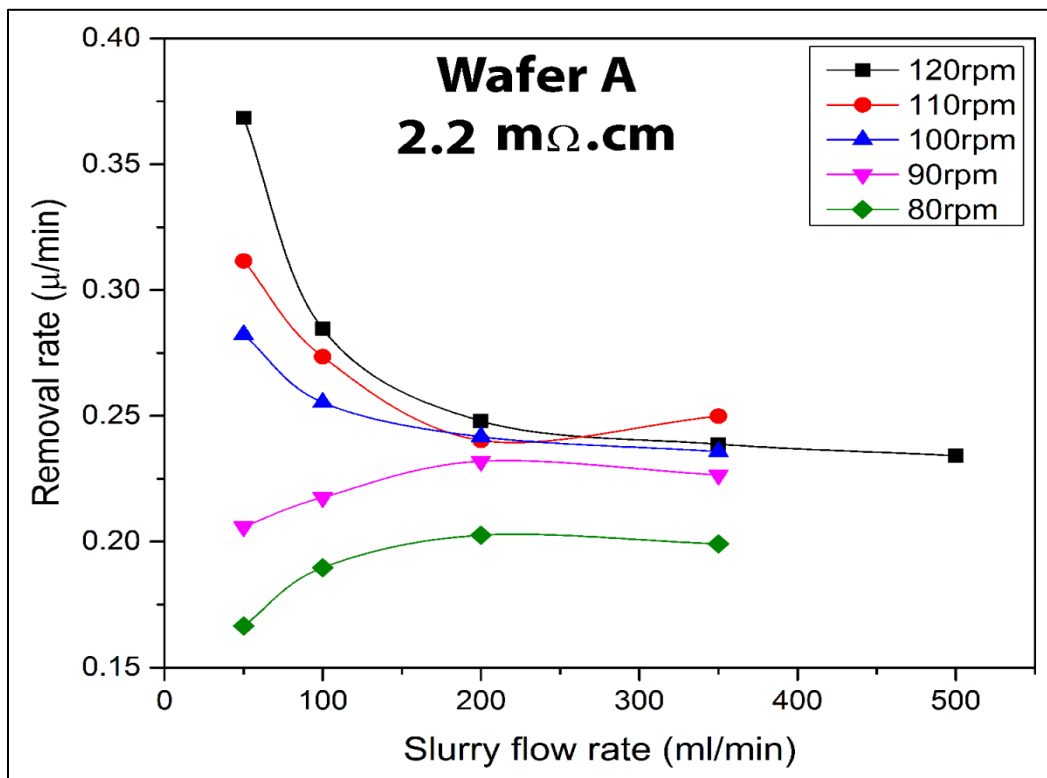


Figure 6-2. SRP and SIMS results for the 2.2 mΩ.cm sample.

In order to compare the polish rate at different doping levels, a relatively high polish condition, high pressure (6psi) and moderate-high velocity (80-120rpm) over a wide flow rate range (50-350ml/min) was used. The polish rate results are presented in Figure 6-3 and it is apparent that the polish behavior is completely different when the doping level is changed, that is, the polish rate has been significantly increased by reduction of film conductivity. A better comparison of removal rate is shown in Figure 6-4 for a moderate flow rate case (200ml/min). Other flow rates also followed the same trend and are not shown here for simplicity. Wafer A, with high boron concentration as hole donors, has a polish rate approximately 5 times lower than the polish rate for un-doped polysilicon. This difference is more noticeable between the polish rate of wafers A and B where a ~50% decrease in the doping level resulted in ~3 times higher polish rates.



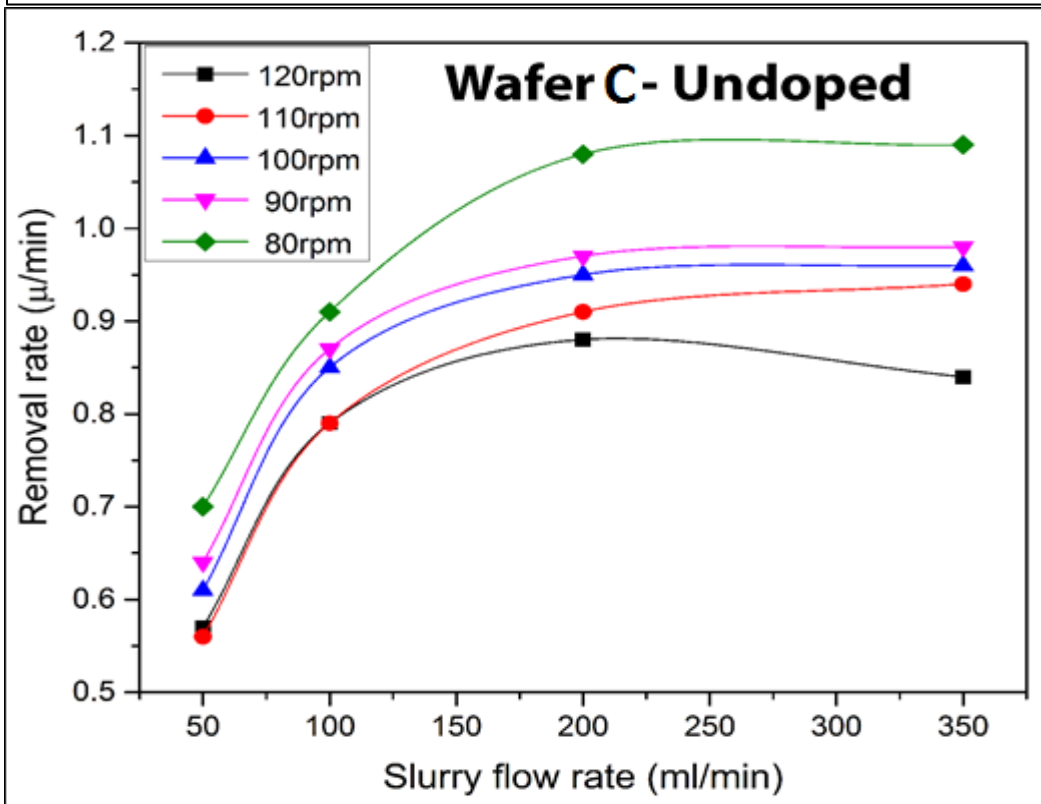
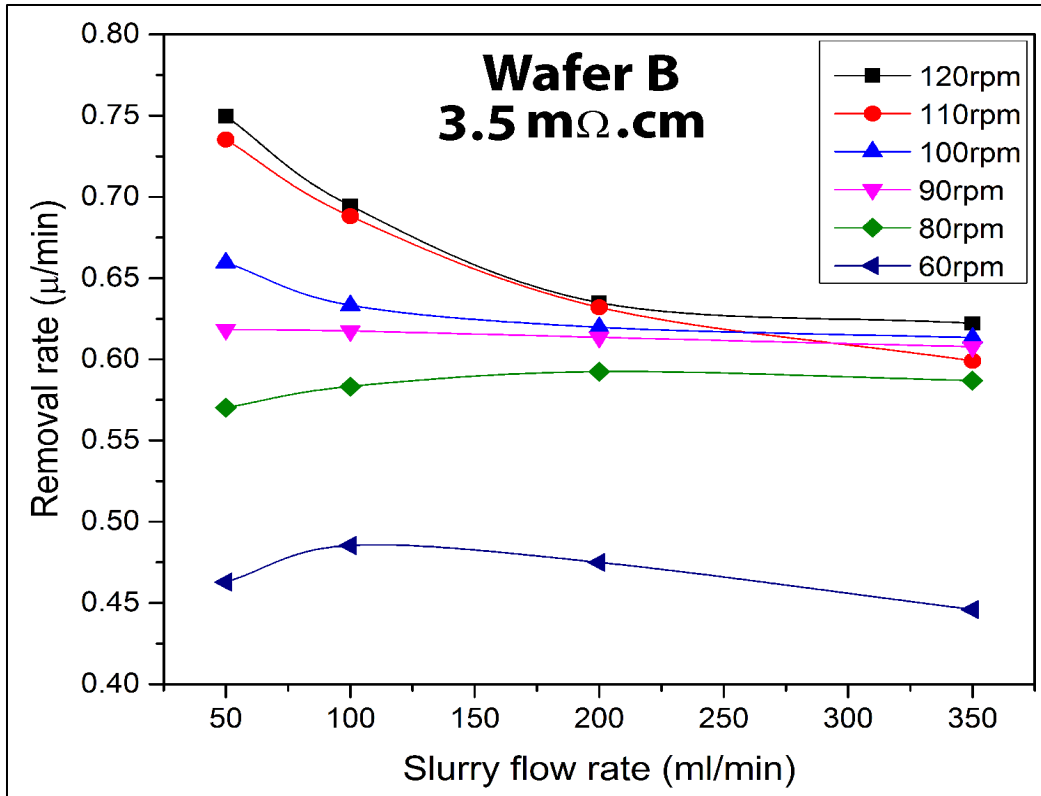


Figure 6-3. Polish rate at different flow rates and velocity with 6psi pressure.

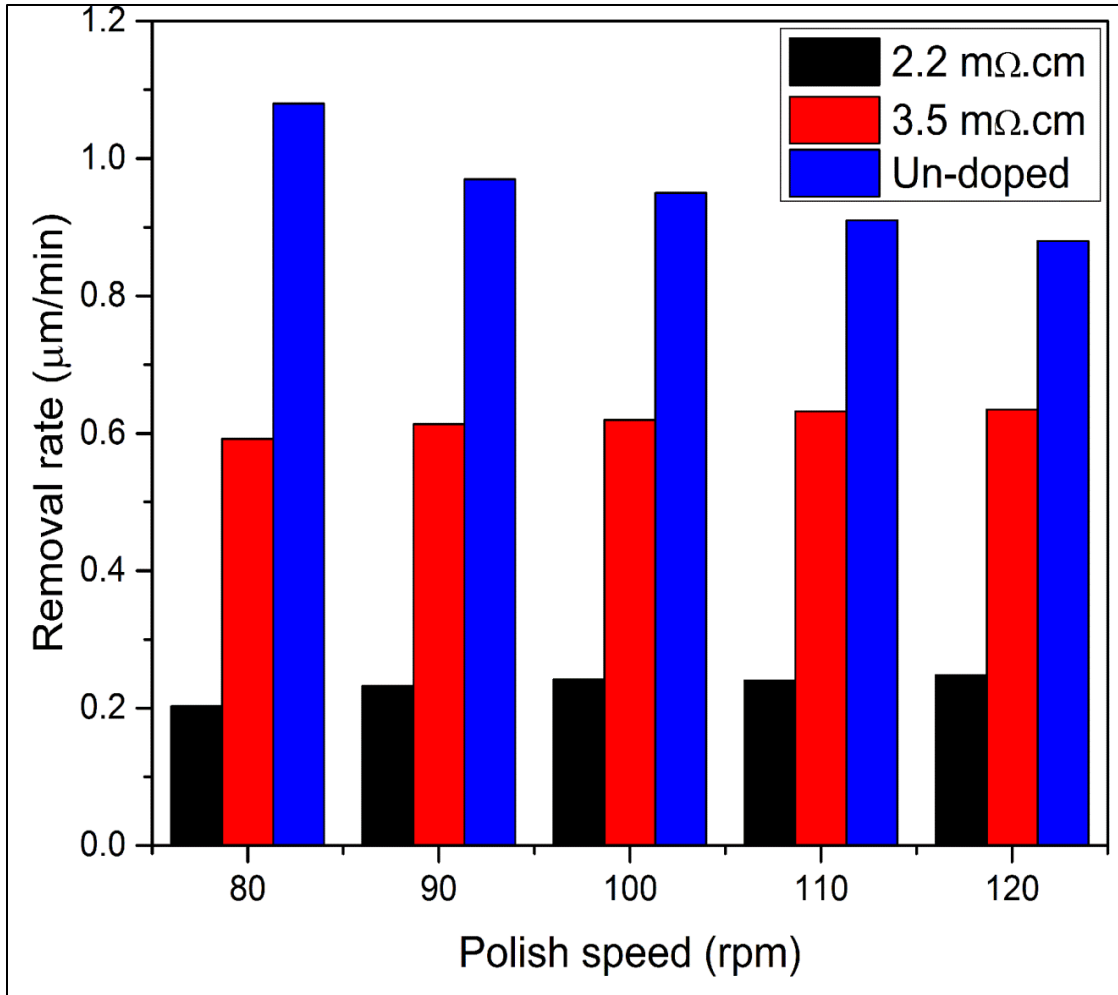


Figure 6-4. Comparison of polish rate as function of doping level for 200ml/min flow rate and 6psi pressure.

The relationship between doping and polish rate is not linear and is expected to have an exponential relationship as indicated by Figure 6-5 for a moderate polish condition (90rpm, 6psi, 200ml/min). This is due to the fact that for low conductivity thin film (un-doped) surface reactions limit surface removal. Since there is no boron in undoped polysilicon to hinder the transportation, no chemical agent transportation limiting occurs. For highly conductive samples the chemical agent transportation limits the process. An exponential equation was fitted to experimental results for different flow rates and polish speeds and is:

$$RR=A\rho^B \quad (6.1)$$

where RR is removal rate in ($\mu\text{m}/\text{min}$), ρ is thin film resistivity in ($\text{m}\Omega.\text{cm}$) and A and B are fitting terms, coefficient and power, respectively. Increasing A and reducing B leads to the decrease in the power of the equation. This indicates that the removal rate of a conductive thin film is improved and approaches the undoped polysilicon polish rate. A and B values were calculated to be in the range of 0.29-0.52 and 0.091-0.006, respectively, in this experiment. Higher values of A and lower values of B occurred under mechanically dominant conditions such as high polish speeds and low flow rates. This agrees with the hypothesis of this study that high mechanical and frictional forces are the main route to improve the heavily boron-doped polysilicon polish rate.

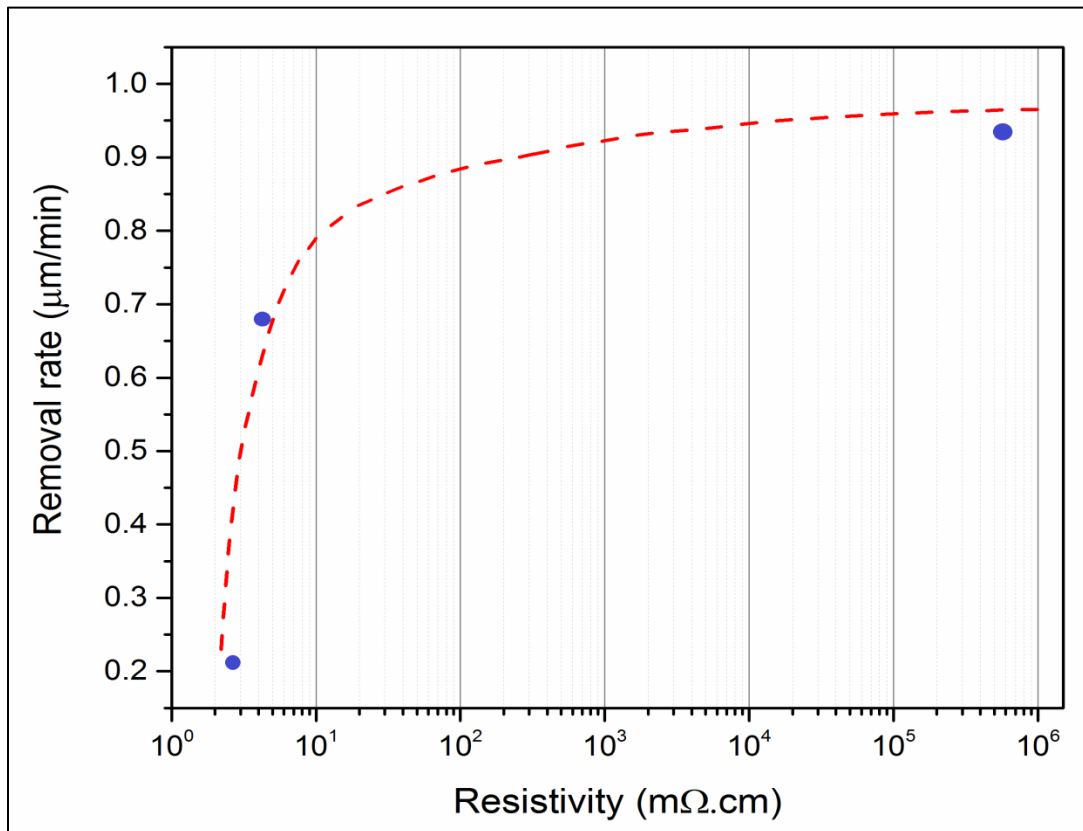


Figure 6-5. The effect of boron-doped polysilicon conductivity on the CMP rate, for the condition of 6pi pressure, 90rpm speed and 200ml/min flow rate. Other conditions follow the same trend as well.

For all three samples the polish rate seems to become independent of the flow rate at above ~ 200 ml/min. Thus, the 200 ml/min will be called the optimum flow rate. As mentioned before, boron doping significantly affects the polysilicon polish rate. By comparing the graphs in Figure 6-3, it is evident that other than polish rate, the trend of the curves is also different. Wafer A shows two different behaviors depending on the polish speed. At high polish speeds, reducing the slurry flow showed a significant polish rate increase. While for moderate velocities the effect was opposite. This was discussed in Chapter 4. Comparing the polishing trends for wafers A and B shows that by decreasing the boron concentration the slope of the curve decreases. In other words, wafer B showed less dependency of polish rate on slurry flow rate. The discrepancies in the slope are due to the change in wafer conductivity. Wafer C has a different trend for all polish speeds; the polish rate improves with increasing flow rate. To quantify this, the ratio of removal rate at the lowest flow rate (50ml/min) with maximum mechanical forces to the optimum flow rate (200ml/min) is shown in Figure 6-6. It is clear that the flow rate has more effect on wafer A. This proves our hypothesis that the chemical force suppression plays the key role in the dependency of polish rate on the doping level. The slope of the graphs in Figure 6.6 represents the ratio of mechanical forces to chemical forces. The results shown in Figure 6-6 indicate that for wafer A, with maximum carrier concentration and at high polish speeds, the mechanical effects are more dominant since the ratio exceeds 1. For wafer C the ratio is below 1 for all the polish speeds, and the curve shows a slope close to zero. Since mechanical effects for the three tested wafers can be assumed to be similar (because the polish condition is the same for the tested wafers), the decrease in the ratio and the slope can be

attributed to the increase in the chemical components of polishing. From wafer A to C the dependency of polish on the mechanical factors and friction force decreases.

Hydroxyl anion repulsion in the presence of boron makes the effect of mechanical interactions more significant and by changing the flow rate and consequently moving from the boundary lubrication regime to the dry lubrication regime; the rapid change of removal rate is observed.

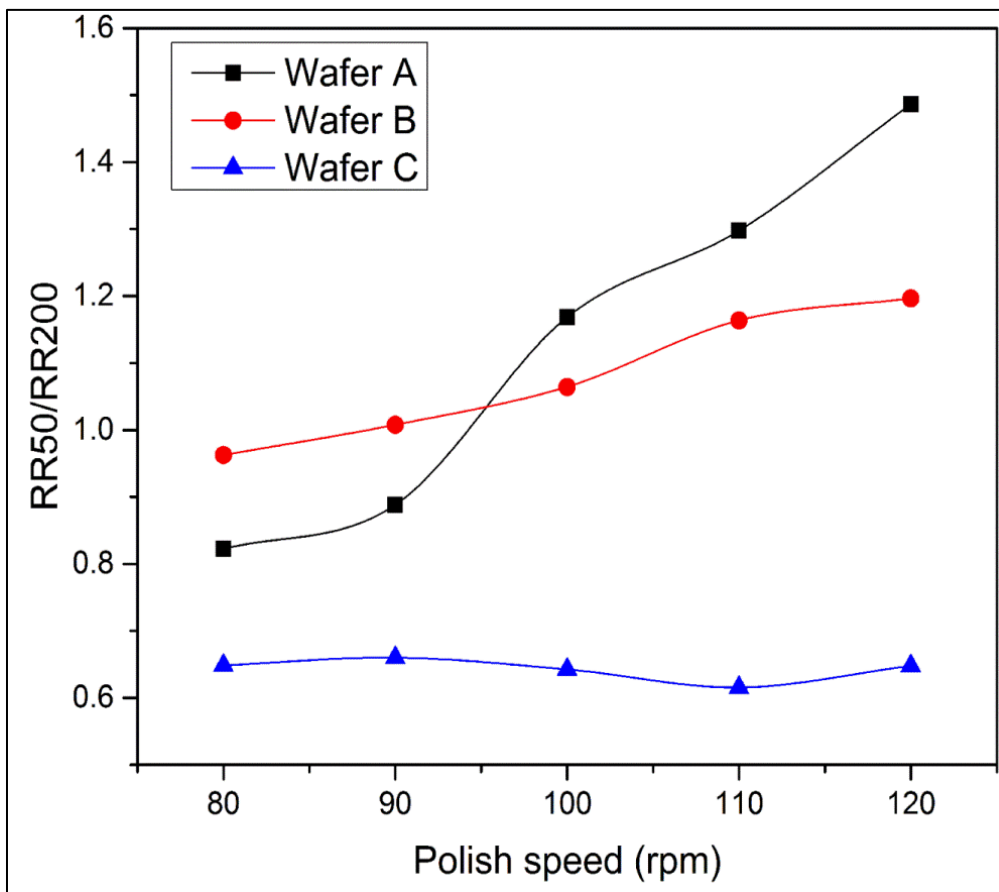


Figure 6-6. Removal rate ratio at highly mechanical condition of 50ml/min (RR50) and optimum flow rate of 200ml/min (RR200) vs. the polish velocity.

6.1 Conclusion

Boron doping showed a significant effect on the polysilicon polish rate. The un-doped polysilicon shows approximately 5 times higher polish rate than the heavily boron-doped polysilicon. In this chapter we suggested that the limitation of the slurry chemical agent transportation on the wafer surface is responsible for this retardation effect. The aim of this work was to examine this hypothesis by comparing the chemical and mechanical components of polishing. An exponential relation between the boron doping level and material removal rate was observed. At high doping levels (low resistivities) the hydroxyl ion transportation limited the etching process, while at lower doping levels (high resistivities) the surface reaction was responsible for the limiting of the process. It was also shown that by reducing the doping level, the role of surface chemical etching is reduced.

Chapter 7. Summary

Increasing the conductivity of polysilicon by boron doping has been shown to have a significant CMP rate suppression. In this work, it is hypothesized that this effect is due to limiting of the transportation of chemical agents of the CMP slurry (hydroxyl anion) on the wafer surface. The hypothesis was tested by investigating the nature of the boron-doped polysilicon polishing. This was carried out through studying the process parameters such as polish pressure, temperature, velocity and flow rate, and slurry properties such as chemistry and abrasives, and the doping level effects. The outcome of this thesis is briefly described below.

- The lubrication behavior of CMP had a significant effect on the polish rate. Altering the lubrication regime from hydrodynamic lubrication with low mechanical interactions to boundary and dry lubrication with maximum wafer-pad contact was responsible for approximately 8 times increase in the polish rate. Polishing under hydroplaning conditions showed a small polish rate due to minimum friction force between the wafer and the pad. This means that increasing the slurry flow rate does not always increase the polish rate.
- Influence of chemical and mechanical components of polishing on removal rate was studied separately. Heating the slurry mimicked a chemically dominant CMP condition by improving the chemical etching effects and reducing the pad hardness. It was also shown that mechanical forces are the dominant factor for heavily boron-doped polysilicon polishing. By improving

the mechanical interactions and friction force between the wafer and the pad the polish rate was increased significantly.

- The slurry chemistry and abrasive properties also affected the polish rate. The optimum pH of the colloidal silica solution is between pH~11-12. Presence of abrasives is also critical to the achievement of acceptable polish rates. Polishing with abrasive-less slurry showed almost zero surface removal. The most common abrasive used for polysilicon polishing is colloidal silica with high stability at basic pH values. The particle size showed greater effect on polishing than abrasive concentration. Using silica with higher surface area ($300\text{m}^2/\text{g}$) gave a ~40% higher polish rate than larger abrasives with $30\text{m}^2/\text{g}$ surface area. On the other hand, 3-6wt% of abrasive concentration was enough for polishing, and using higher concentrations of silica abrasives had a small effect on the removal rate.
- The effect of boron doping level on the polish rate of polysilicon was investigated and an exponential relation between the removal rate and thin film resistivity was observed. By heavily boron-doping the polysilicon thin film, the polish rate was reduced significantly (more than 5 times). It was shown that the boron chemical retardation of polishing is responsible for this. By increasing the polysilicon resistivity the role of chemical forces become more evident.
- In this study we were able to achieve higher removal rates by enhancement of both the mechanical and chemical components of polishing. By modifying the polish methodology the removal rate was increased up to ~100% and by using

a high pH silica slurry the removal rate was improved up to ~40%. A brief comparison of the mentioned polish rate progress is shown in Figure 7-1. The surface quality after

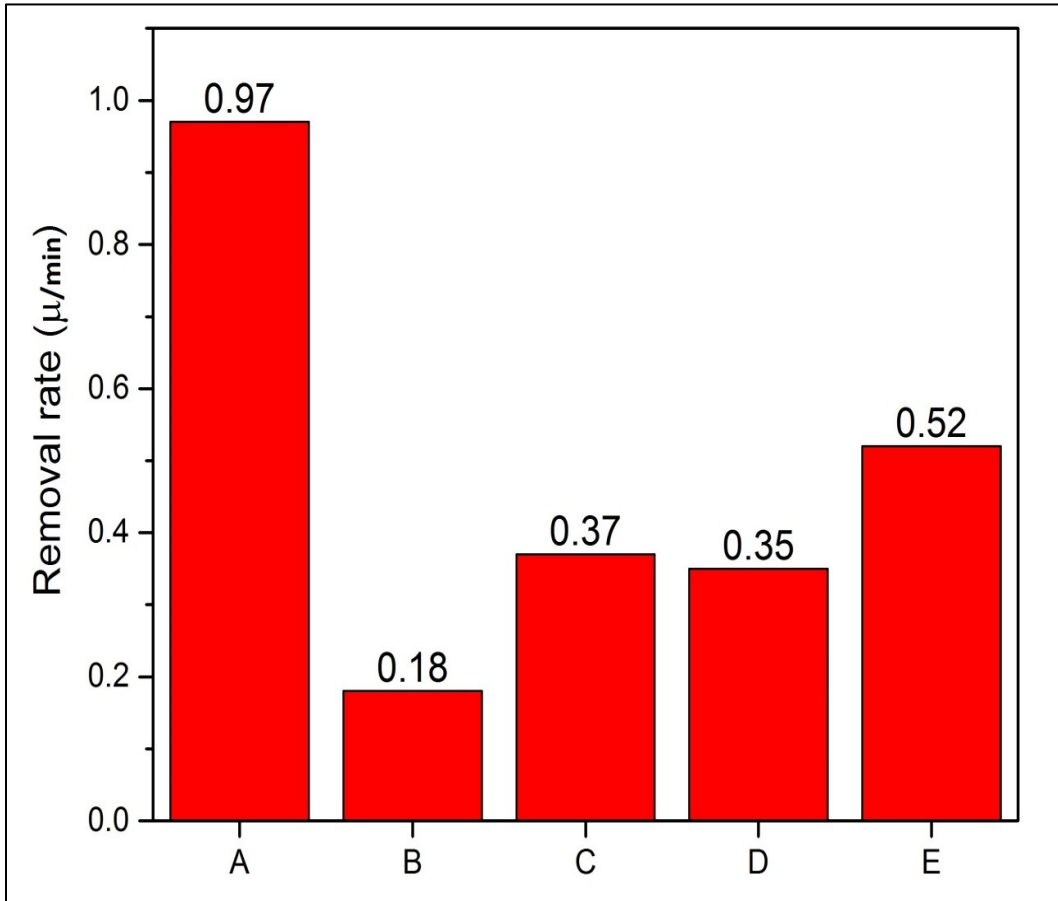


Figure 7-1. Polish rate comparison for different conditions: A. Undoped poly, commercial polish slurry (Fujimi) and moderate polish condition (6psi pressure, 80rpm speed, 200ml/min flow rate) B. Heavily boron-doped poly, commercial polish slurry and moderate polish condition C. Heavily boron-doped poly, commercial polish slurry and mechanically enhanced condition D. Heavily boron-doped poly, moderate polish condition and developed silica slurry E. Heavily boron-doped poly, mechanically enhance polish condition and developed silica slurry.

Future work

The focus of this work is on the removal rate of highly boron-doped polysilicon. In order to confirm the proposed mechanism for the role of boron on polysilicon polishing and developing a commercial high pH slurry, some other experiments are required. This section identifies the specific areas which require further work.

- Heavily boron-doped amorphous silicon: As discussed earlier, it is expected that the electrically activated boron atoms are responsible for the polish rate reduction. In amorphous boron doped films, the boron is not activated and the polish rate is expected to increase with respect to a polysilicon film with the same boron concentration. This fabrication process requires relatively low deposition temperatures (below 500°C) and therefore the deposition rate is much lower than polysilicon deposition.
- Deposition at lower temperatures: Deposition of boron-doped polysilicon at temperatures below 600 °C resulted in higher conductivity. This effect and the polish rate of this sample need to be studied in future.
- Interactions between pad, wafer and abrasives on the nanoscale: This can be carried out by surface force apparatus (SFA) to investigate the attraction, repulsion and friction force between materials.
- Using abrasives with other morphologies: There have been a few studies focusing on the role of abrasive morphology on the polish behavior. It is expected to increase the polish rate by using abrasives with rough surface shape instead of perfectly spherical. This is due to the increase of specific surface area and interactions between abrasives and wafer.

- Studying the polish rate selectivity: In commercial applications a polysilicon slurry must have a much higher polish rate than the underlying SiO_2 or Si_3N_4 film. Organic chemical additives such as amino acids can be added to the slurry to suppress the polish rate of these underlying films and increase the polish rate selectivity.

Bibliography

- [1] G. E. Moore, “Cramming More Components onto Integrated Circuits,” *Proceedings of the IEEE*, vol. 86, no. 1, pp. 82–85, 1998.
- [2] P. Van Zant, *Microchip fabrication*. McGraw-Hill, 2000.
- [3] Y. Li, Ed., *Microelectronic applications of chemical mechanical planarization*. Wiley Interscience, 2007.
- [4] H. Hocheng and Y. Huang, “A comprehensive review of end point detection in chemical mechanical polishing for deep-submicron integrated circuits manufacturing,” *Engineering*, no. 6, pp. 1–18, 2002.
- [5] Y. Eineli and D. Starosvetsky, “Review on copper chemical–mechanical polishing (CMP) and post-CMP cleaning in ultra large system integrated (ULSI)—An electrochemical perspective,” *Electrochimica Acta*, vol. 52, no. 5, pp. 1825–1838, Jan. 2007.
- [6] P. B. Zantye, A. Kumar, and a. K. Sikder, “Chemical mechanical planarization for microelectronics applications,” *Materials Science and Engineering: R: Reports*, vol. 45, no. 3–6, pp. 89–220, Oct. 2004.
- [7] M. R. Oliver, Ed., *Chemical-Mechanical Planarization of Semiconductor Materials*. Springer, 2004.
- [8] K. Cadien, L. Nolan, H. Pirayesh, Z. Dawkins, and Z. Xu, “Electrodeposition and surface finishing,” S. Djokic, Ed. Springer, 2013.
- [9] L. M. Cook, “Chemical Processes in Glass Polishing,” *Journal of non-crystalline solids*, vol. 120, pp. 152–171, 1990.
- [10] R. K. Iler, *The Chemistry of Silica: Solubility, Polymerization, Colloid and Surface Properties and Biochemistry of Silica*. Wiley-Interscience, 1979.
- [11] P. Garrou, C. Bower, and P. Ramm, Eds., *Handbook of 3D Integration: Volume 1-Technology and Applications of 3D Integrated Circuits*. Wiley Interscience, 2012.
- [12] D. Henry, X. Baillin, V. Lapras, M. Vaudaine, J. Quemper, N. Sillon, B. Dunne, C. Hernandez, and E. Vigier-Blanc, “Via first technology development based on high aspect ratio trenches filled with doped polysilicon,” in *2007 Proceedings 57th Electronic Components and Technology Conference*, 2007, pp. 830–835.

- [13] G. Parès, N. Bresson, S. Moreau, V. Lapras, D. Henry, and N. Sillon, "Effects of Stress in Polysilicon VIA - First TSV Technology," in *12th Electronics Packaging Technology Conference*, 2010, pp. 333–337.
- [14] C. Su, T. Tsai, Y. Liou, Z. Lin, and H. Lin, "Gate-All-Around Junctionless Transistors With Heavily Doped Polysilicon Nanowire Channels," *IEEE Electron Device Letters*, vol. 32, no. 4, pp. 521–523, 2011.
- [15] Y. Laghla, E. Scheid, H. Vergnes, and J. P. Couderc, "Electronic properties and microstructure of undoped, and B- or P-doped polysilicon deposited by LPCVD," *Solar Energy Materials and Solar Cells*, vol. 48, no. 1–4, pp. 303–314, Nov. 1997.
- [16] P. R. D. Veera, A. Natarajan, S. Hegde, and S. V Babu, "Selective Polishing of Polysilicon during Fabrication of Microelectromechanical Systems Devices," 2009.
- [17] H. Pirayesh and K. Cadien, "High rate chemical mechanical polishing of boron-doped polycrystalline silicon," *ECS Journal of Solid State Science and Technology*, vol. 3, no. 6, pp. P213–P218, May 2014.
- [18] J. Mihaychuk, "Toshiba TSV technology in a back (side) illuminated sensor," 2011. [Online]. Available: <http://www.chipworks.com/en/technical-competitive-analysis/resources/blog/toshiba-tsv-technology-in-a-back-side-illuminated-sensor/>.
- [19] G. J. Pietsch, G. S. Higashi, and Y. J. Chabal, "Chemomechanical polishing of silicon: surface termination and mechanism of removal," *Applied Physics Letters*, vol. 64, no. 23, p. 3115, 1994.
- [20] G. J. Pietsch and G. S. Higashi, "The atomic-scale removal mechanism during chemo-mechanical polishing of Si (100) and Si (111)," *Surface Science*, vol. 333, pp. 395–401, 1995.
- [21] M.-Y. Lee, H.-G. Kang, M. Kanemoto, U. Paik, and J.-G. Park, "Effect of Alkaline Agent in Colloidal Silica Slurry for Polycrystalline Silicon Chemical Mechanical Polishing," *Japanese Journal of Applied Physics*, vol. 46, no. 8A, pp. 5089–5094, Aug. 2007.
- [22] R. P. Venkatesh, Y. N. Prasad, T.-Y. Kwon, Y.-J. Kang, and J.-G. Park, "Effect of Alkaline pH on Polishing and Etching of Single and Polycrystalline Silicon," *Japanese Journal of Applied Physics*, vol. 51, p. 071301, Jun. 2012.
- [23] K. Park, H. Kang, M. Kanemoto, and J. Park, "Effects of the Size and the Concentration of the Abrasive in a Colloidal Silica (SiO₂) Slurry with Added TMAH on Removal Selectivity of Polysilicon and Oxide Films in Polysilicon Chemical Mechanical Polishing," vol. 51, no. 1, pp. 214–223, 2007.
- [24] S. M. Sze, *VLSI Technology*. McGraw-Hill Book Company, 1983.

- [25] J. R. Senna, R. L. Smith, I. D. P. Espaciais, and S. J. Campos, "Gallium doping for silicon etch stop in KOH," in *8th International Conference on Solid-State Sensors and Actuators, and Eurosensors*, 1995, pp. 194–197.
- [26] J. Watanabe, G. Yu, O. Eryu, I. Koshiyama, K. Izumi, K. Nakashima, M. Umeno, T. Jimbo, and K. Kodama, "High precision chemical mechanical polishing of highly-boron-doped Si wafer used for epitaxial substrate," *Precision Engineering*, vol. 29, no. 2, pp. 151–156, Apr. 2005.
- [27] W. L. Yang, C. Cheng, M. Tsai, D. Liu, and M. Shieh, "Retardation in the Chemical – Mechanical Polish of the Boron-Doped Polysilicon and Silicon," *IEEE Electron Device Letters*, vol. 21, no. 5, pp. 218–220, 2000.
- [28] M. Forsberg, N. Keskitalo, and J. Olsson, "Effect of dopants on chemical mechanical polishing of silicon," *Microelectronic Engineering*, vol. 60, pp. 149–155, 2002.
- [29] D. Liu, M. Tsai, W. L. Yang, and C. C. C., "Effects of impurities on removal of polysilicon in chemical-mechanical polish," *Journal of electrochemical society*, vol. 30, no. 1, pp. 53–58, 2001.
- [30] S. Oh and J. Seok, "Modeling of chemical–mechanical polishing considering thermal coupling effects," *Microelectronic Engineering*, vol. 85, no. 11, pp. 2191–2201, Nov. 2008.
- [31] P. R. Veera Dandu, B. C. Peethala, N. K. Penta, and S. V. Babu, "Role of amines and amino acids in enhancing the removal rates of undoped and P-doped polysilicon films during chemical mechanical polishing," *Colloids and Surfaces A: Physicochemical and Engineering Aspects*, vol. 366, no. 1–3, pp. 68–73, Aug. 2010.
- [32] Y. Wang, Y. W. Zhao, and X. Chen, "Chemical Mechanical Planarization from Macro-Scale to Molecular-Scale," *Materials and Manufacturing Processes*, vol. 27, no. 6, pp. 641–649, Jun. 2012.
- [33] L. Hong and C. David, *Tribology in Chemical-Mechanical Planarization*. Taylor & Francis Group, 2005.
- [34] J. Williams, *Engineering Tribology*. Cambridge University Press, 2005.
- [35] L. Charns and a. Philipossian, "Tribology and Removal Rate Characteristics of Chemical Mechanical Planarization Pads Containing Water Soluble Particles," *Japanese Journal of Applied Physics*, vol. 45, no. 7, pp. 5696–5701, Jul. 2006.
- [36] T. Kasai and B. Bhushan, "Physics and tribology of chemical mechanical planarization," *Journal of Physics: Condensed Matter*, vol. 20, no. 22, p. 225011, Jun. 2008.

- [37] T.-Y. Kwon, M. Ramachandran, and J.-G. Park, "Scratch formation and its mechanism in chemical mechanical planarization (CMP)," *Friction*, vol. 1, no. 4, pp. 279–305, Nov. 2013.
- [38] A. Y. Moon, "The Effect of Slurry Film Thickness Variation in CMP," University of California, Berkeley, 1999.
- [39] J. X. Su, J. X. Du, X. L. Liu, H. N. Liu, and R. K. Kang, "Study on lubricating behavior in chemical mechanical polishing," *Key Engineering Materials*, vol. 487, pp. 243–247, Jul. 2011.
- [40] D. Rosales-Yeomans, L. Borucki, T. Doi, L. Lujan, and a. Philipossian, "Implications of Wafer-Size Scale-up on Frictional, Thermal, and Kinetic Attributes of Interlayer Dielectric CMP Process," *Journal of The Electrochemical Society*, vol. 153, no. 4, p. G272, 2006.
- [41] R. Hellmann, "The albite-water system : Part II . The time-evolution of the stoichiometry function of pH at 100 , 200 , and 300 ° C of dissolution as a," vol. 59, no. 9, pp. 1669–1697, 1995.
- [42] Y. Niibori, M. Kunita, O. Tochiyama, and T. Chida, "Dissolution Rates of Amorphous Silica in Highly Alkaline Solution," no. May 2013, pp. 37–41.
- [43] K. B. Sundaram, A. Vijayakumar, and G. Subramanian, "Smooth etching of silicon using TMAH and isopropyl alcohol for MEMS applications," *Microelectronic Engineering*, vol. 77, no. 3–4, pp. 230–241, Apr. 2005.
- [44] H. J. Kim, Y.-J. Jang, J. Choi, B. Kwon, K. Lee, and Y. Ko, "Tribological approaches to material removal rate during chemical mechanical polishing," *Metals and Materials International*, vol. 19, no. 2, pp. 335–339, Mar. 2013.
- [45] Y. Sampurno, L. Borucki, Y. Zhuang, S. Misra, K. Holland, D. Boning, and A. Philipossian, "Characterization of thermoset and thermoplastic polyurethane pads, and molded and non-optimized machined grooving methods for oxide chemical mechanical planarization applications," *Thin Solid Films*, vol. 517, no. 5, pp. 1719–1726, Jan. 2009.
- [46] A. J. Nijdam, "Anisotropic Wet-chemical Etching of Silicon Pits, Peaks, Principles, Pyramids and Particles," University of Twente, 2001.
- [47] M. S. Kulkarni and H. F. Erk, "Acid-Based Etching of Silicon Wafers: Mass-Transfer and Kinetic Effects," *Journal of The Electrochemical Society*, vol. 147, no. 1, p. 176, 2000.
- [48] Y. Chen, L. C. Zhang, J. a. Arsecularatne, and C. Montross, "Polishing of polycrystalline diamond by the technique of dynamic friction, part 1: Prediction of the

- interface temperature rise,” *International Journal of Machine Tools and Manufacture*, vol. 46, no. 6, pp. 580–587, May 2006.
- [49] T. N. Farris, “Polishing and Lapping Temperatures,” vol. 1, no. January, 1997.
- [50] H. Hocheng and Y.-L. Huang, “In Situ Endpoint Detection by Pad Temperature in Chemical–Mechanical Polishing of Copper Overlay,” *IEEE Transactions on Semiconductor Manufacturing*, vol. 17, no. 2, pp. 180–187, May 2004.
- [51] F. W. Preston, “The Theory and Design of Plate Glass Polishing Machines,” *Journal of The Society of Glass Technology*, pp. 214–256, 1927.
- [52] Y. Homma, “Dynamical Mechanism of Chemical Mechanical Polishing Analyzed to Correct Preston’s Empirical Model,” *Journal of The Electrochemical Society*, vol. 153, no. 6, p. G587, 2006.
- [53] W.-T. Tseng and Y.-L. Wang, “Re-examination of Pressure and Speed Dependences of Removal Rate during Chemical-Mechanical Polishing Processes,” *Journal of The Electrochemical Society*, vol. 144, no. 2, p. L15, 1997.
- [54] W. Tseng, J. Chin, and L. Kang, “A Comparative Study on the Roles of Velocity in the Material Removal Rate during Chemical Mechanical Polishing,” vol. 146, no. 5, pp. 1952–1959, 1999.
- [55] L. Wu and C. Yan, “Modeling of the Effect of Wafer Topography on Chemical Mechanical Polishing Processes Based on 3D Analysis,” *Journal of The Electrochemical Society*, vol. 158, no. 3, p. H239, 2011.
- [56] J. Xin, W. Cai, and J. a. Tichy, “A fundamental model proposed for material removal in chemical–mechanical polishing,” *Wear*, vol. 268, no. 5–6, pp. 837–844, Feb. 2010.
- [57] S. K. Wang and D. L. Butler, “The evaluation and modeling of the CMP removal rate for polysilicon,” *International Journal of Nanoscience*, vol. 4, no. 4, pp. 753–760, 2005.
- [58] S. Oh and J. Seok, “An integrated material removal model for silicon dioxide layers in chemical mechanical polishing processes,” *Wear*, vol. 266, no. 7–8, pp. 839–849, Mar. 2009.
- [59] H. Shi and T. a. Ring, “Analytical solution for polish-rate decay in chemical–mechanical polishing,” *Journal of Engineering Mathematics*, vol. 68, no. 2, pp. 207–211, Mar. 2010.
- [60] G. Ahmadi and X. Xia, “A Model for Mechanical Wear and Abrasive Particle Adhesion during the Chemical Mechanical Polishing Process,” *Journal of The Electrochemical Society*, vol. 148, no. 3, p. G99, 2001.

- [61] G. Fu, A. Chandra, S. Guha, and G. Subhash, "A plasticity-based model of material removal in chemical-mechanical polishing (CMP)," *IEEE Transactions on Semiconductor Manufacturing*, vol. 14, no. 4, pp. 406–417, 2001.
- [62] M. Bastaninejad and G. Ahmadi, "Modeling the Effects of Abrasive Size Distribution, Adhesion, and Surface Plastic Deformation on Chemical-Mechanical Polishing," *Journal of The Electrochemical Society*, vol. 152, no. 9, p. G720, 2005.
- [63] D. O. Ouma, D. S. Boning, J. E. Chung, W. G. Easter, V. Saxena, S. Misra, and a. Crevasse, "Characterization and modeling of oxide chemical-mechanical polishing using planarization length and pattern density concepts," *IEEE Transactions on Semiconductor Manufacturing*, vol. 15, no. 2, pp. 232–244, May 2002.
- [64] D. Ouma, D. Boning, J. Chung, G. Shim, L. Olsen, and J. Clark, "An Integrated Characterization and Modeling M[ethodology for CMP Dielectric Planarization," pp. 67–69, 1998.
- [65] B. A Closed-form Analytic Model for ILD Thickness Variation in CMP Processes Stine, D. Ouma, R. Divecha, D. Boning, J. Chung, D. L. Hetherington, S. N. Laboratories, I. Ali, G. Shinn, J. Clark, T. Instruments, O. S. Nakagawa, S. Oh, H. P. Co, and P. Alto, "A Closed-form Analytic Model for ILD Thickness Variation in CMP Processes," pp. 1–8, 1997.
- [66] V. H. Nguyena and F. G. Shia, "Modeling of the removal rate in chemical mechanical polishing," vol. 4181, pp. 161–167, 2000.
- [67] L. Nolan and K. Cadien, "Nanofabrication: Techniques and Principles," E. M. Stepanova and S. Dew, Eds. Springer, 2012.
- [68] L. Nolan and K. Cadien, "Copper CMP: The Relationship between Polish Rate Uniformity and Lubrication," *ECS Journal of Solid State Science and Technology*, vol. 1, no. 4, pp. P157–P163, Aug. 2012.
- [69] I. D. Marinescu, E. Uhlmann, and T. K. Doi, Eds., *Handbook of Lapping and Polishing*. CRC Press Taylor & Francis Group, 2007.
- [70] Z. J. Pei, "Measurement Methods of Pad Properties for Chemical Mechanical Polishing," in *IMECE2007*, 2007, pp. 11–16.
- [71] S. Raghavan, "Particulate Science and Technology in the Engineering of Slurries for Chemical Mechanical Planarization," vol. 26, no. 26, pp. 94–105, 2008.
- [72] E. Matijević and S. V Babu, "Colloid aspects of chemical-mechanical planarization.," *Journal of colloid and interface science*, vol. 320, no. 1, pp. 219–37, Apr. 2008.

- [73] K. Park, H. Kang, M. Kanemoto, and J. Park, "Effects of the Size and the Concentration of the Abrasive in a Colloidal Silica (SiO₂) Slurry with Added TMAH on Removal Selectivity of Polysilicon and Oxide Films in Polysilicon Chemical Mechanical Polishing," vol. 51, no. 1, pp. 214–223, 2007.
- [74] H. J. Kim, H. Y. Kim, H. Do Jeong, S. H. Lee, and D. Dornfeld, "Kinematic Analysis of Chemical Mechanical Polishing and its Effect on Polishing Results," *Key Engineering Materials*, vol. 238–239, pp. 229–234, 2003.
- [75] H. Lee and H. Jeong, "A wafer-scale material removal rate profile model for copper chemical mechanical planarization," *International Journal of Machine Tools and Manufacture*, vol. 51, no. 5, pp. 395–403, May 2011.
- [76] J. a. Chen, "Hydrodynamic characteristics of the thin fluid film in chemical-mechanical polishing," *IEEE Transactions on Semiconductor Manufacturing*, vol. 15, no. 1, pp. 39–44, 2002.
- [77] P. W. Carter and T. Werts, "A method for measuring frictional forces and shaft vibrations during chemical mechanical polishing," *Journal of The Electrochemical Society*, vol. 154, no. 1, p. H60, 2007.
- [78] Y.-K. Hong, J.-H. Han, T.-G. Kim, J.-G. Park, and A. a. Busnaina, "The Effect of Frictional and Adhesion Forces Attributed to Slurry Particles on the Surface Quality of Polished Copper," *Journal of The Electrochemical Society*, vol. 154, no. 1, p. H36, 2007.
- [79] W. Choi, S. Lee, and R. K. Singh, "Dynamic contact characteristics during chemical mechanical polishing (CMP)," *Materials Research Society Symposium*, vol. 767, pp. 10.1–10.6, 2003.
- [80] K. Tamai, H. Morinaga, T. K. Doi, S. Kurokawa, and O. Ohnishi, "Analysis of Chemical and Mechanical Factors in CMP Processes for Improving Material Removal Rate," *Journal of The Electrochemical Society*, vol. 158, no. 3, p. H333, 2011.
- [81] F. Ilie, T. Laurian, and C. Tita, "Relating Friction and Processes Development during Chemical - Mechanical Polishing (CMP)," in in *Advanced Tribology*, J. Luo, Y. Meng, T. Shao, and Q. Zhao, Eds. Springer-Berlin Heidelberg, 2010, pp. 571–575.
- [82] L. Nolan, "Achieving High Rates and High uniformity in copper chemical mechanical polishing," University of Alberta, 2012.
- [83] "Four-Probe Resistivity and Hall Voltage Measurements with the Model 4200-SCS." [Online]. Available: www.keithley.com/data?asset=15222.
- [84] G. L. Vick and K. M. Whittle, "Solid Solubility and Diffusion Coefficients of Boron in Silicon," *Journal of The Electrochemical Society*, vol. 116, no. 8, p. 1142, 1969.

- [85] W. Treberspurg, T. Bergauer, M. Dragicevic, J. Hrubec, M. Krammer, and M. Valentan, "Measuring doping profiles of silicon detectors with a custom-designed probe station," *Journal of Instrumentation*, vol. 7, no. 11, pp. P11009–P11009, Nov. 2012.
- [86] Y. Jiao, X. Liao, C. Wu, S. Theng, Y. Zhuang, Y. Sampurno, M. Goldstein, and A. Philipossian, "Tribological, thermal and kinetic attributes of 300 vs. 450 mm chemical mechanical planarization processes," *Journal of the Electrochemical Society*, vol. 159, no. 3, pp. H255–H259, Jan. 2012.
- [87] A. K. Sikder, F. Giglio, J. Wood, A. Kumar, and M. Anthony, "Optimization of tribological properties of silicon dioxide during the chemical mechanical planarization process," *Journal of Electronic Materials*, vol. 30, no. 12, pp. 1520–1526, Dec. 2001.
- [88] S. Dutta, M. Imran, P. Kumar, R. Pal, P. Datta, and R. Chatterjee, "Comparison of etch characteristics of KOH, TMAH and EDP for bulk micromachining of silicon (110)," *Microsystem Technologies*, vol. 17, no. 10–11, pp. 1621–1628, Sep. 2011.
- [89] G. J. Pietsch, Y. J. Chabal, and G. S. Higashi, "Infrared-absorption spectroscopy of Si(100) and Si(111) surfaces after chemomechanical polishing," *Journal of Applied Physics*, vol. 78, no. 3, p. 1650, 1995.
- [90] D. G. Thakurta, C. L. Borst, D. W. Schwendeman, R. J. Gutmann, and W. N. Gill, "Pad porosity, compressibility and slurry delivery effects in chemical-mechanical planarization: modeling and experiments," *Thin Solid Films*, vol. 366, no. 1–2, pp. 181–190, May 2000.
- [91] C. Liu, B. Dai, W. Tseng, and C. Yeh, "Modeling of the Wear Mechanism during Chemical-Mechanical Polishing," *Journal of electrochemical society*, vol. 143, no. 2, pp. 716–721, 1996.
- [92] A. Philipossian and S. Olsen, "Effect of Slurry Flow Rate on Pad Life during Interlayer Dielectric CMP," *Journal of The Electrochemical Society*, vol. 151, no. 6, p. G436, 2004.
- [93] Y. G. Wang, L. C. Zhang, and A. Biddut, "Chemical effect on the material removal rate in the CMP of silicon wafers," *Wear*, vol. 270, no. 3–4, pp. 312–316, Jan. 2011.
- [94] C. Rogers, J. Coppeta, L. Racz, A. Philipossian, F. B. Kaufman, and D. Bramono, "Analysis of flow between a wafer and pad during CMP processes," *Journal of Electronic Materials*, vol. 27, no. 10, pp. 1082–1087, Oct. 1998.
- [95] A. Philipossian and S. Olsen, "Fundamental tribological and removal rate studies of inter-layer dielectric chemical mechanical planarization," *Japanese Journal of Applied Physics*, vol. 42, no. Part 1, No. 10, pp. 6371–6379, Oct. 2003.

- [96] H. Kim, H. Kim, H. Jeong, E. Lee, and Y. Shin, "Friction and thermal phenomena in chemical mechanical polishing," *Journal of Materials Processing Technology*, vol. 130–131, pp. 334–338, Dec. 2002.